# Rocky Mountain Friends of the Pleistocene
# Henry Mountains, Utah
# 15-17 October 2010

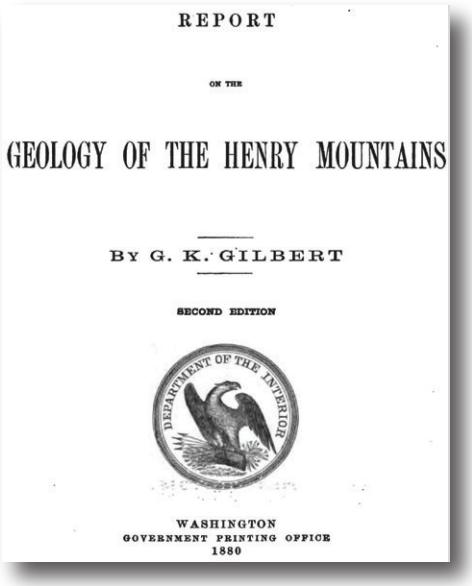
REPORT

ON THE

GEOLOGY OF THE HENRY MOUNTAINS

BY G. K. GILBERT

SECOND EDITION

DEPARTMENT OF THE INTERIOR

WASHINGTON
GOVERNMENT PRINTING OFFICE
1880

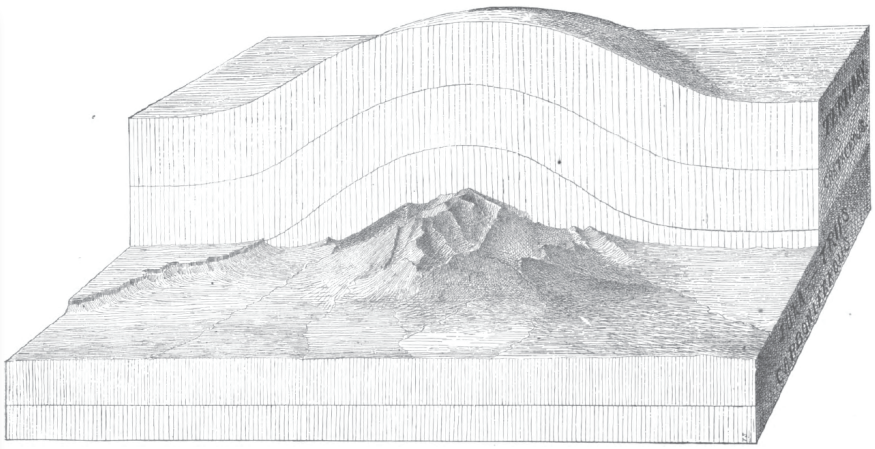

*Frontispiece from G.K. Gilbert's Report on the Geology of the Henry Mountains*

*"But while the Henry Mountains contribute almost nothing to our direct material interests, they offer in common with the plateaus which surround them a field of surpassing interest to the student of structural geology. The deep carving of the land which renders it so inhospitable to the traveler and the settler, is to the geologist a dissection which lays bare the very anatomy of the rocks, and the dry climate which makes the region a naked desert, soilless and almost plantless, perfects the preparation for his examination."*

*- G.K. Gilbert*


ASU School of Earth & Space Exploration
Arizona State University
The University of Texas at Austin
Jackson School of Geosciences

Arjun Heimsath, Roman DiBiase, Matt Jungers,
Matt Rossi, Andy Darling, Kelin Whipple

Joel Johnson, Lindsay Olinde, Peter Polito


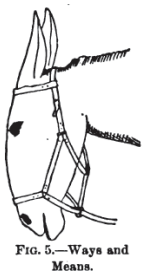
FIG. 5.—Ways and Means.


MAP
of the
HENRY MOUNTAINS.
by G.K.Gilbert.
Photographed from a model in relief.
Scale of Miles.
BAD LANDS
Marine Butte
Bow Creek
Ellen Butte
Mt. Ellen
BLUE GATE PLATEAU
Newberry
Peale
The Crescent
Crescent Creek
Penellen Pass
Sentinel
MASUK PLATEAU
Trachyte Creek
Howell
Mt. Pennell
B
C
Steward
D
BLUE GATE PLATEAU
Mt. Hillers
TUNUNK PLATEAU
Pine Arroyo Creek
Mt. Holmes
HENRYS FORK PLATEAU
Mt. Ellsworth
Colorado River

# Regional Map

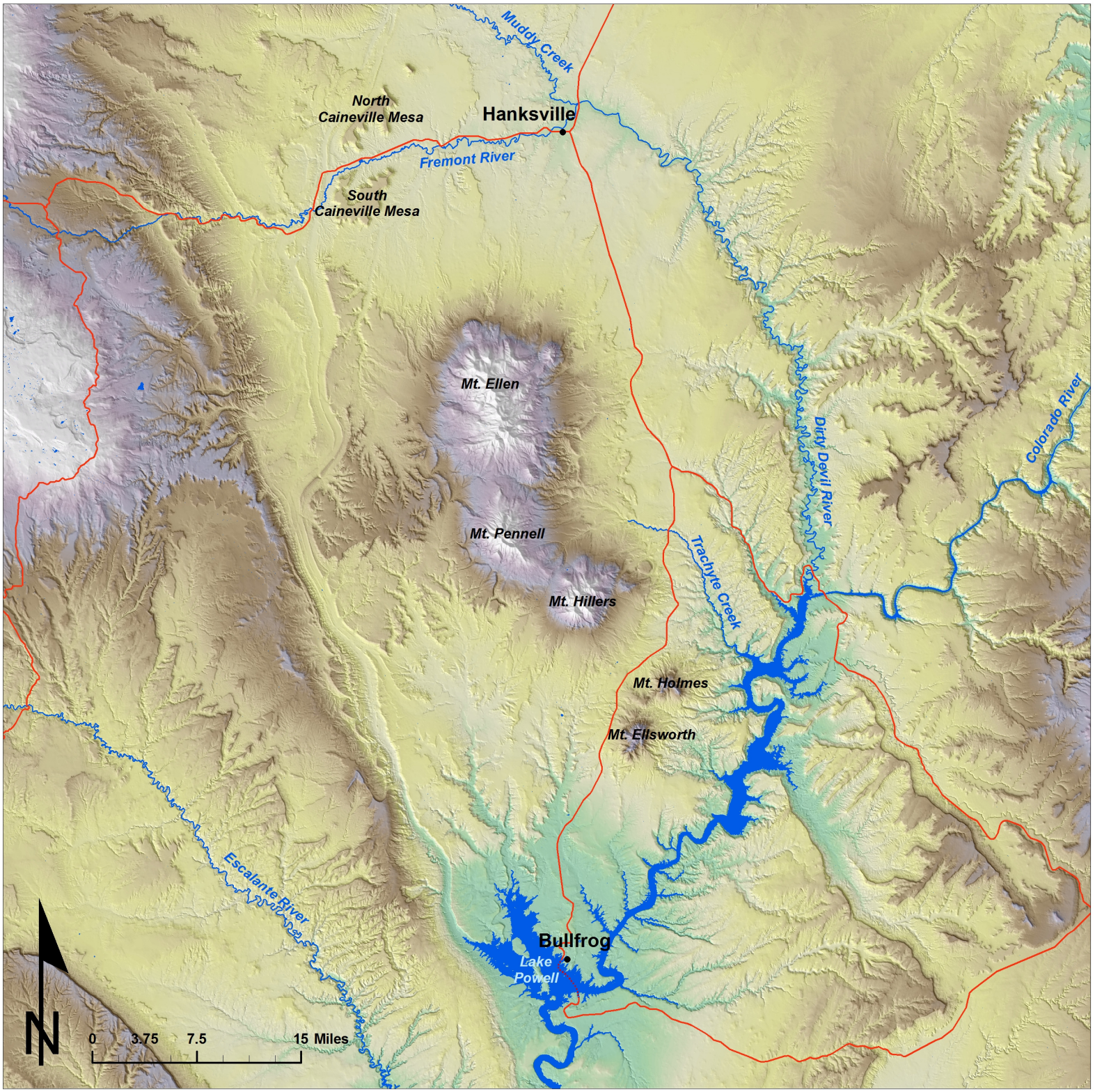

*"The Basin of the Colorado offers peculiar facilities for the study of the origin of topographic forms, and its marvelous sculpture has excited the interest of every observer."* *- G.K. Gilbert (as are the rest)*

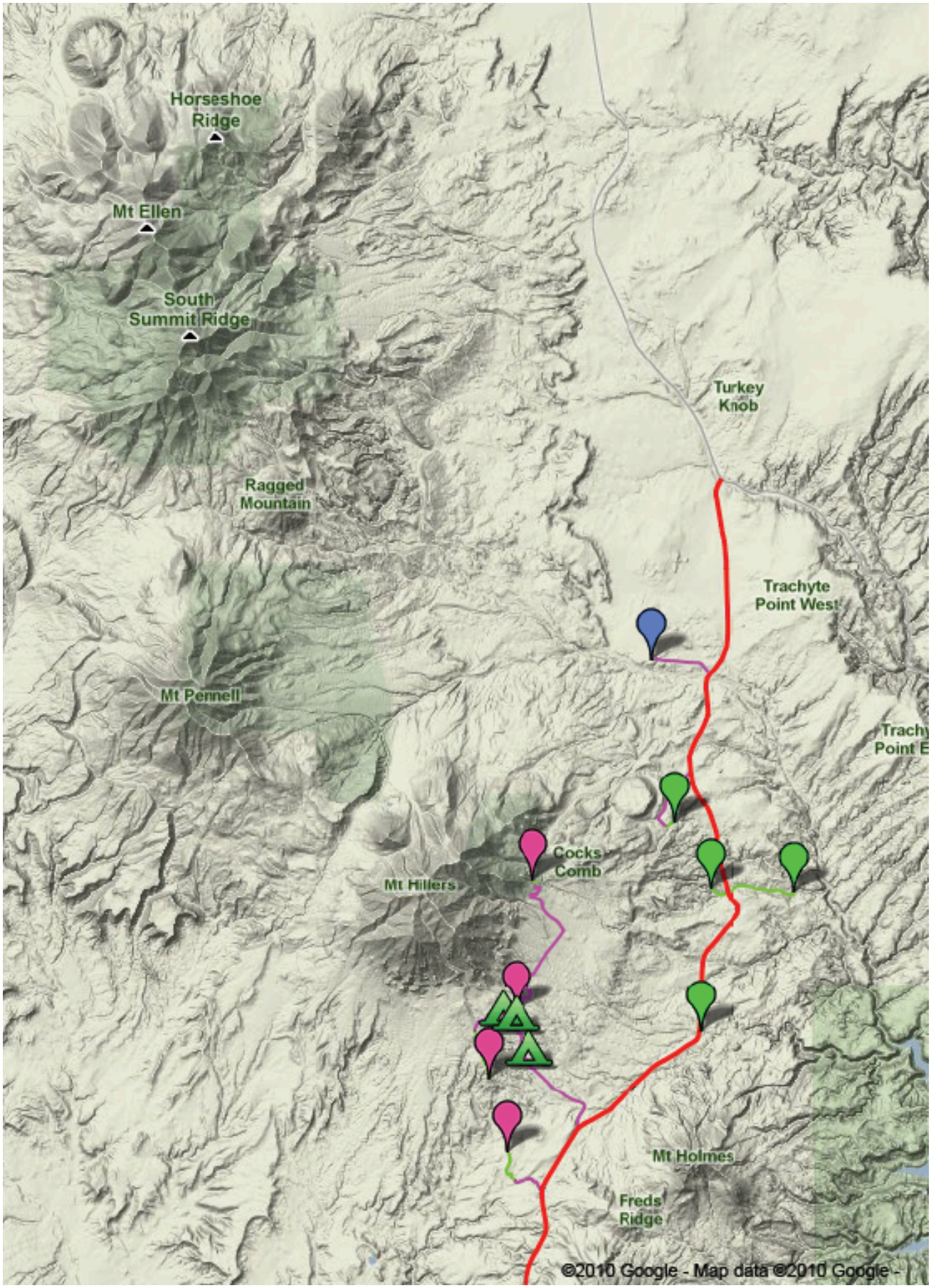


Day 1: Red

Day 2: Green

Day 3: Blue

**The Trip On A Page**

**Day 1: Hillslopes – Form, Process and Sediment Production & Transport**

**Stop 1**: **Organization, introductions and trip overview**
- Meet at Base Camp at 9 a.m.
- Brief Henry Mountains geologic history: Mt. Holmes as a backdrop

**Stop 2**: **Intro to hillslope morphology: hypotheses/questions**
- Is this landscape supply- or transport-limited? Threshold slopes.
- Soil vs. Bedrock dominated landscapes and dominant processes.
- Impact of fire on hillslope erosion and sediment supply.

**Stop 3: Convex Hillslopes on the Shoulders of Gilbert**
- Short hike through a soil-mantled landscape south of Mt. Hillers.
- Lunch break: convex hillslopes and hillslope sediment transport.
- Panorama Knoll – hillslope response to falling base level.

**Stop 4: Pediments, Badlands, and Closing Discussion**
- View from Mt. Hillers south to Bullfrog Bay
- Panorama of badlands, pediments/piedmonts, and convex hillslopes.
- How old are all these features, and how are they related to one another?

**Day 2: Rivers – Form, Process and Bedrock Incision**

**Stop 1: Swett Creek Erosion Monitoring Site**
- Flash flood & snowmelt hydrographs, erosion rates,
- morphological adjustment, and inner channels.
- Compare to flume experiments

**Stop 2: Trail Canyon (just upstream of road)**
- Comparison of mainstem and two tributaries
- Discussion of pothole formation

**Stop 3: Trail Canyon Epigenetic Gorges (downstream of road)**
- Hike downstream to epigenetic gorges, and discuss over lunch

**Stop 4: Bedrock Incision Across a Laccolith**
- Discuss feedbacks between hillslope sedimentation and channel response.

**Day 3: Dating surfaces, incision rates, and connections to the Colorado**

**Stop 1 (and only): Trachyte Creek Surfaces**
- Trachyte Creek surfaces used for incision rate study.
- Cosmogenic nuclide dating of surfaces
- Closing remarks and additional spots for the drive home!

## Day 1: Hillslopes – Form, Process and Sediment Production & Transport

Overview of Stops and rough schedule:

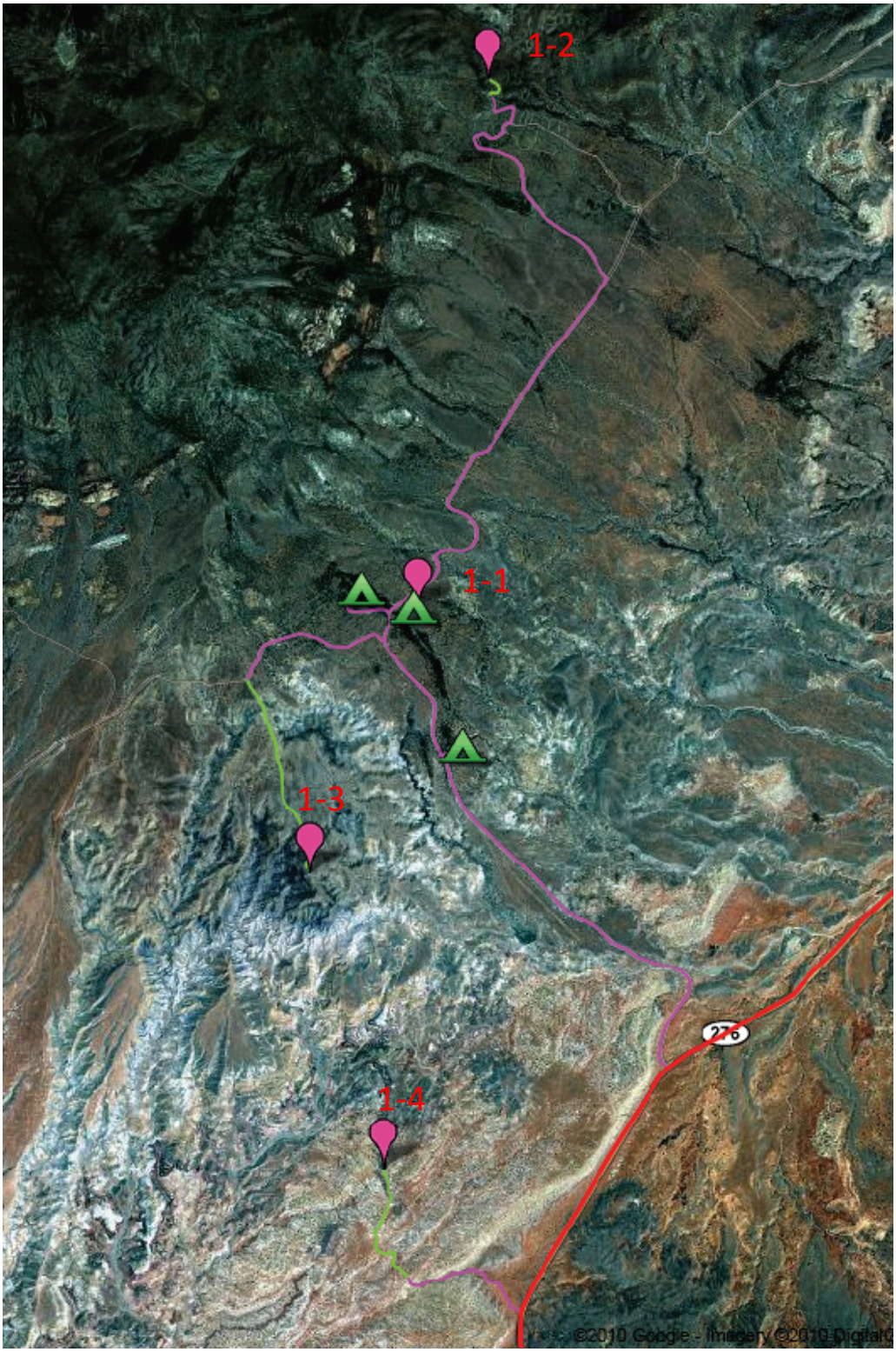


Schedule, Fri. Oct. 15, 2010

1-1: Fire Pit Camp
8:30 – 9:30

1-2: Trail Cyn Headwaters
10:00 – 11:30

1-3: Panorama Knoll
12:00 – 3:00

1-4: Shitamaring Lookout
3:30 – whenever …

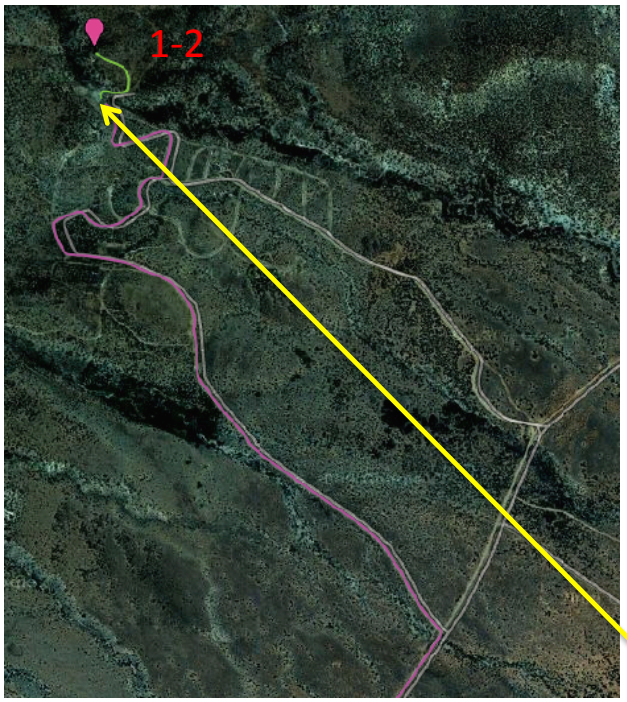


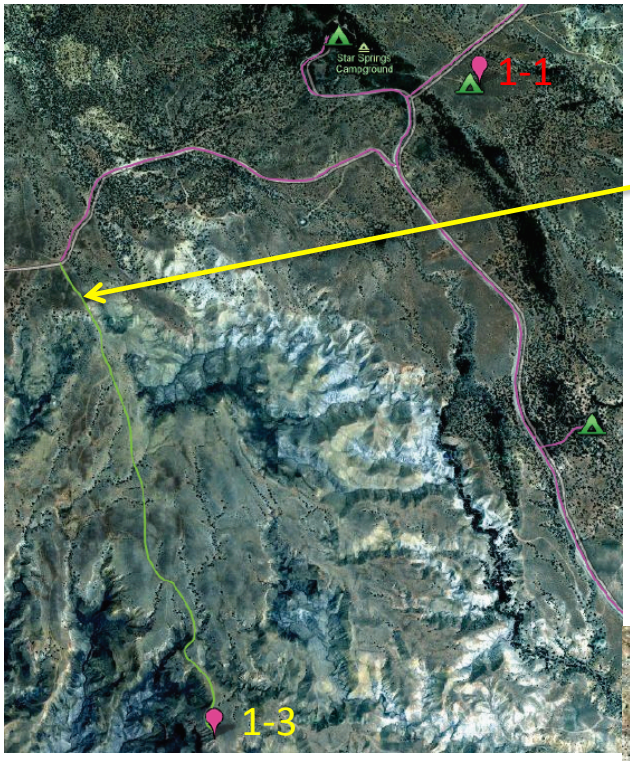


# Parking and Logistics, Fri. Oct. 15, 2010

**Stop 1-1: Fire Pit Camp – 8:30 – 9:30 AM**

This is "base camp" for us and is less than 1 km from Star Springs Campground. We will gather "first thing" and go through introductions and the regional setting of the Henry Mountains, as well as introduce the field trip and the stops we've had planned – to give everyone an outline of the rest of the trip.

**Stop 1-2: Trail Canyon Headwaters – 10:00 – 11:30 AM**

This stop can be approached from two dirt roads that head uphill from the road that Fire Pit Camp is off of. The last uphill stretch is likely rutted, and only has limited parking and turnaround area at the end of the arrow. We will hike to the top of a small ridge to show/discuss.

**Stop 1-3: Panorama Knoll – 12:00 – 3:00 PM**

Parking will be at the top of the main ridge and we'll have a couple hours worth of gentle hiking here to get across the soil-mantled hills to the edge of more badland-like topography. **BRING LUNCH AND WATER**.

**Stop 1-4: Shitamaring Lookout – 3:30 – whenever…**

Turn right on a dirt road off Rt. 276 about 2.5-3 km south from the road up to Star Springs. The first km or so is good dirt and then it's likely to be rough. We will direct parking and admire the view accordingly. (*below zoom*)

# Geology Overview of Mt. Hillers Area

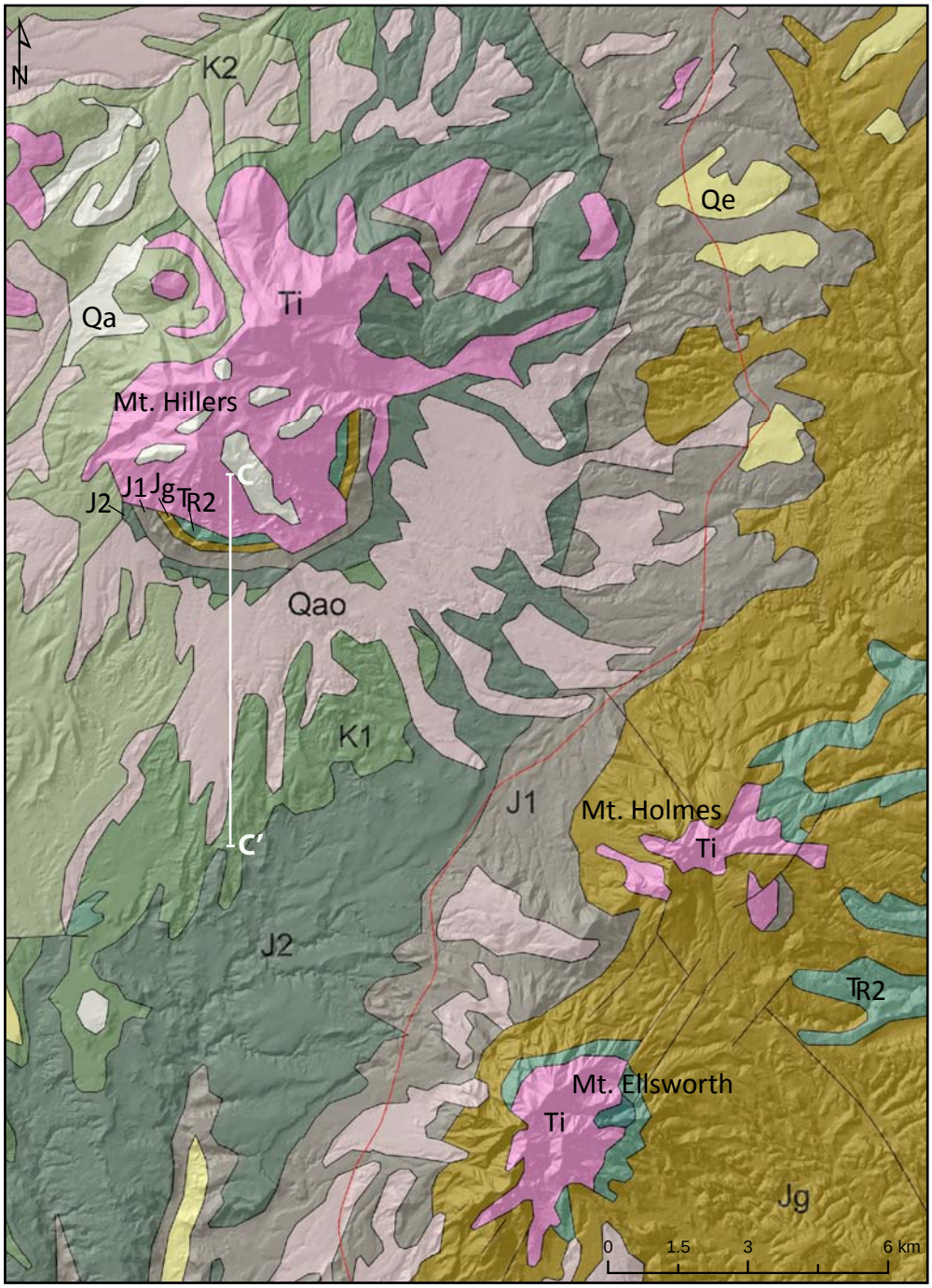


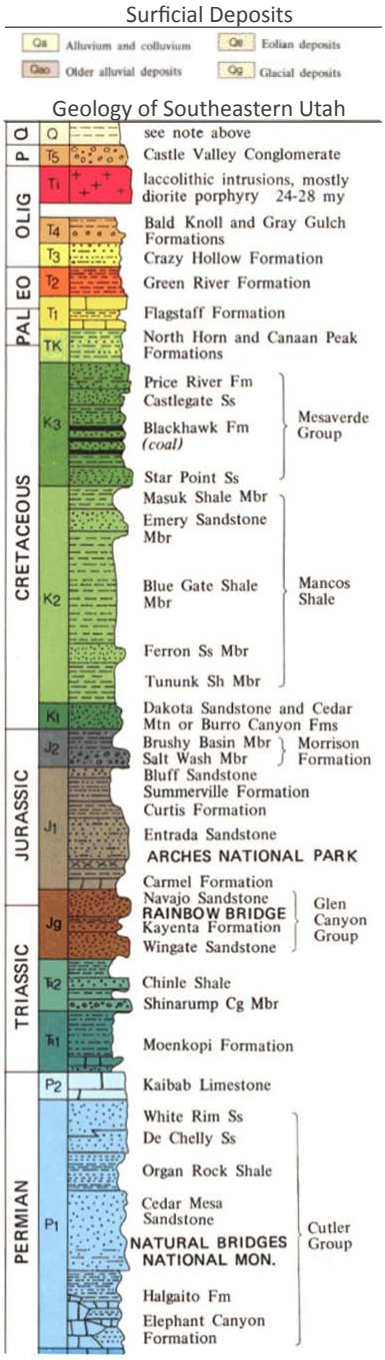


Digital Geologic Map of Utah 2000; Utah Geological Survey
*Note that cross section line (C to C') is approximate

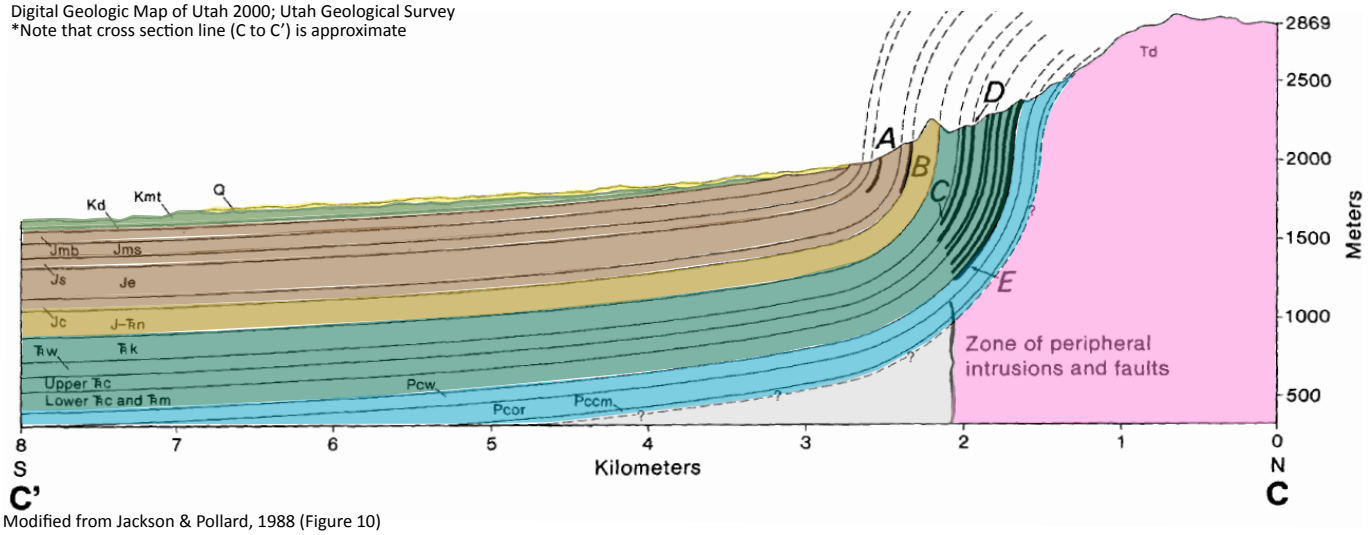


Modified from Jackson & Pollard, 1988 (Figure 10)

# Day 1, Stop 2: Hillslope process and form

**Soil-mantled**

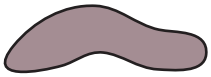

**Scree-mantled**

**Bedrock**

**low slopes, convex up**

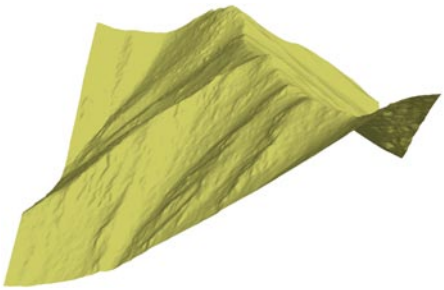

**steep, planar slopes**

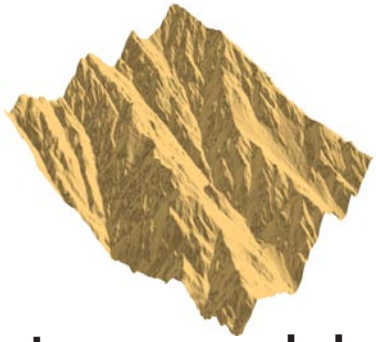

**steep, rugged slopes**

## Which processes are active/dominant in each zone?

"Plants often pry apart rocks by the growth of their roots, but their chief aid to erosion is by increasing the solvent power of percolating water" -Gilbert

# Day 1, Stop 2: Quantifying hillslope form

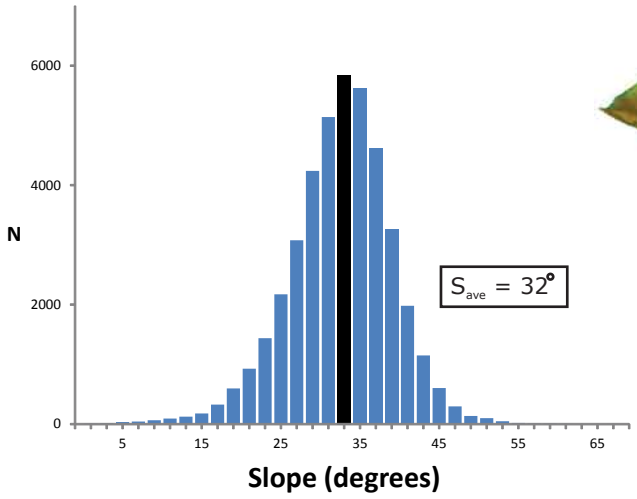


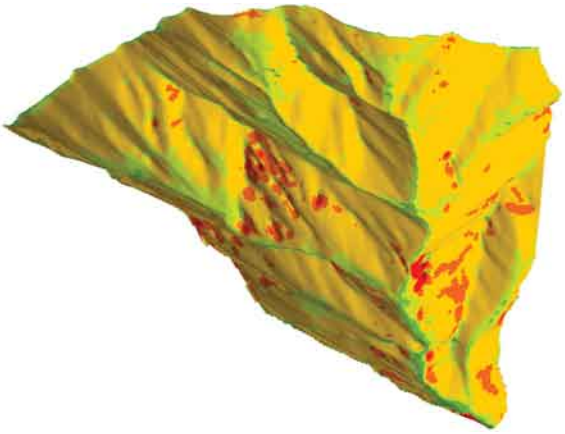

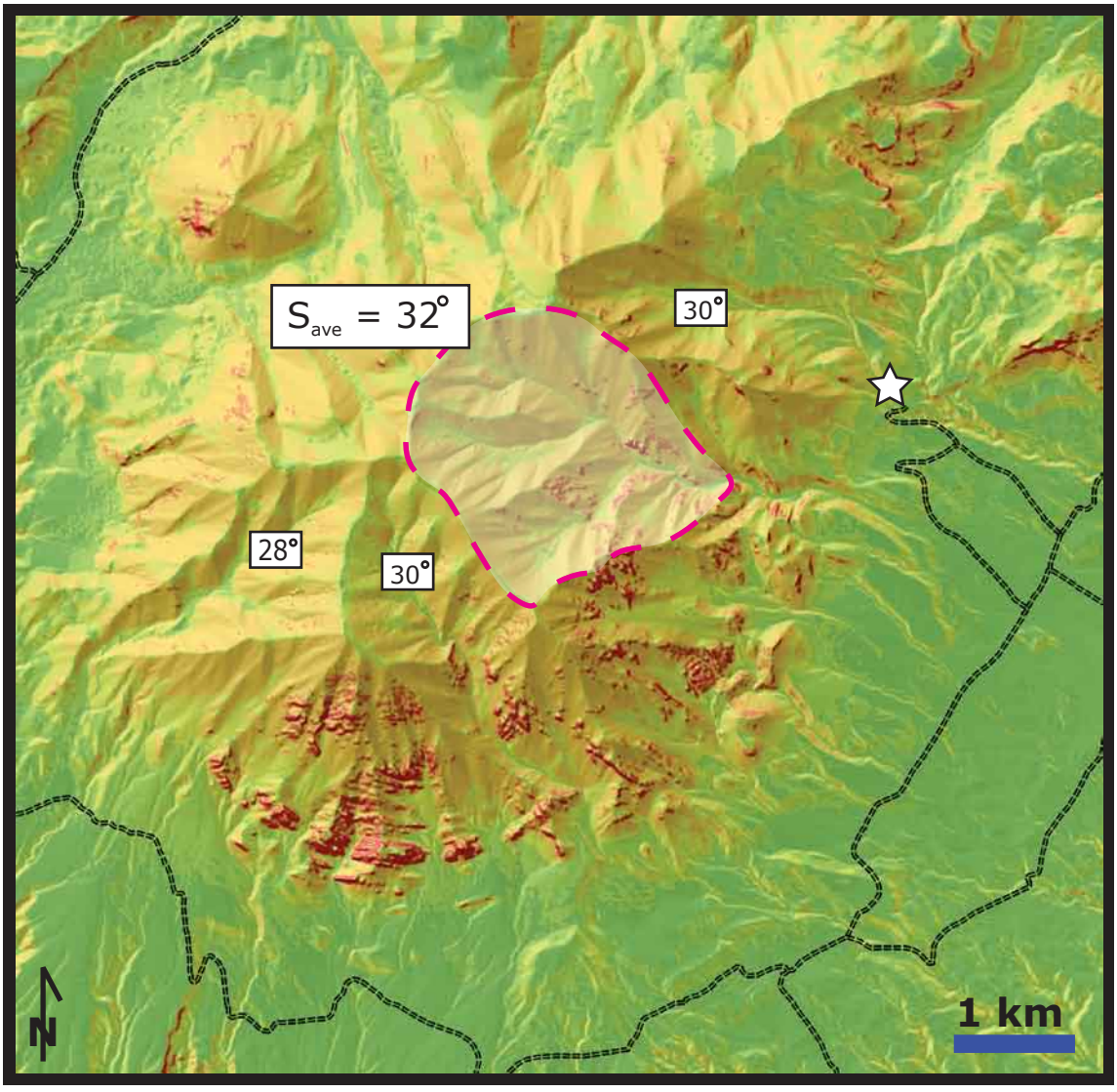


Slope (degrees)

- 0-10
- 10-20
- 20-30
- 30-40
- 40-50
- >50

# Day 1, Stop 2: Rates of hillslope processes

Catchment-averaged erosion rates from in situ cosmogenic $^{10}$Be

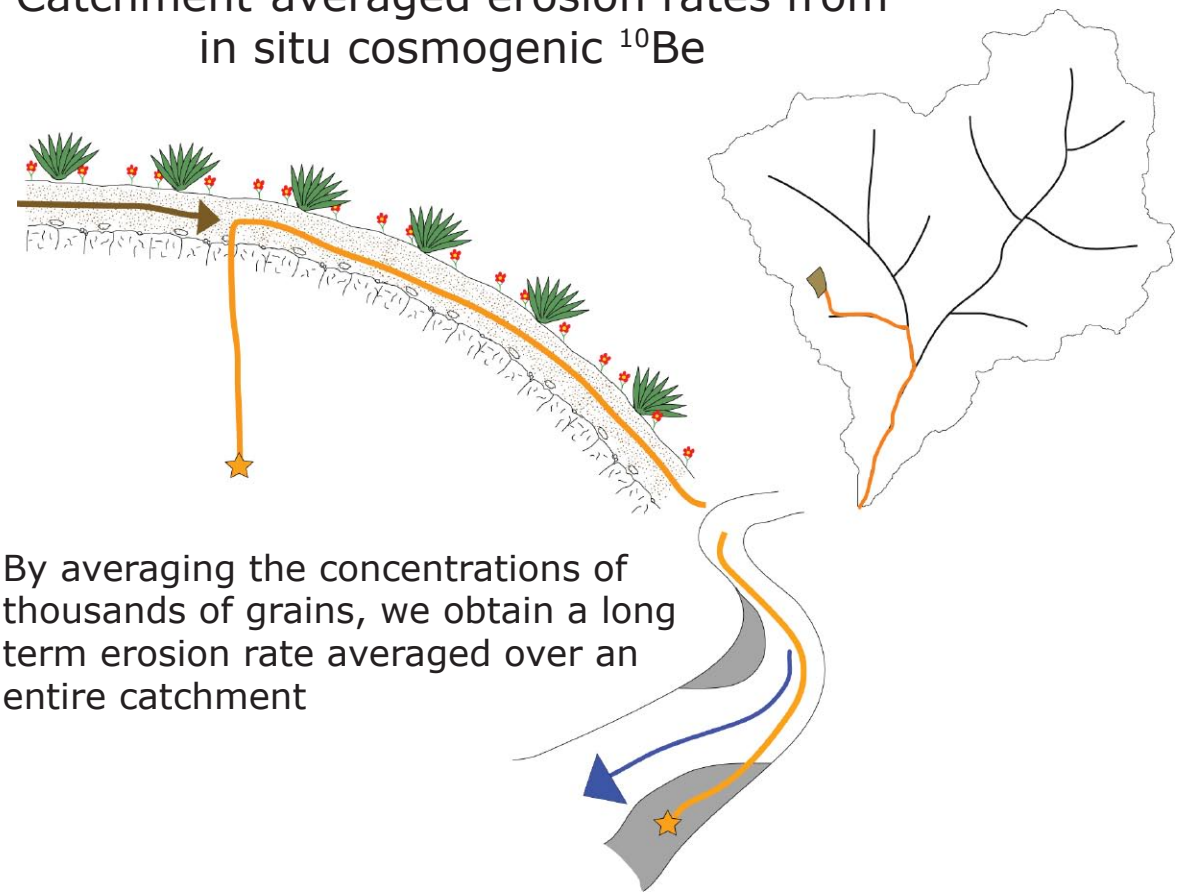

By averaging the concentrations of thousands of grains, we obtain a long term erosion rate averaged over an entire catchment

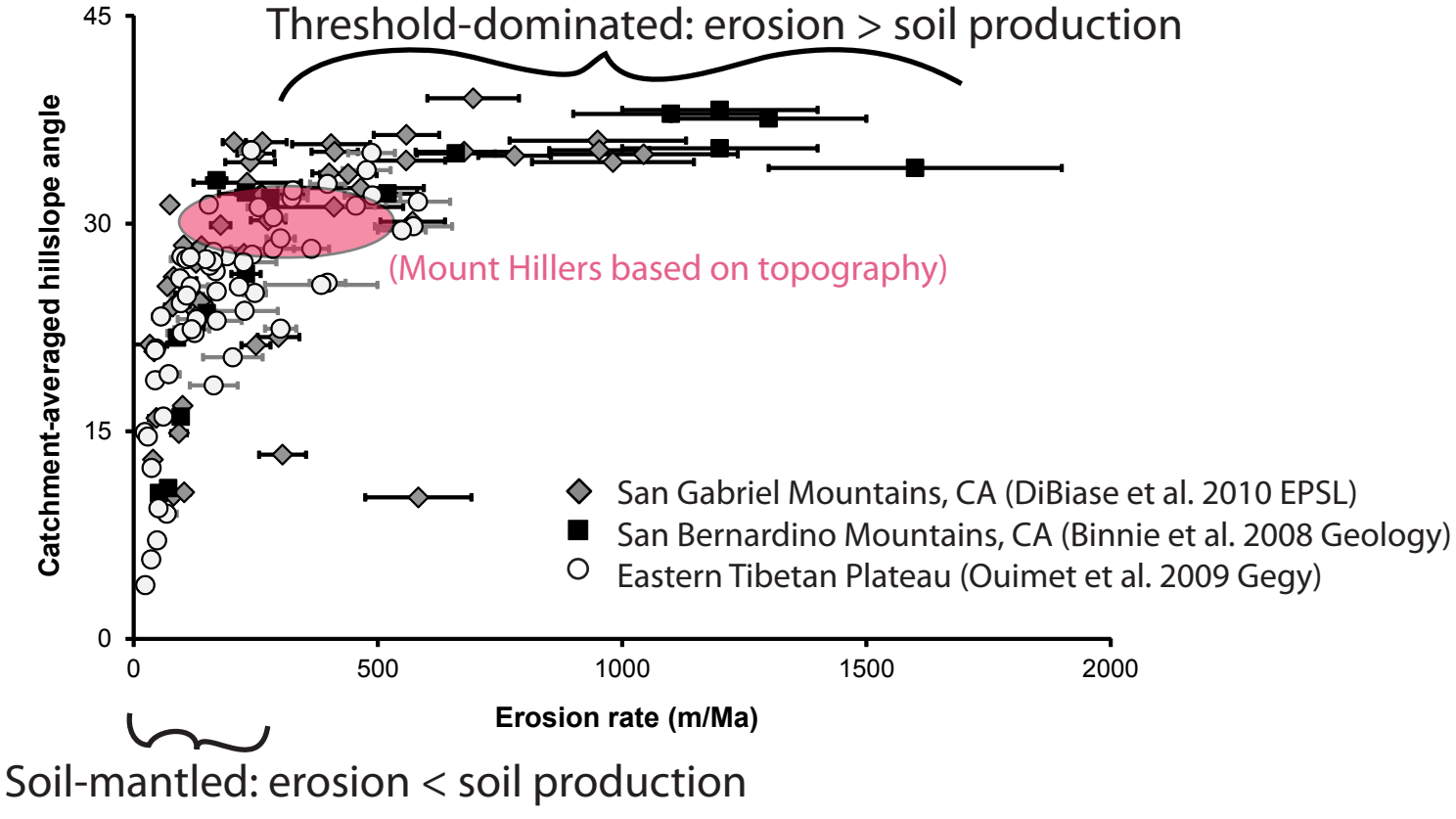

*"Consider now the effect of creep on the law of slope. As we are speaking of mature topography only, we may assume the rate of degradation to be the same on all parts of the slope, so that the two lines in the schematic* [next page] *represent the surface of the ground at two epochs…."*

## Day 1 Stop 3: Convex Hillslopes on the Shoulders of Gilbert

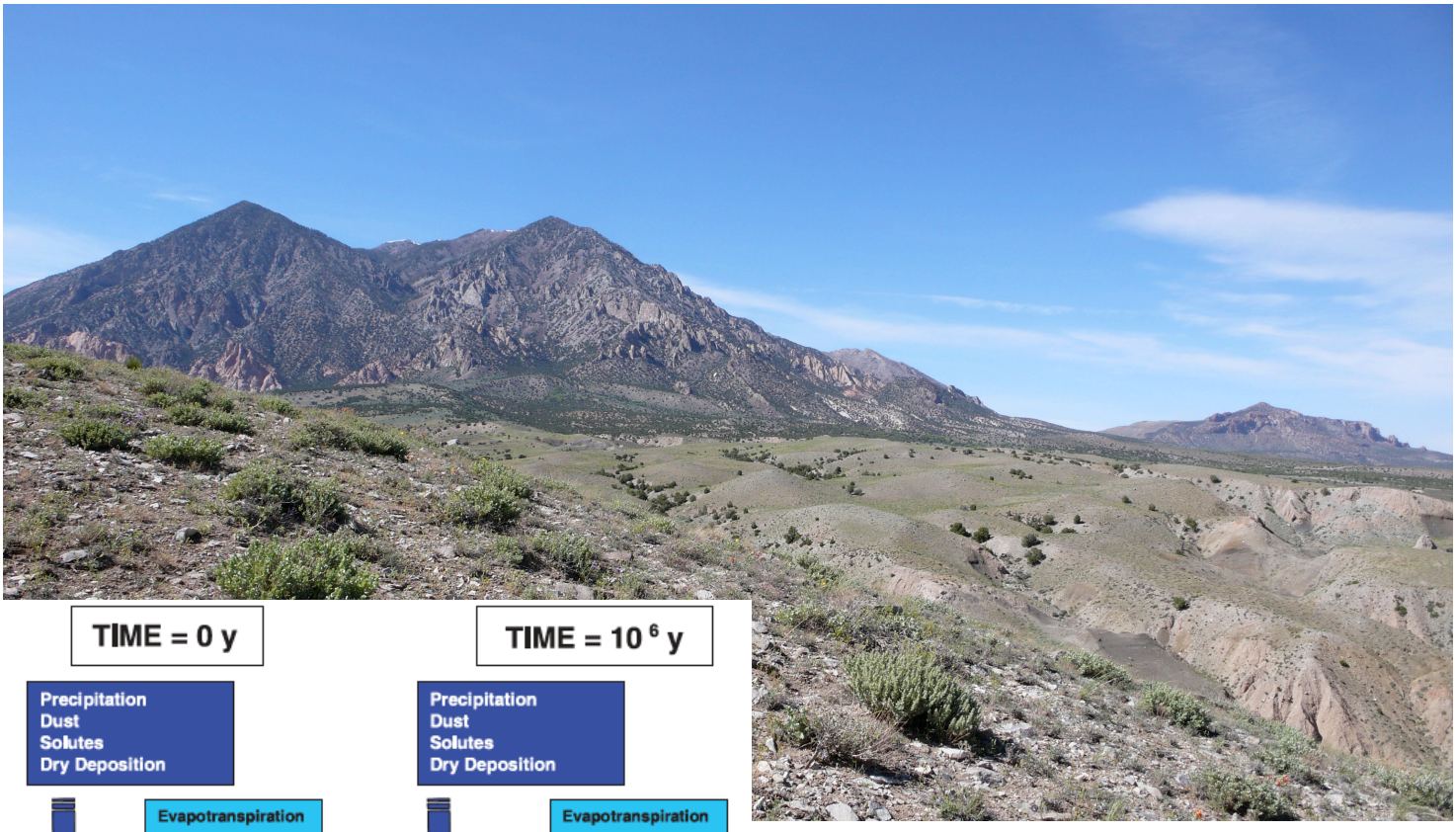

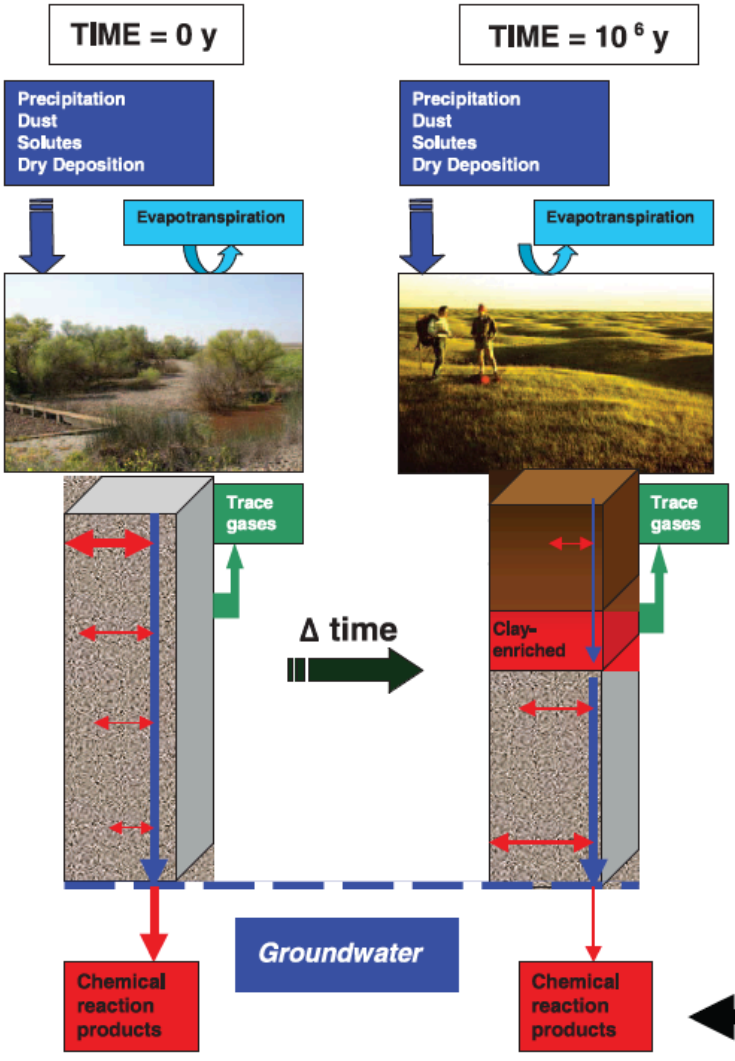


Gilbert's perspectives on such landforms spawned numerous studies and helps motivate study of the Earth's Critical Zone.

*Figures from Amundson et al. 07*

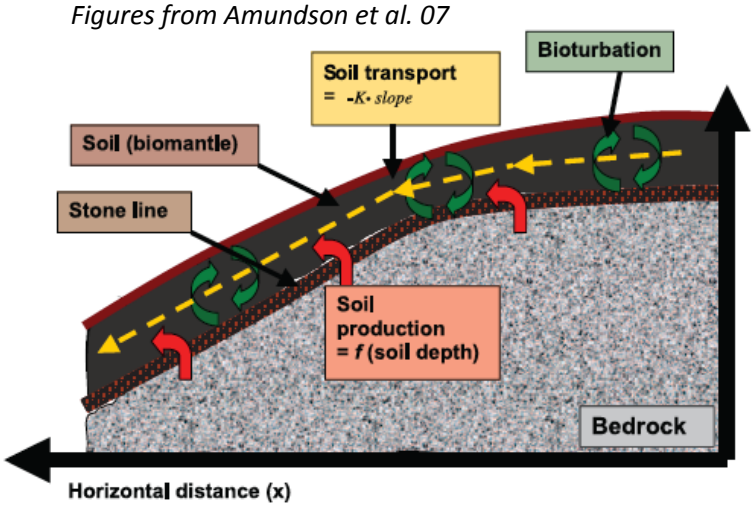

**From Anderson's "Little Book of Geomorphology"**

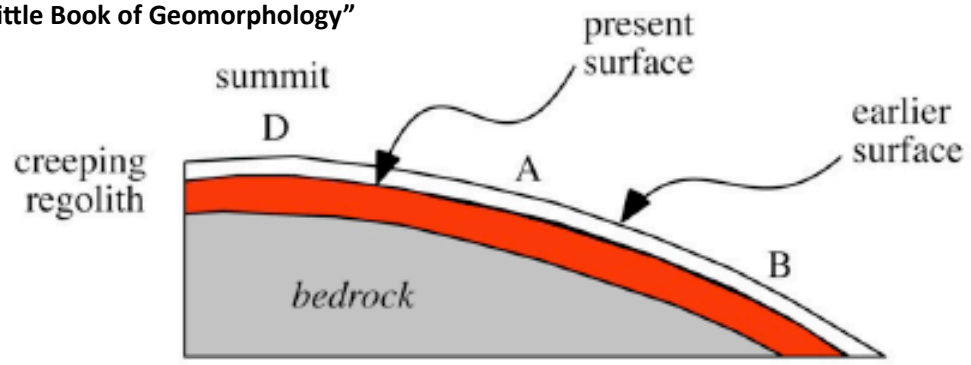


Schematic cross-section of a steady state convex hilltop. Summit at D and two equally spaced points A and B are shown. Surface of the hill is shown at two times, early (dashed) and present. The entire hilltop has been lowered by the same amount. Bedrock weathers to mobile regolith at the bedrock-regolith interface. Regolith produced between the summit, D, and the point A must be transported past A by creep, while all regolith produced between D and B must be transported past B. If the transport process is slope-dependent, the slope at B must be twice that at A. This is the essence of convex hilltops. (after Gilbert, 1909, Figure 1)

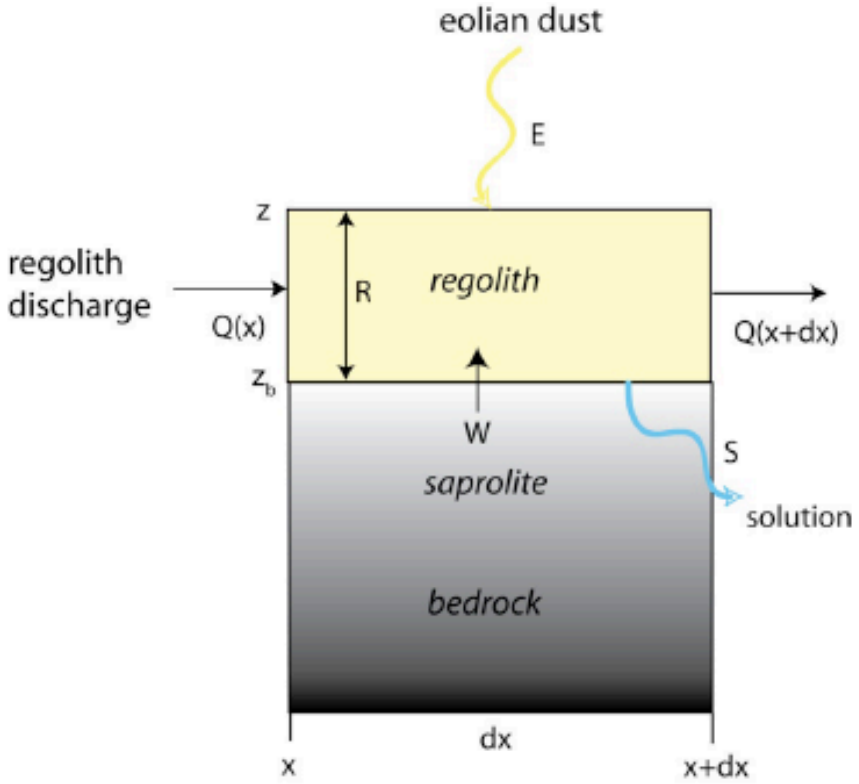


The word statement representing conservation of regolith is:

| rate of change of regolith mass [M/T] | = | rate of regolith inputs [M/T] | - | rate of regolith outputs [M/T] |
|---|---|---|---|---|

*"In a maturely developed topography, hilltops composed of unconsolidated materials are upwardly convex in profile … In creep the chief disturbing agencies are expansion and contraction, and these are caused by freezing and thawing, heating and cooling, wetting and drying … Prominent among other disturbing agencies are plant roots …. Animals promote creep in a more direct way…"* Gilbert's recognition of processes & form

## Stop 3: Using morphology to deduce process and hypothesize rates

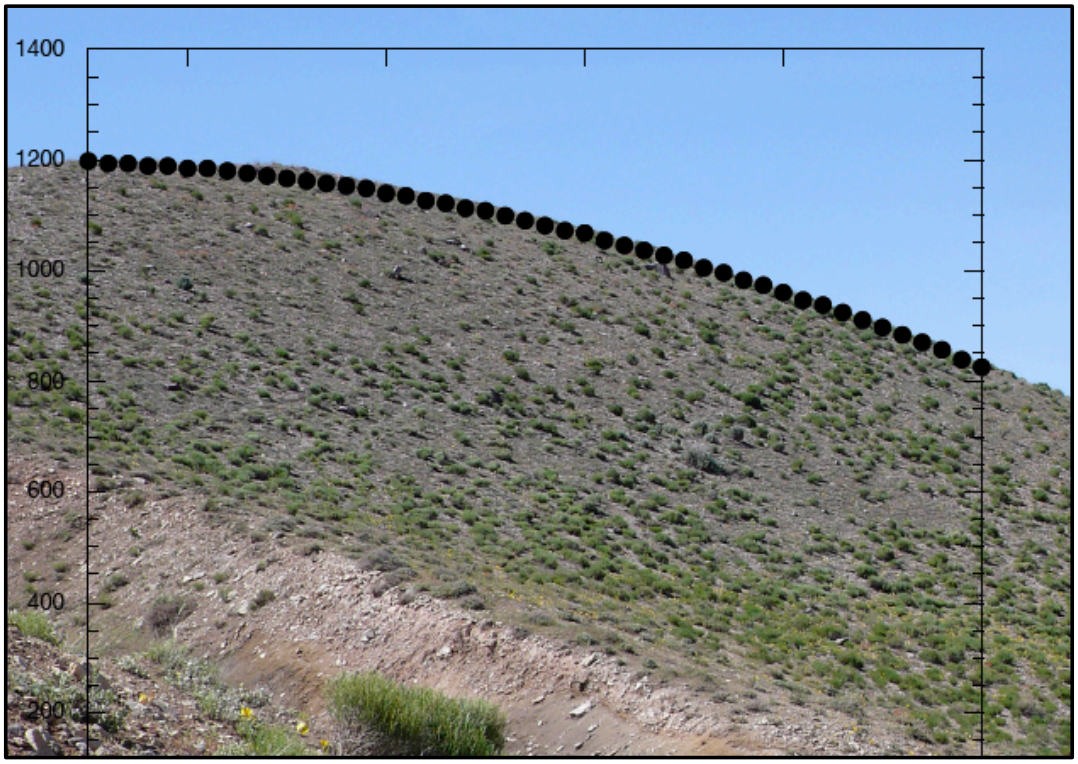


1. $Q_s = -K(dz/dx)$ K = transport coefficient ($L^2$/time)

   *Assume, as Gilbert suggests, sediment flux is linearly dependant on slope*.

2. $E = -(dz/dt)=(dQ_s/dx)$ - Recall, from mass balance

3. Substitute eq. 1 into eq. 2:

   $E = \mathbf{-(dz/dt) = -K(d^2z/dx^2)}$ ► $E/K = -(d^2z/dx^2)$ = *constant, as above photo…*

   *Integrate*: $\mathbf{-dz/dx = E/K(x)}$ (E and K are constants; dz/dx = 0 @ x = 0)

So, the profile of a hillside can yield an Erosion Rate or transport coefficient…

***i.e. plot Slope vs. distance and the slope of the line = E/K.***

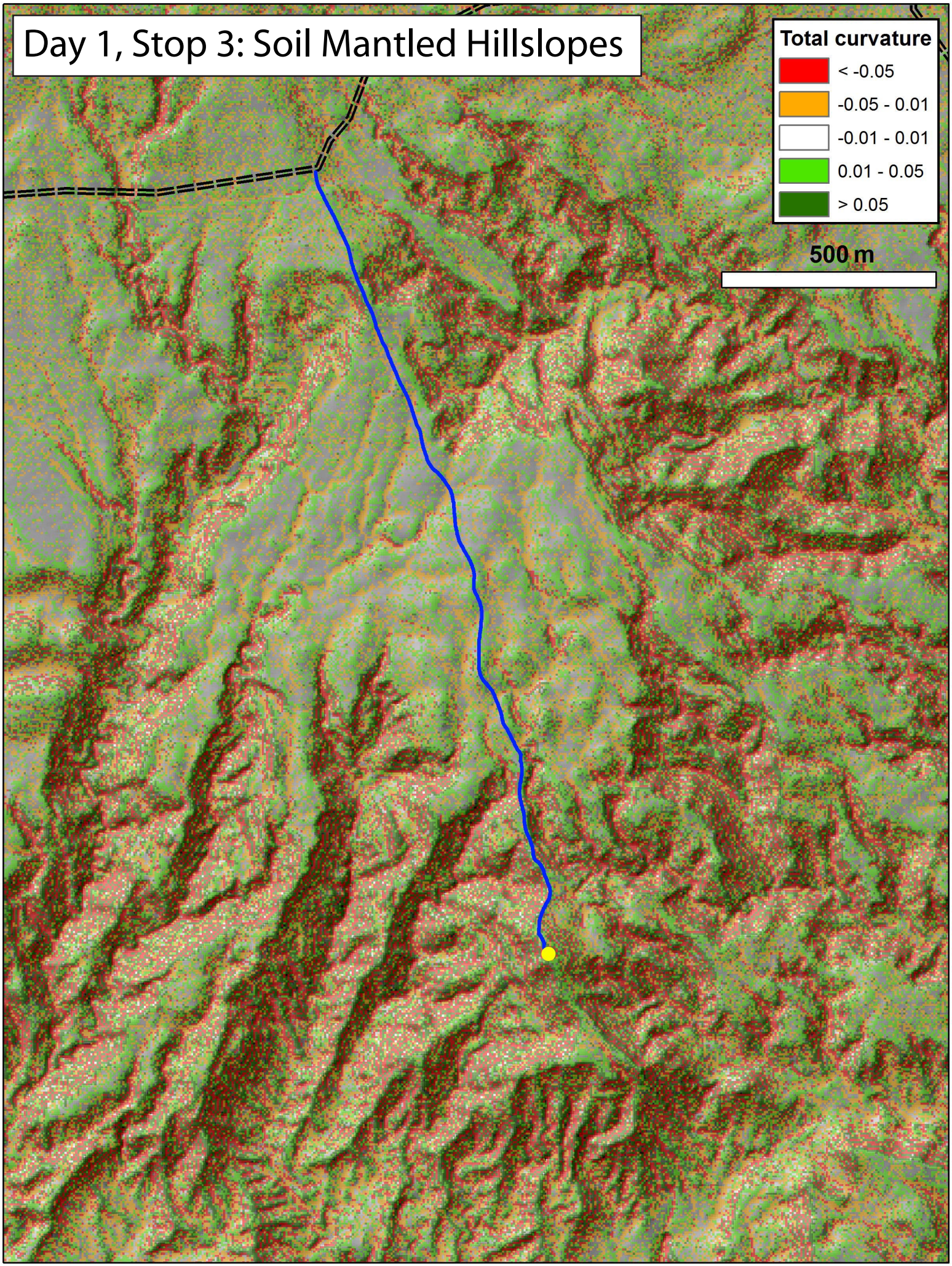
Day 1, Stop 3: Soil Mantled Hillslopes
Total curvature
< -0.05
-0.05 - 0.01
-0.01 - 0.01
0.01 - 0.05
> 0.05
500 m

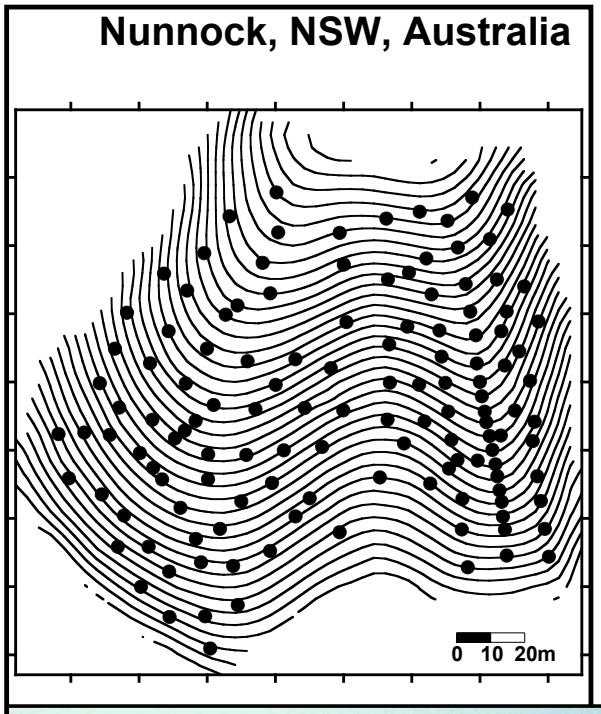
Nunnock, NSW, Australia
0 10 20m

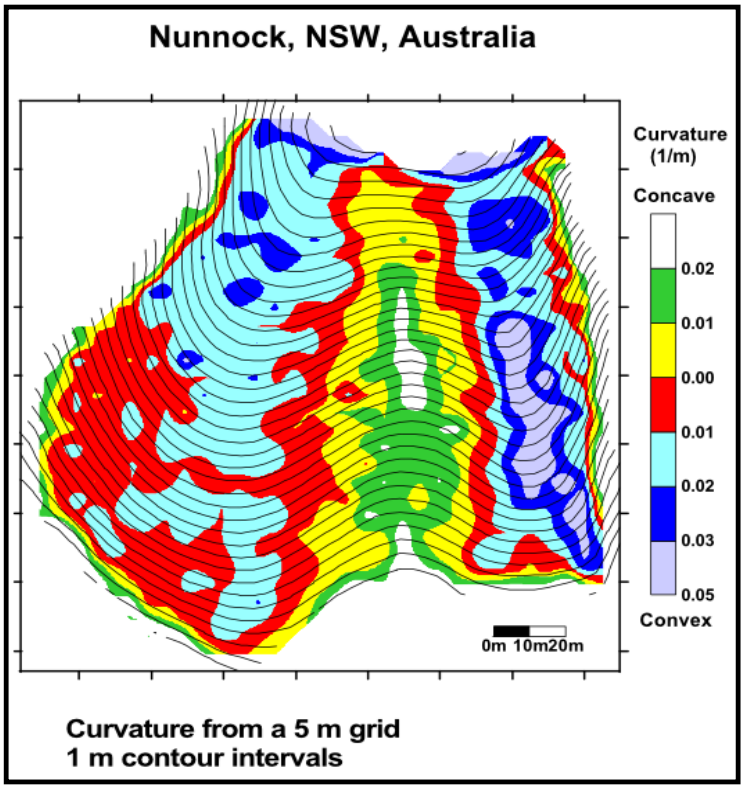
Nunnock, NSW, Australia
Curvature (1/m)
Concave
0.02
0.01
0.00
0.01
0.02
0.03
0.05
Convex
0m 10m20m
Curvature from a 5 m grid
1 m contour intervals

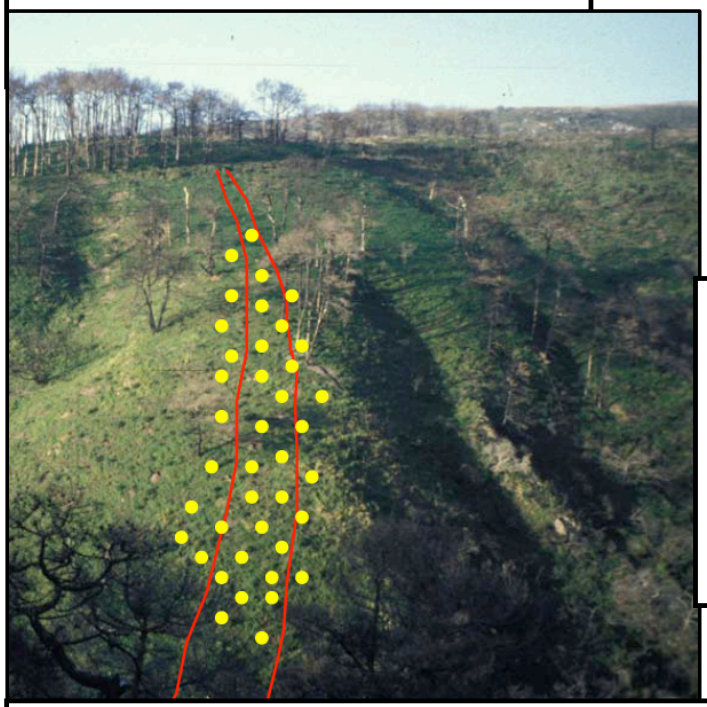

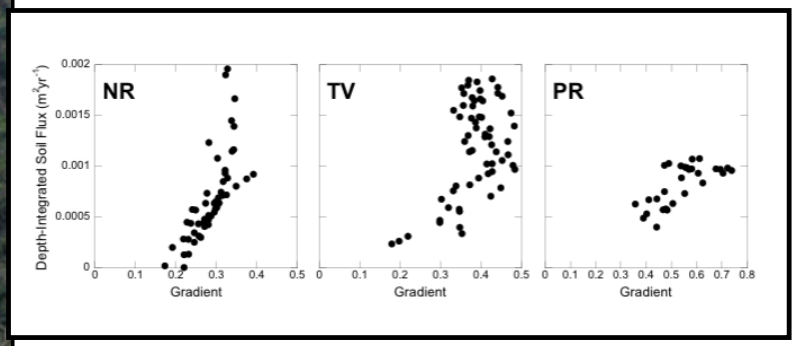
NR
TV
PR
Depth-Integrated Soil Flux (m²yr⁻¹)
Gradient

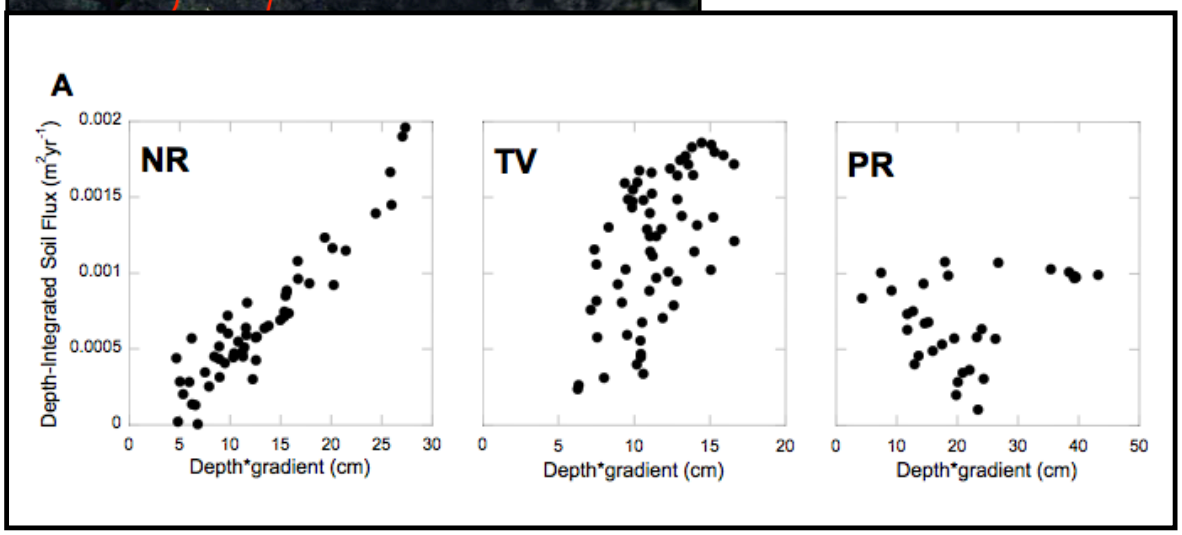
A
NR
TV
PR
Depth-Integrated Soil Flux (m²yr⁻¹)
Depth*gradient (cm)

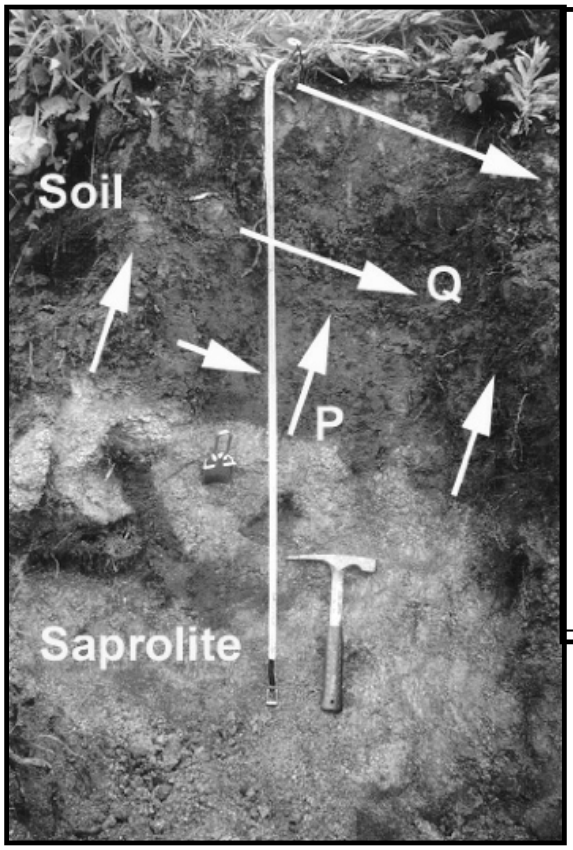


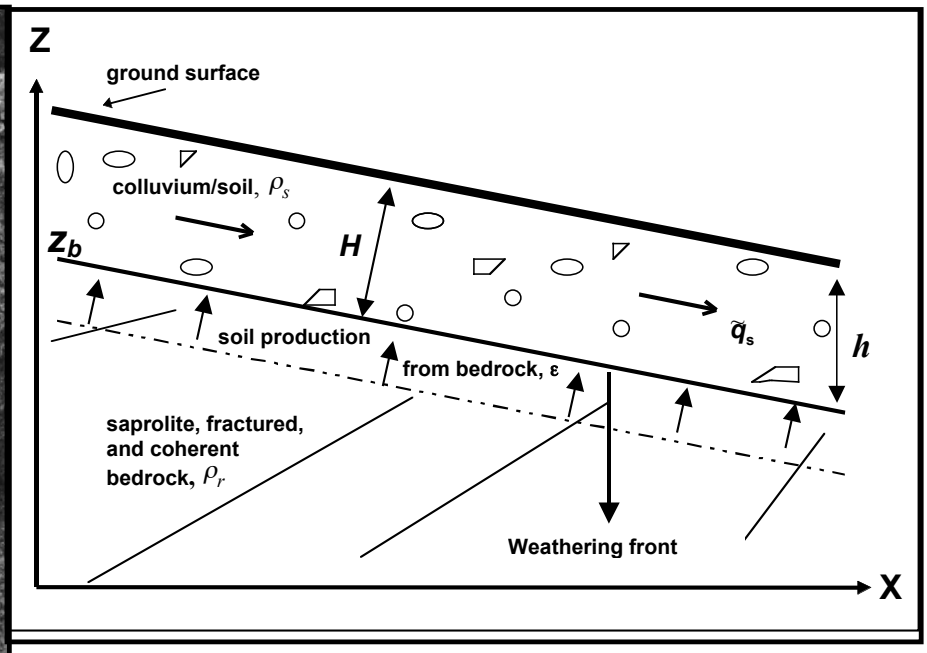


$$\frac{\partial z}{\partial t} = -\nabla \cdot \tilde{Q}_s + Tectonics$$

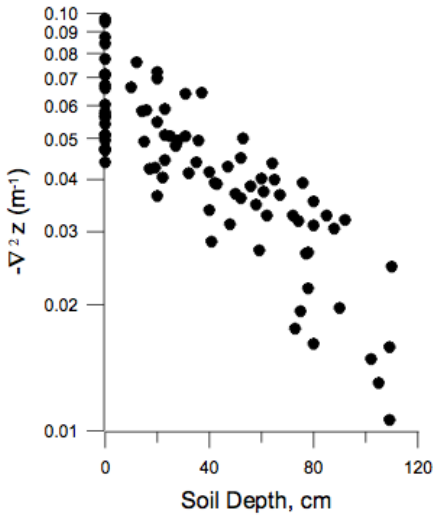


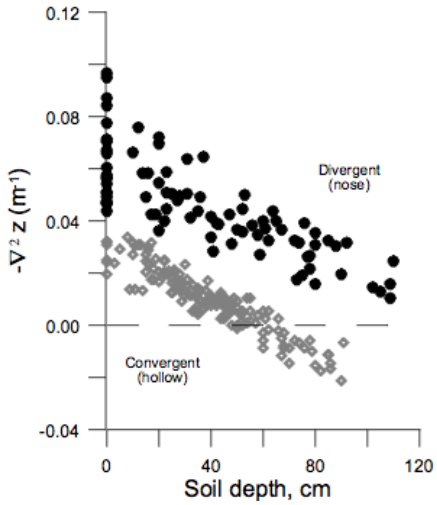


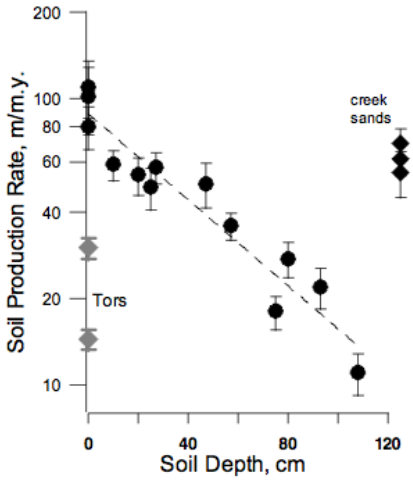


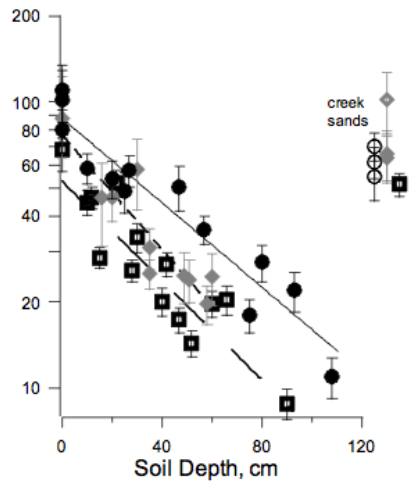

# Quantifying hillslope sediment transport with cosmogenic nuclides

## Meteoric $^{10}$Be, McKean et al., 1993

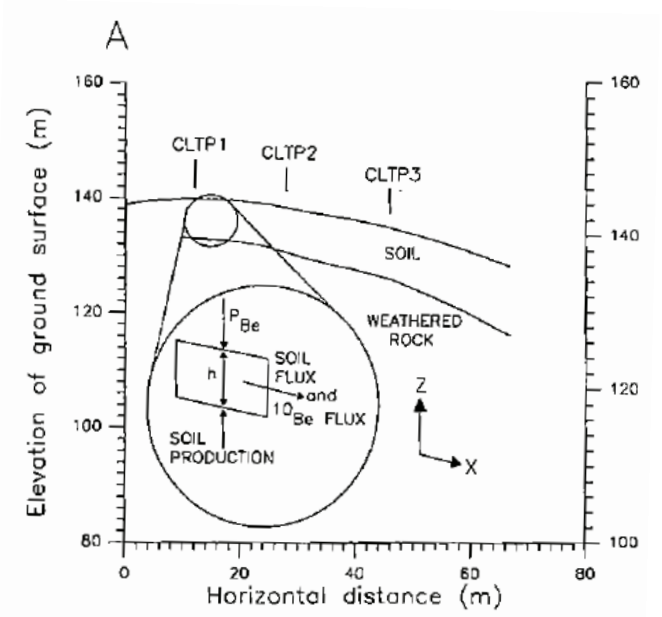


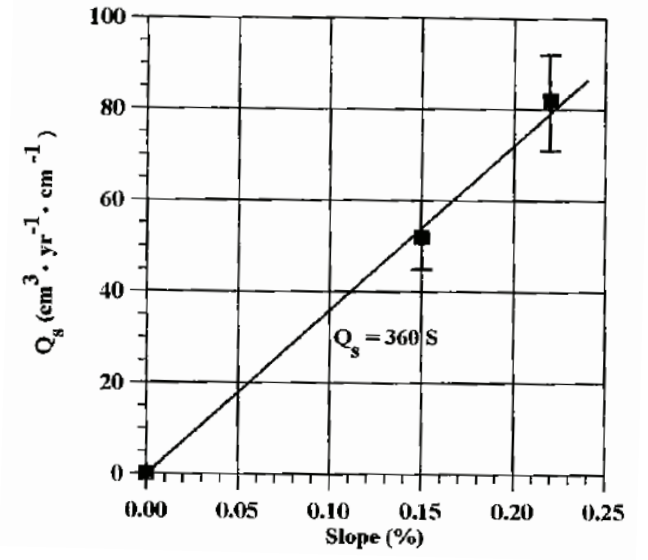


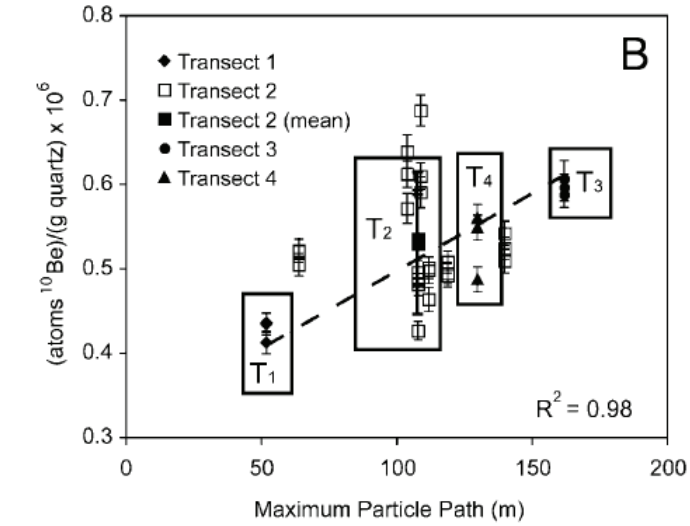


## *In situ*-produced $^{10}$Be, Small et al., 1999

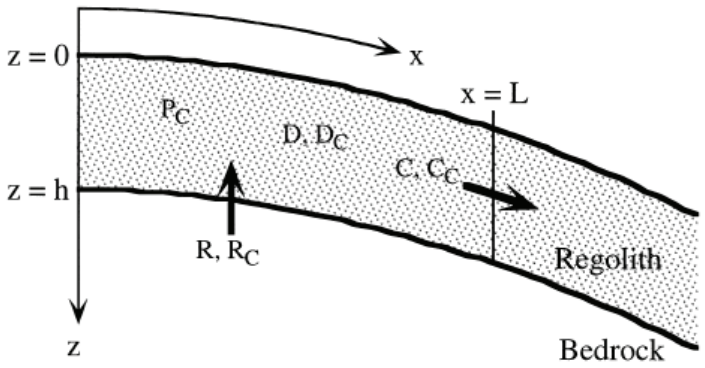


Fig. 2. This scheme was used to evaluate hillslope mass (total and quartz) and CRN balance. No subscript indicates component of mass balance. Subscript (C) indicates component of CRN balance. Regolith production (R) adds mass and CRNs to the hillslope element, whereas regolith dissolution (D) and regolith creep (C) remove mass and CRNs. In addition, in situ production ($P$) of CRNs within the regolith adds CRNs.

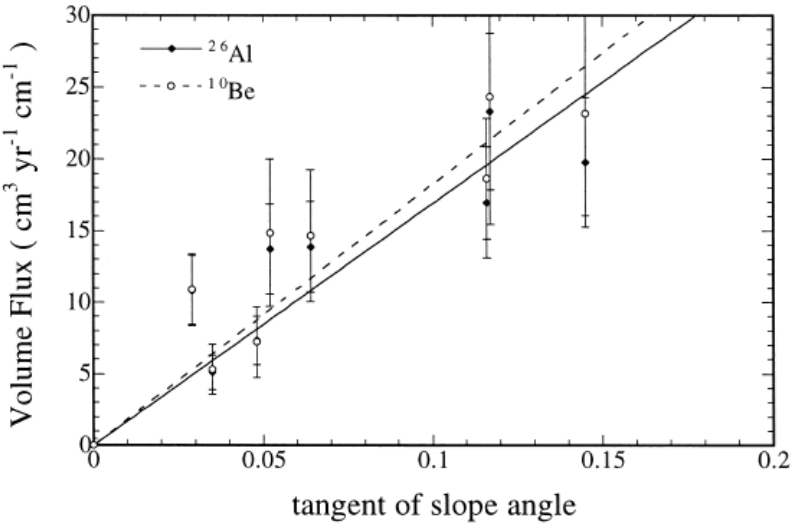


<--Jungers et al., 2009

> Inventories of both *in situ* and meteoric $^{10}$Be suggest transport velocities of ~1-2 cm/yr

> Concentration of cosmogenic nuclides is highest in sediment with longest potential particle paths (particle paths determined using airborne LiDAR)

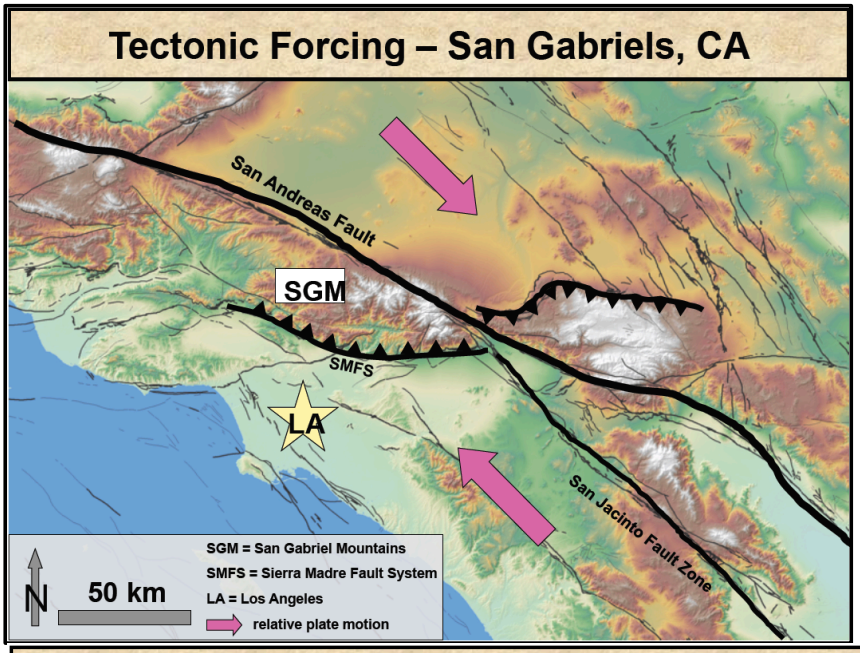


Examining erosion and soil production rates where we have a gradient of external forcing: The San Gabriel Mtns., CA

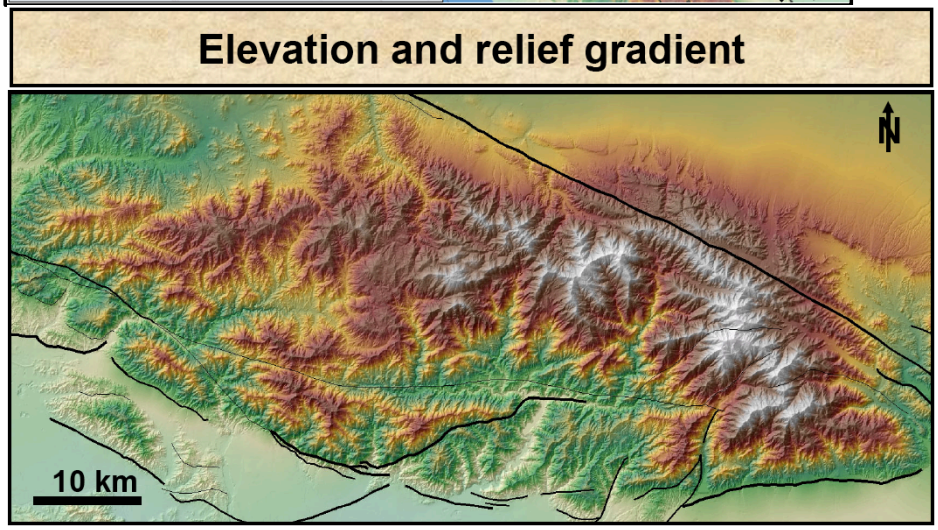


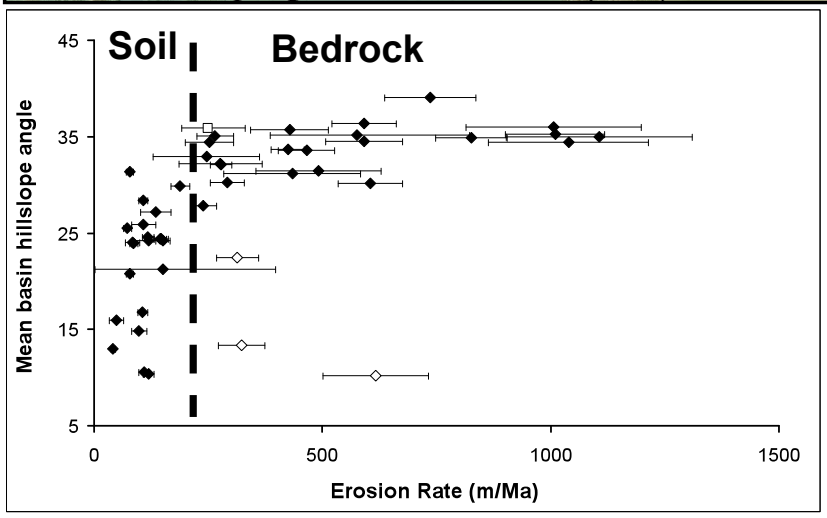


Max. Soil Pro Rate: ~ 200 m/Ma

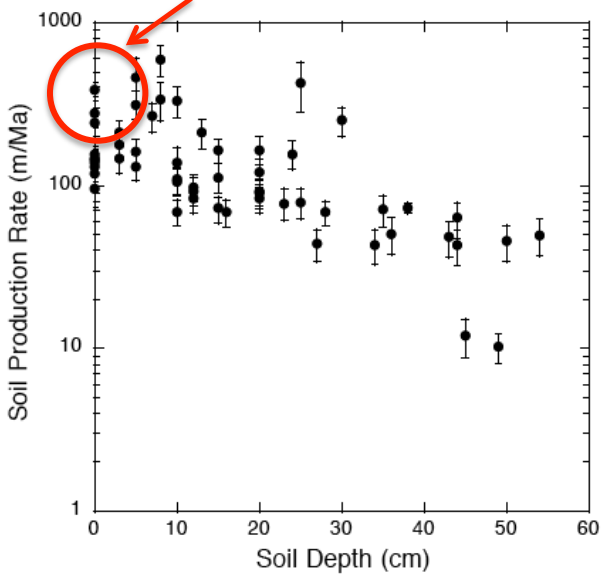


*"…the rapid removal of the products of weathering stimulates its action … If however the power of transportation is so great as to remove completely the products of weathering, the work of disintegration is thereby checked; for the soil which weathering tends to accumulate is a reservoir to catch rain …"*

# Climate-driven processes of hillslope weathering

Jean L. Dixon[1]*, Arjun M. Heimsath[1]*, James Kaste[2]*, and Ronald Amundson[3]*
[1]School of Earth and Space Exploration, Arizona State University, 548 Physical Sciences F-wing, Tempe, Arizona 85287, USA
[2]Department of Geology, College of William and Mary, 217 McGlothlin-Street Hall, Williamsburg, Virginia 23187, USA
[3]Department of Environmental Science, Policy and Management, University of California–Berkeley, 137 Mulford Hall, Berkeley, California 94720, USA

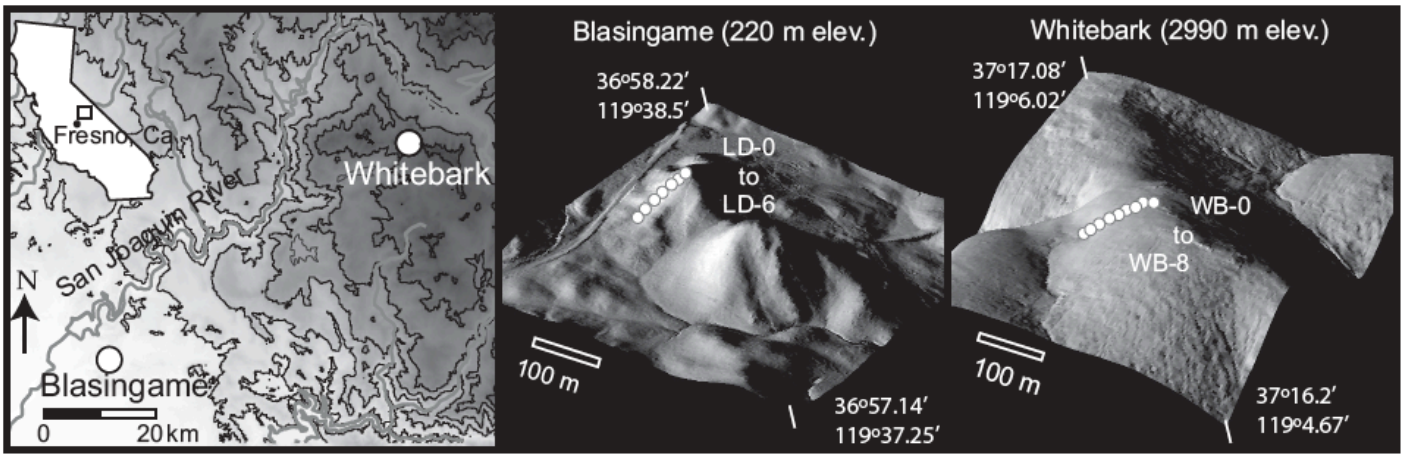


**Figure 1. Location of field area showing low-elevation grassland site, Blasingame, and high-elevation subalpine site, Whitebark. Light ranging and detection data (provided by National Center for Airborne Laser Mapping) were used to derive slope and curvature and produce shaded relief images.**

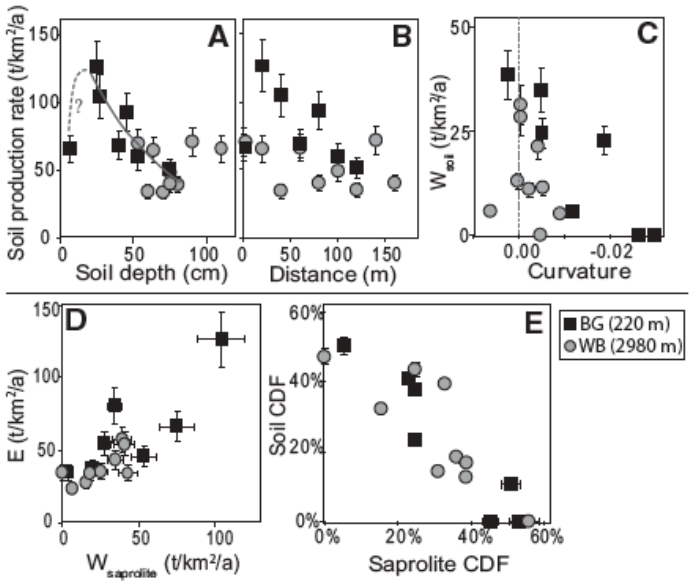


**Figure 2. Average $^{10}$Be-derived soil production rates ($P_{soil}$) are higher at Blasingame (BG) than Whitebark (WB) (one-tailed *t*-test, $t = 7.28$, $p = 0.02$). A: At BG, these rates decrease with soil thickness ($P_{soil} = 77e^{-0.017h}$, $r^2 = 0.81$). B: At BG, these rates decrease with distance from crest ($r^2 = 0.81$, $p < 0.01$). Hill crest alone deviates from these trends, suggesting either exponential soil production function with hill crest held up by slower eroding feature such as emergent tor, or humped production function, whereby production rates peak at some finite soil thickness. C: Soil chemical weathering rates ($W_{soil}$) decrease with increasing convexity (negative curvature) at BG ($r^2 = 0.75$, $p = 0.05$), and insignificantly at WB ($r^2 = 0.31$, $p = 0.19$). D: Physical erosion rates increase with chemical weathering rate of saprolite ($W_{saprolite}$) at both sites (all data: $r^2 = 0.68$, $p = 0.02$; BG: $r^2 = 0.48$, $p = 0.04$; WB: $r^2 = 0.69$, $p < 0.01$). Average rates of erosion are faster at warmer and drier BG (one-tailed *t*-test, $p = 0.04$), compared to colder and wetter WB, although saprolite weathering rates are not significantly different ($p = 0.13$). E: Soil and saprolite weathering extents, shown by chemical depletion fractions (CDF), are negatively correlated (all data: $r^2 = 0.78$, $p < 0.01$; BG: $r^2 = 0.87$, $p < 0.01$; WB: $r^2 = 0.69$, $p < 0.01$).**

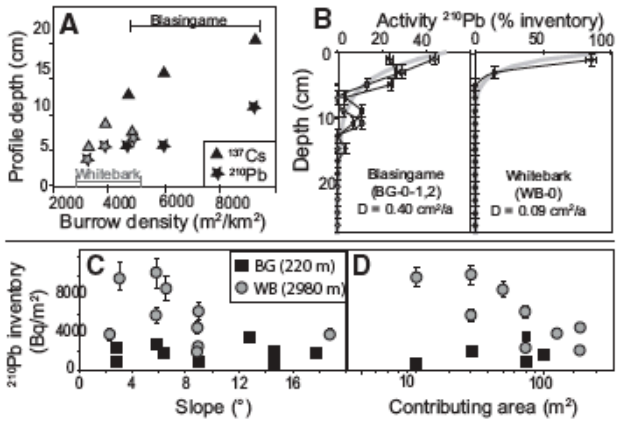


**Figure 3. A: Surface burrowing activities from three transects at Blasingame (BG) and Whitebark (WB) increase with associated profile depths for fallout nuclide $^{210}Pb_{excess}$ ($r^2 = 0.95$, $p < 0.01$) and $^{137}Cs$ ($r^2 = 0.85$, $p < 0.01$). Profile depth is defined as soil depth at 95% cumulative nuclide inventory. B: Fallout profiles show nuclide activity versus depth for hill crests at BG (two profiles shown are 2 m apart) and WB (one profile) and are deeper at BG. We calculated diffusion-like mixing coefficients (*D*) for each profile (shown by broad gray line) by best fit to the diffusion equation: $a(z) = a_0 * \exp\left[\frac{V - \sqrt{V^2 + 4\lambda D}}{2D}(z)\right]$, where $a(z)$ and $a_0$ are nuclide activity at depth ($z$) and surface, respectively, and $\lambda$ is nuclide decay. Here, we assume that advection velocity ($V$) is zero. Diffusive mixing coefficients of hill crests are shown, and average hillslope values at each site are 0.28 ± 0.05 cm²/a at BG and 0.15 ± 0.02 cm²/a at WB. Also shown are inventories of $^{210}Pb_{excess}$ and $^{137}Cs$ for downslope soils at low-elevation BG site (gray squares) and high-elevation WB site (black circles). Inventory data points reflect those calculated from individual soil profiles, and activities of additional bulk soil samples gathered downslope. C: Nuclide inventories at high elevation are lower at high slopes; however, no statistically significant correlation exists. D: At BG, inventories do not change markedly, while at WB, nuclide inventories decrease with distances downslope and increasing contributing area ($r^2 = 0.63$, $p = 0.01$). Symbols contain error if not otherwise labeled. Nuclide activities were measured using gamma-ray spectrometry on a broad energy germanium detector at Dartmouth College (Hanover, New Hampshire). Downslope profiles of $^{210}Pb_{excess}$ for each pit, including modeled mixing coefficients, are provided in Data Repository (see footnote 1).**

# The critical role of climate and saprolite weathering in landscape evolution

**Jean L. Dixon,[1]* Arjun M. Heimsath[1] and Ronald Amundson[2]**
[1] School of Earth and Space Exploration, Arizona State University, Tempe, AZ, USA
[2] Department of Environmental Science, Policy and Management, University of California, Berkeley, CA, USA

Received 26 June 2008; Revised 13 April 2009; Accepted 21 April 2009

* Correspondence to: Jean L. Dixon, PSF 686, P.O. Box 871404, Tempe, AZ 85287-1404, USA. E-mail: jean.dixon@asu.edu

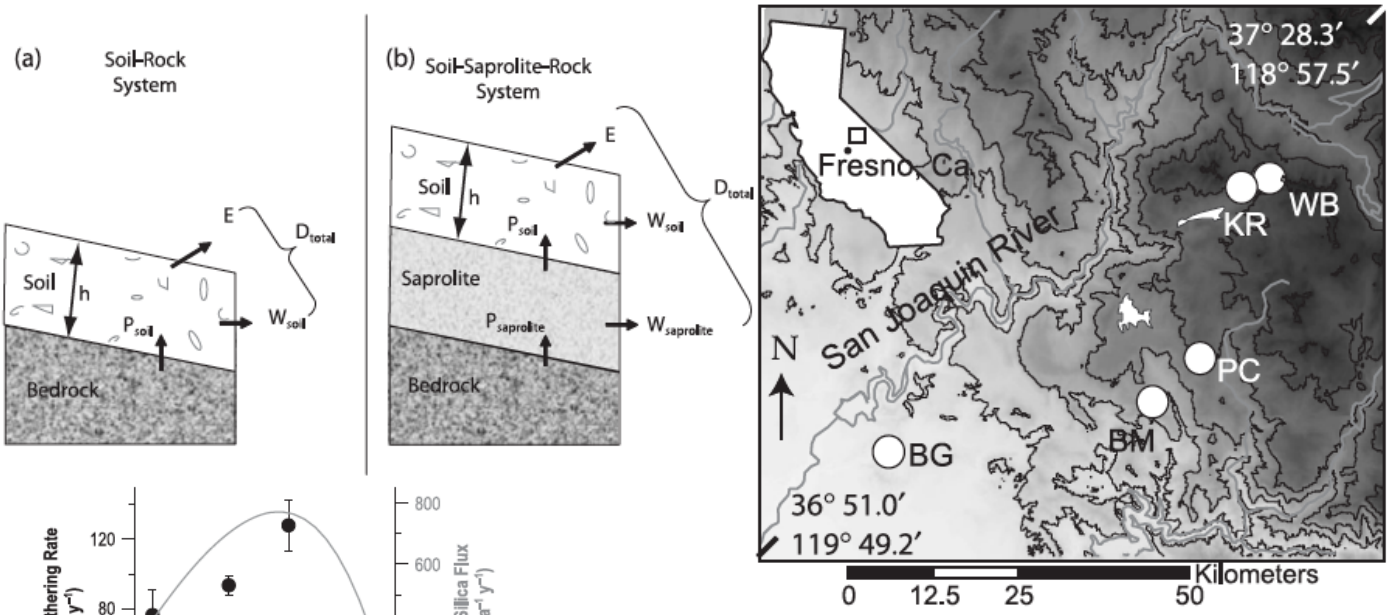


**Figure 2.** Study sites follow an elevation transect up the western front of the Sierra Nevada (200–3000 m elevations). The low elevation site BG is located approximately 40 km northwest from Fresno, California. Sites fall within the San Joaquin and Kings River Drainages, and occupy distinct climate zones. Regional topography is shown by 500 m shaded elevation contours.

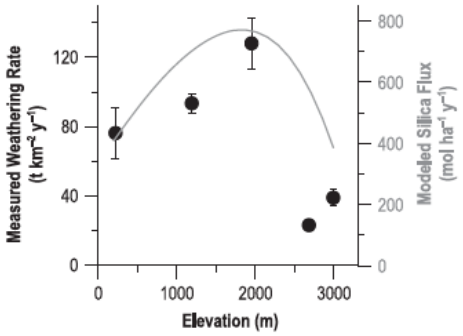


**Figure 7.** Modeling the coupled effects of temperature and precipitation on weathering. Silica fluxes (line) were modeled from Equation 1 using values of $E_a$ and $a_i$ parameterized by field data from White and Blum (1995) ($E_a$ = 59·4 kJ mol$^{-1}$, $a_i$ = 0·456, $T_0$ = 5 °C). Measured average rates of chemical weathering (circles) follow similar patterns as modeled fluxes along the climate gradient. Error bars represent the standard error about the mean for total chemical weathering rates at each climate zone.

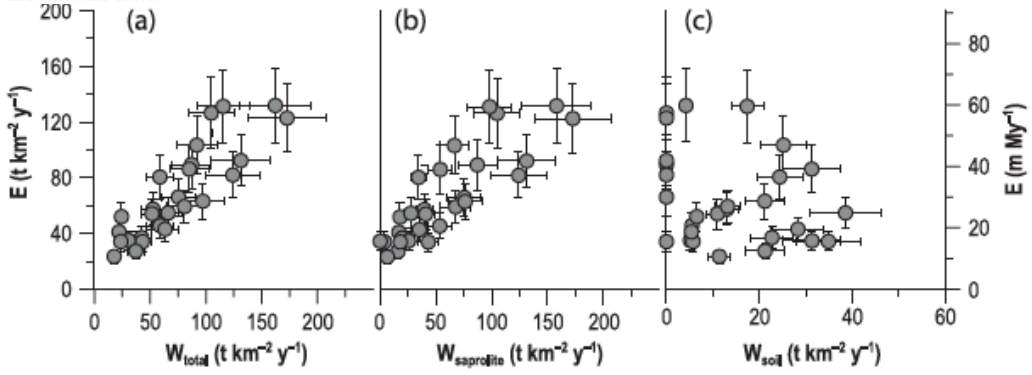


**Figure 3.** Physical erosion rates increase with total weathering (a) and saprolite weathering (b) rates, however links with soil weathering (c) are not as clear. Linear regressions suggest strong links between erosion rates and both total and saprolite weathering rates ($r^2$ = 0·69 and 0·65 respectively).

*"Mountain forms in general depend more on the law of divides than on the law of structure, but their independence of structure is rarely perfect, and it is difficult to discriminate the results of the two principles. For the investigation of the workings of the law of divides it is better to select examples from regions which afford no variety of rock texture and are hence unaffected in their erosion by the law of structure. Such examples are found in bad-lands."*

## Stop 4: Badlands as natural laboratories

1. Arid—lack vegetation
2. Weak—loosely consolidated sedimentary rock
3. Homogenous—uniform substrate
4. Steep—recently exposed to erosion

*If channels drive landscape lowering, why do we see convex hilltops everywhere?*

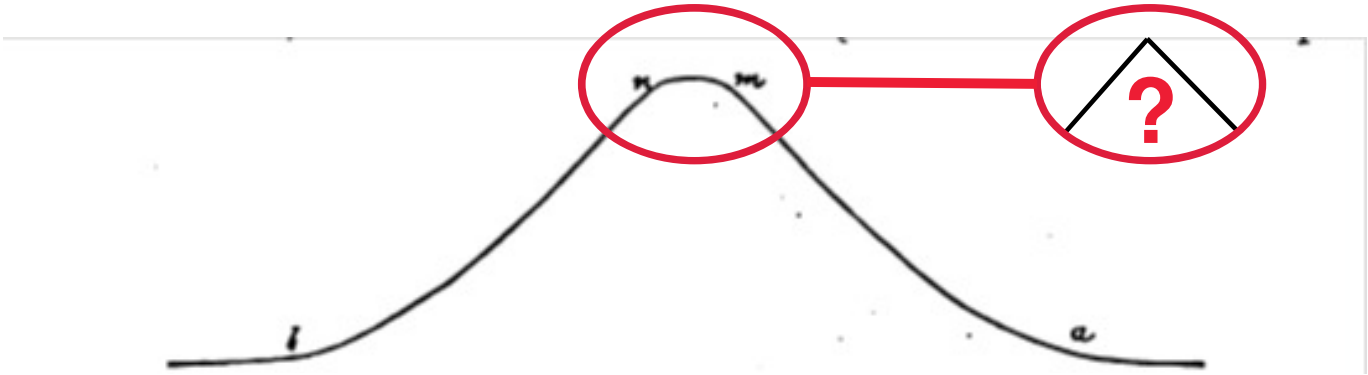


**Fig 60:** Cross-profile of a Bad-Land Divide *(adapted from Gilbert, 1892)*

*Drainage density as a metric to interpret the balance between mass-wasting and fluvial transport processes:*

*photo by Steve DeLong*

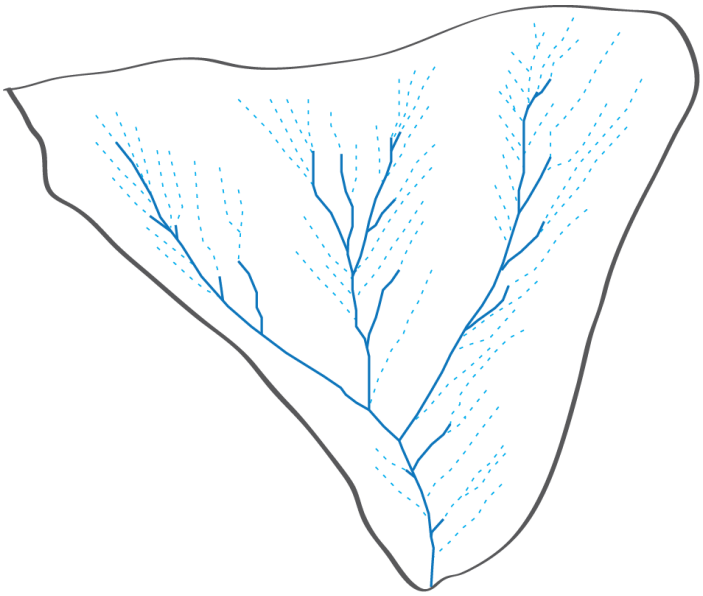

$$\textbf{Drainage Density} = \frac{\textbf{Total length of channels}}{\textbf{Drainage area}}$$

# Stop 4: Badland modeling and observations *(Howard, 1997)*

**Fig 1: Badlands in Mancos Shale (North Caineville Mesa):** *Asterisks mark early Wisconsin pediment surface.*

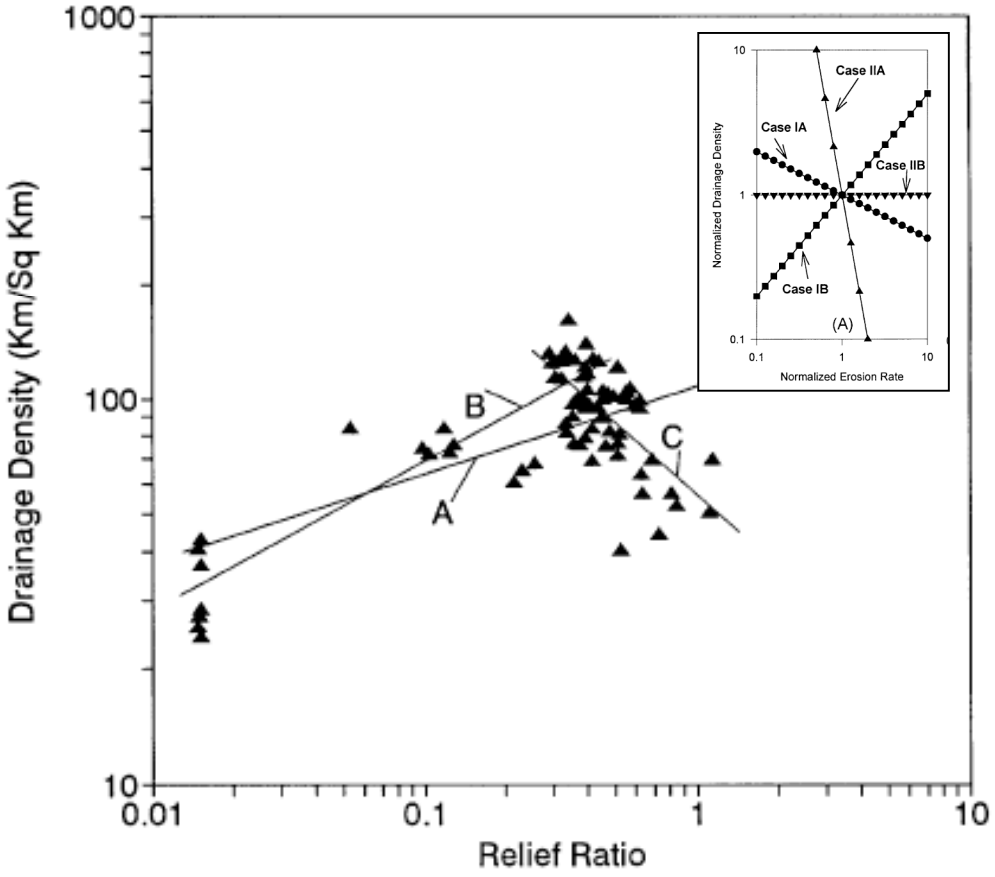


**Main—Fig 6: Observed dependence of drainage density on relief** *Measured from aerial photographs (~1:12000). Ephemeral rills not included in the calculation.*

**Inset—Fig 3A: Modeled dependence of drainage density on erosion**
*Four scenarios modeled: Case I uses a linear diffusion model and Case II uses a threshold hillslope model for hillslope transport. "A" indicates that no threshold for fluvial erosion is imposed and "B" indicates that a threshold is used. Drainage density is determined by evaluating where the hillslope delivery of sediment is balanced by fluvial export of sediment.*

## *Two process regimes:*

**Observations:** In low relief areas, drainage density increases with higher relief.
**Interpretation:** The threshold for fluvial erosion controls channel heads . So, as relief increases , the critical drainage area goes down (Case IB).

**Observations:** In high relief areas, drainage density decreases with higher relief.
**Interpretation:** As threshold slopes are approached, hillslopes get more efficient and channels increase their critical drainage area to keep up (Case IIA).

# Stop 4: Pediments *(Cook et al., 2009)*

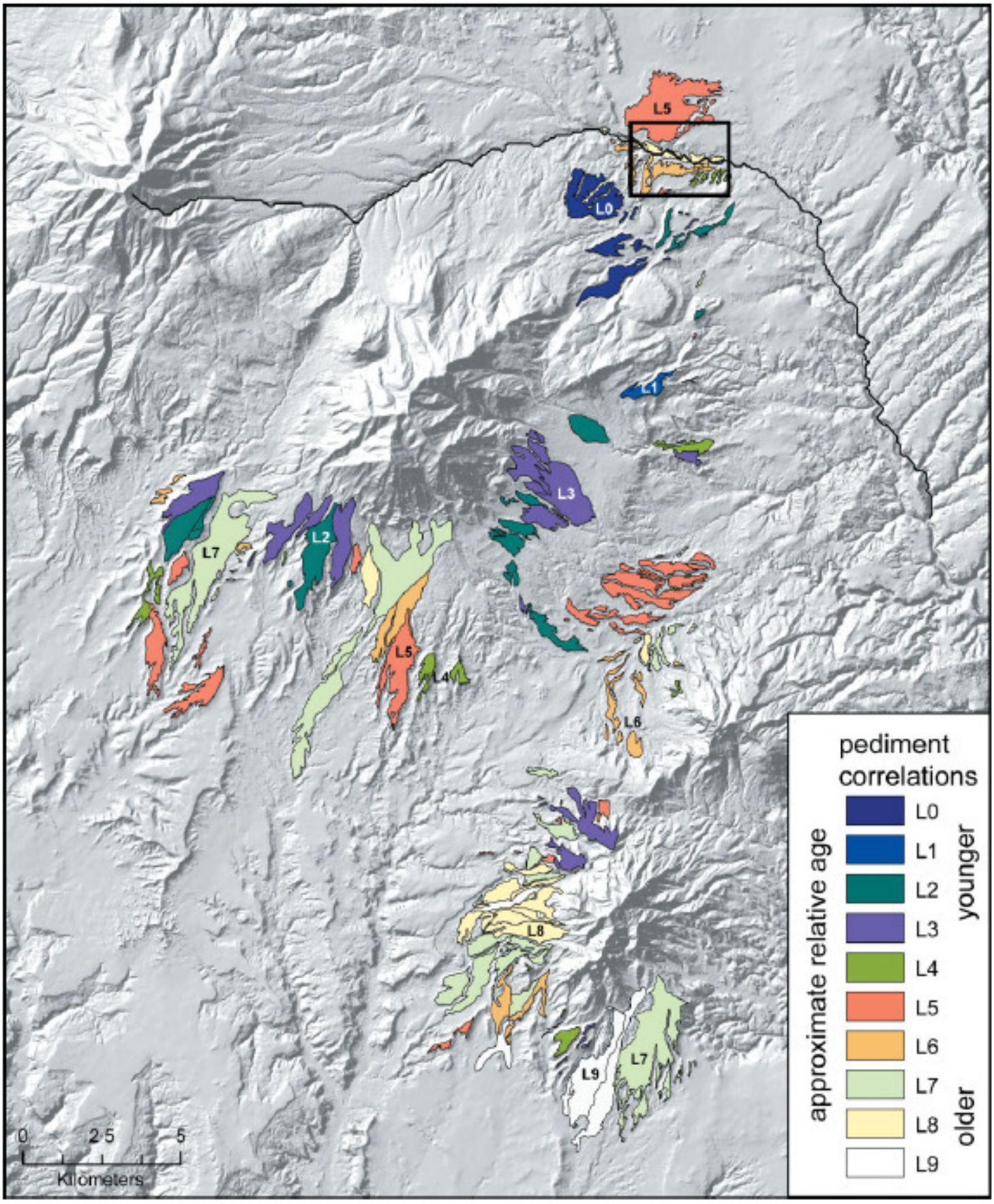


**Fig 6: Relative ages of pediment surfaces** *The distribution and inferred relative ages are based on aerial photographs and field observation.*

# Day 2: Sediment supply controls on river incision and canyon formation

## Overview of stops:

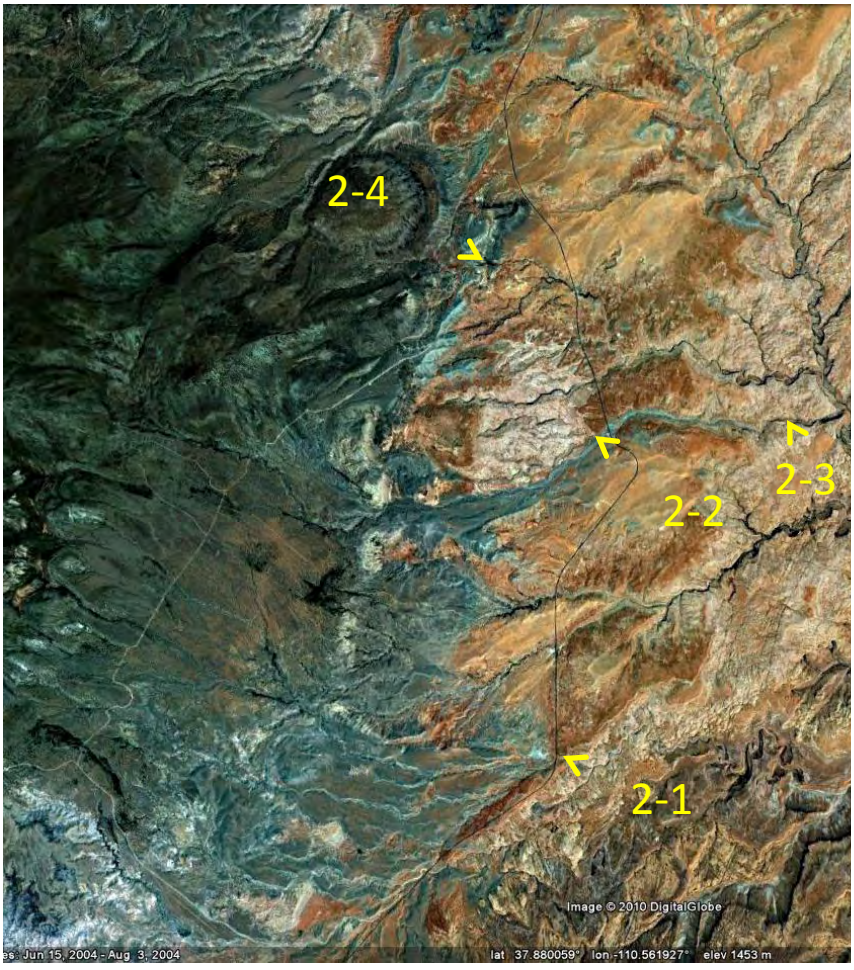


2 km

Schedule, Saturday Oct. 16 2010

2-1: Swett Creek
8:00-9:30 AM

2-2: Trail Canyon and tributaries, and slot canyon, just upstream of highway.
9:45-11:30 AM

2-3: Epigenetic Gorges, downstream Trail Canyon
NOTE: we will be away from the vehicles for several hours. BRING WATER and LUNCH!
11:30-12:45 Hike downstream
12:45-1:30 Lunch
1:30-2:30 Hike back to cars

2-4: Bedrock incision across a laccolith
2:45 until you stop exploring


## Parking and logistics, Saturday Oct. 16 2010

Stop 2-1: Swett Creek
8:00-9:30 AM

- Between Hwy 276 milemarkers 13 (to the north) and 14.
- Park in small pull-off area or on shoulder where hwy crosses filled-in canyon.
- Discussion will take place down in canyon, but right here where road crosses canyon.


2-2 and 2-3: Trail Canyon, just upstream of highway.
9:45-11:30 for stop 2-2;
11:30-2:30 for stop 2-3.

- A little north of Hwy 276 milemarker 10.
- Parking area just south of channel.
- We will first walk upstream a little ways and see several channels including a slot canyon (2-2). Bring water.
- After returning to the cars to grab sack lunches, we will then hike downstream ~ 2 miles. Bring water and lunch.

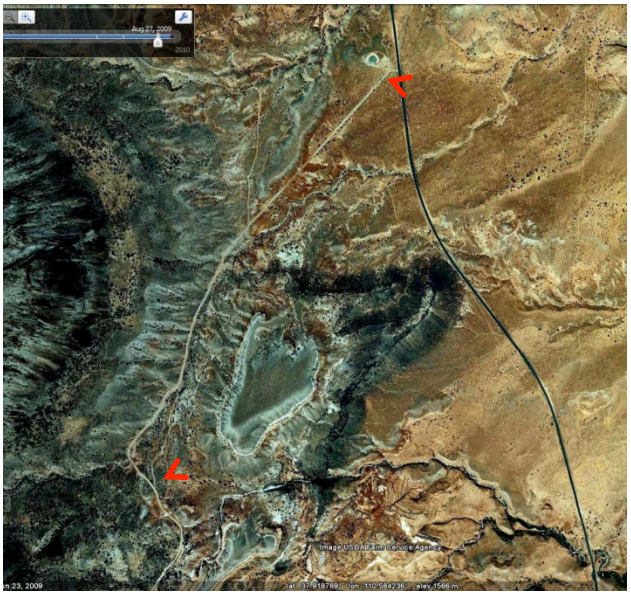

2-4: Bedrock incision across a laccolith
2:45 until you stop exploring

- Take dirt road right next to milemarker 7.
- Drive ~1.5 miles up road; we will have signs/people to indicate where to park.
- Low clearance vehicle people may want to ride with high clearance vehicle people—we will let you know the current road conditions.

## Key reason this landscape is useful for evaluating sediment controls on channel incision:

Systematic differences in coarse diorite sediment supply between channels, based on spatial distribution of diorite intrusions and mountains, pediment deposits, in relation to a given watershed. More on this at stop 2-2.

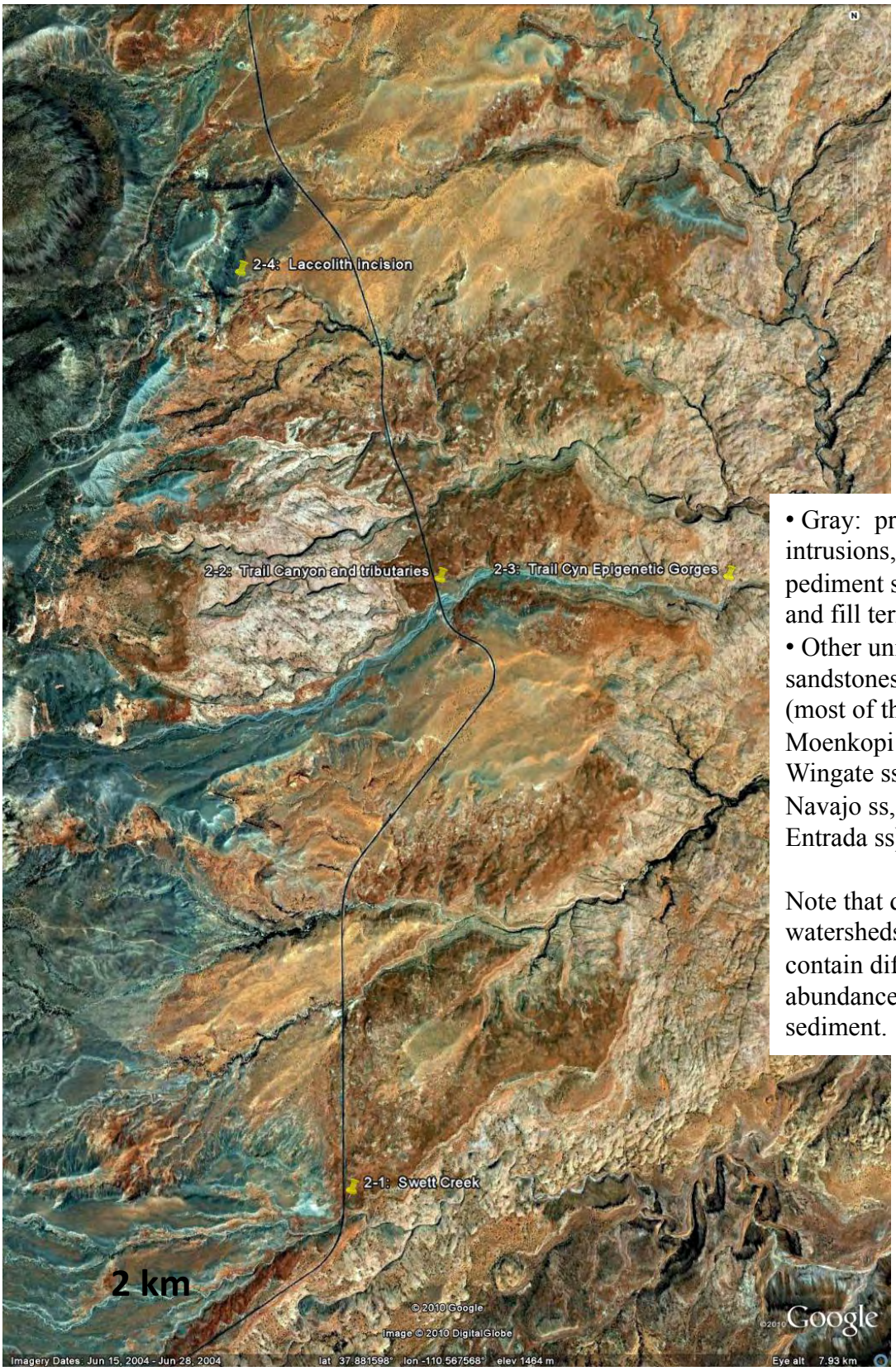


- Gray: primarily diorite intrusions, eroding pediment surface deposits, and fill terraces.
- Other units: weaker sandstones and mudstones (most of this image: Moenkopi and Chinle fm, Wingate ss, Kayenta fm, Navajo ss, Carmel fm, Entrada ss).

Note that different watersheds and channels contain different abundances of gray diorite sediment.

Johnson, Whipple, Sklar and Hanks initially started working in the Henry Mountains to do a field test of the Sklar and Dietrich (2004) *saltation-abrasion model* of bedload transport-dependent bedrock channel incision.

Saltation-abrasion model, inspired by Gilbert's work in the Henry Mountains:

• Tools effect: too little sediment reduces incision rate by limiting the rate of particle impacts

• Cover effect: too much sediment reduces incision rate because alluvium partially mantles the bed, protecting it from particle impacts

Sklar and Dietrich (2004), A mechanistic model for river incision into bedrock by saltating bedload, *Water Resources Research.*

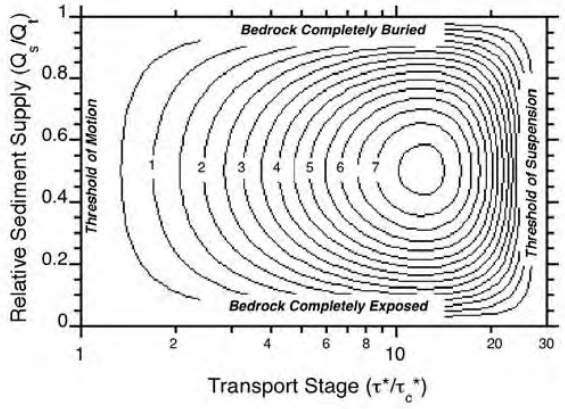


**Figure 16.** Nondimensional erosion rate ($E^*$) $\times$ $10^{-15}$ (contours, axis out of view) as a function of transport stage and relative sediment supply. In this nondimensional framework the saltation-abrasion model collapses to a unique surface for all physically reasonable combinations of discharge, channel slope, width, roughness, rock tensile strength, and coarse sediment grain size ($D_s$ > 0.002 m). Erosion rate goes to zero as each of the four end-member conditions are approached: the thresholds of motion and suspension and a fully alluvial or pure bedrock bed.

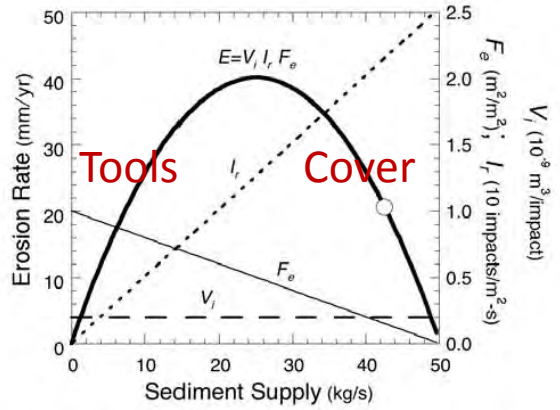


**Figure 10.** Erosion rate as a function of sediment supply predicted by saltation-abrasion model (equation (24a)). Also plotted are the model component terms: volume eroded per unit impact ($V_i$), impact rate per unit area ($I_r$), and the fraction of the bedrock bed exposed ($F_e$). Table 3 lists the values of input variables held constant. The open circle denotes the predicted instantaneous erosion rate at the South Fork Eel reference site.

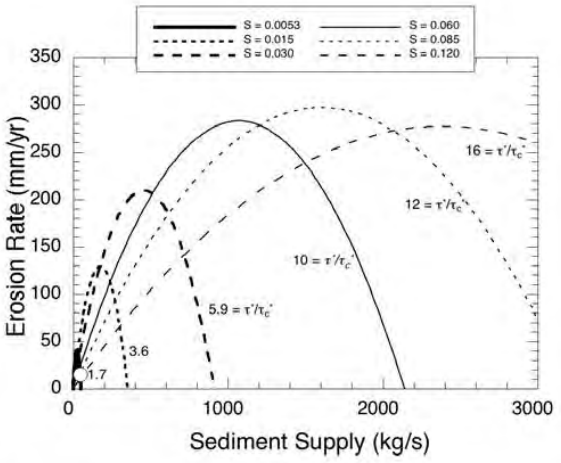


**Figure 11.** Erosion rate as a function of sediment supply for various channel slopes, with corresponding transport stage noted. Thick solid line corresponds to "reference site" conditions (Table 3) and curve of Figure 10.

# Day 2 Stop 1: Bedrock erosion and hydrograph monitoring, Swett Creek

Key topics at this site:
- Hydrograph control on incision and bedload transport rate.
- Rapid maximum bedrock incision rate (~0.5 m in 3 weeks)
- Feedbacks between transport, incision and morphology that lead to inner channel formation; comparison to flume experiments.

Most data and plots in this section are from the following paper:

## Contrasting bedrock incision rates from snowmelt and flash floods in the Henry Mountains, Utah

**Joel P.L. Johnson[1,†], Kelin X. Whipple[2], and Leonard S. Sklar[3]**
[1]*The University of Texas at Austin, Department of Geological Sciences, 1 University Station C9000, Austin, Texas 78712, USA*
[2]*School of Earth and Space Exploration, PSF-686, Arizona State University, P.O. Box 871404, Tempe, Arizona 85287-1404, USA*
[3]*Department of Geosciences, 622 Thorton Hall, San Francisco State University, 1600 Holloway Avenue, San Francisco, California 94132, USA*

*GSA Bulletin*; September/October 2010; v. 122; no. 9/10; p. 1600–1615; doi: 10.1130/B30126.1;

ABSTRACT

Hydrograph variability and channel morphology influence rates of fluvial bedrock incision , but little data exist on these controls in natural channels. **Through field monitoring we demonstrate that (1) short-term bedrock channel incision can be rapid, (2) sustained floods with smaller peak discharges can be more erosive than fl ash floods with higher peak discharges, due to changes in bed alluviation, and (3) bedrock channel morphology varies with local bed slope and controls the spatial distribution of erosion.** We present a three-year record of flow depths and bedrock erosion for a human-perturbed channel reach that drains the Henry Mountains of Utah, USA. Starting from a small and steep (~30% slope), engineered knickpoint in Navajo sandstone, erosion has cut a narrow, deep, and tortuous inner channel in ~35–40 years. Along the inner channel, we measured up to 1/2 m of vertical incision into Navajo sandstone over ~23 days, caused by the 2005 season of exceptional snowmelt flow. In contrast, flash floods caused little bedrock incision even when peak discharges were much higher than the peak snowmelt flow. Flash floods were net depositors of coarse sediment while snowmelt flow cleared alluvial cover. We document the formation of a pothole and interpret that it was abraded by bedload rather than fi ne suspended sediment. Finally, several slot canyons (Peek-a-boo, Spooky, and Coyote Gulch narrows) in the nearby Escalante River drainage basin have erosional morphologies similar to the monitored channel reach. Feedbacks between flow, sediment transport, and transient erosion provide a plausible explanation for the evolution of channel slope, width, and bed roughness of these natural bedrock channels.

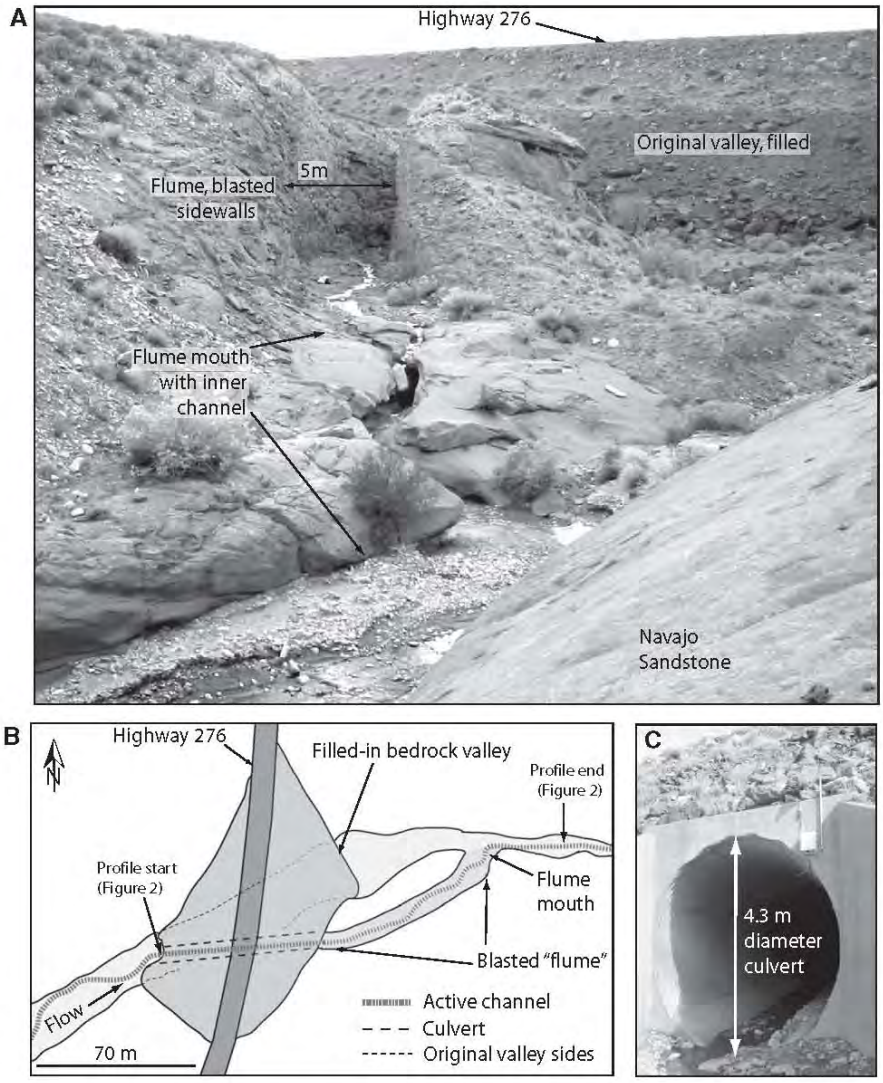


**Figure 1. (A) Photograph looking upstream (east) at the study site. We refer to the blasted slot as the "flume" (because of its similarity to laboratory flumes with rectangular cross sections) and the steep downstream bedrock surface with an incised inner channel as the "flume mouth." Clasts evident in the downstream natural channel (foreground) are primarily composed of diorite. (B) Sketch map view from above, showing the old valley filled in with rubble in order to construct the highway and the culvert and blasted slot through which the channel was diverted. Location is latitude 37.842N, longitude –110.578W. (C) Upstream end of the culvert. The bottom has a curved but smooth concrete lining. Note the solar panel and data logger mounted on the culvert face.**

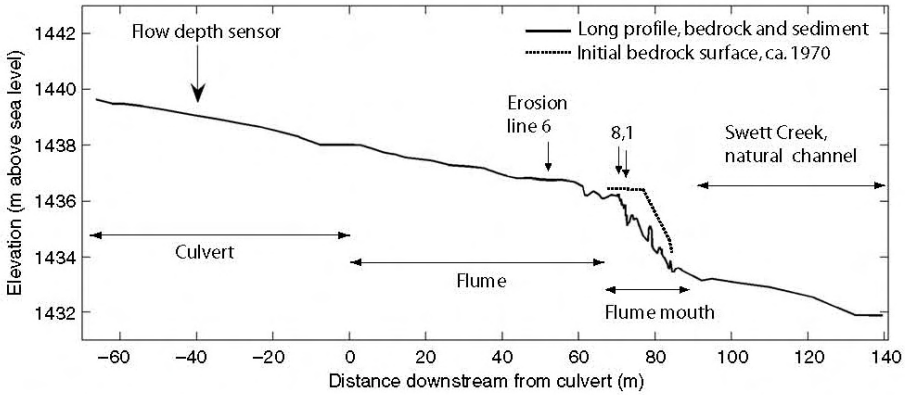


**Figure 2. Longitudinal channel profile for the section of Swett Creek diverted through the culvert, blasted flume, and over the steep and eroding flume mouth before returning to the original channel. The location in the culvert of the sonic flow-depth sensor is indicated, as well as the locations of surveyed topographic cross sections where erosion was measured.**

# Comparing snowmelt and flash flood hydrographs

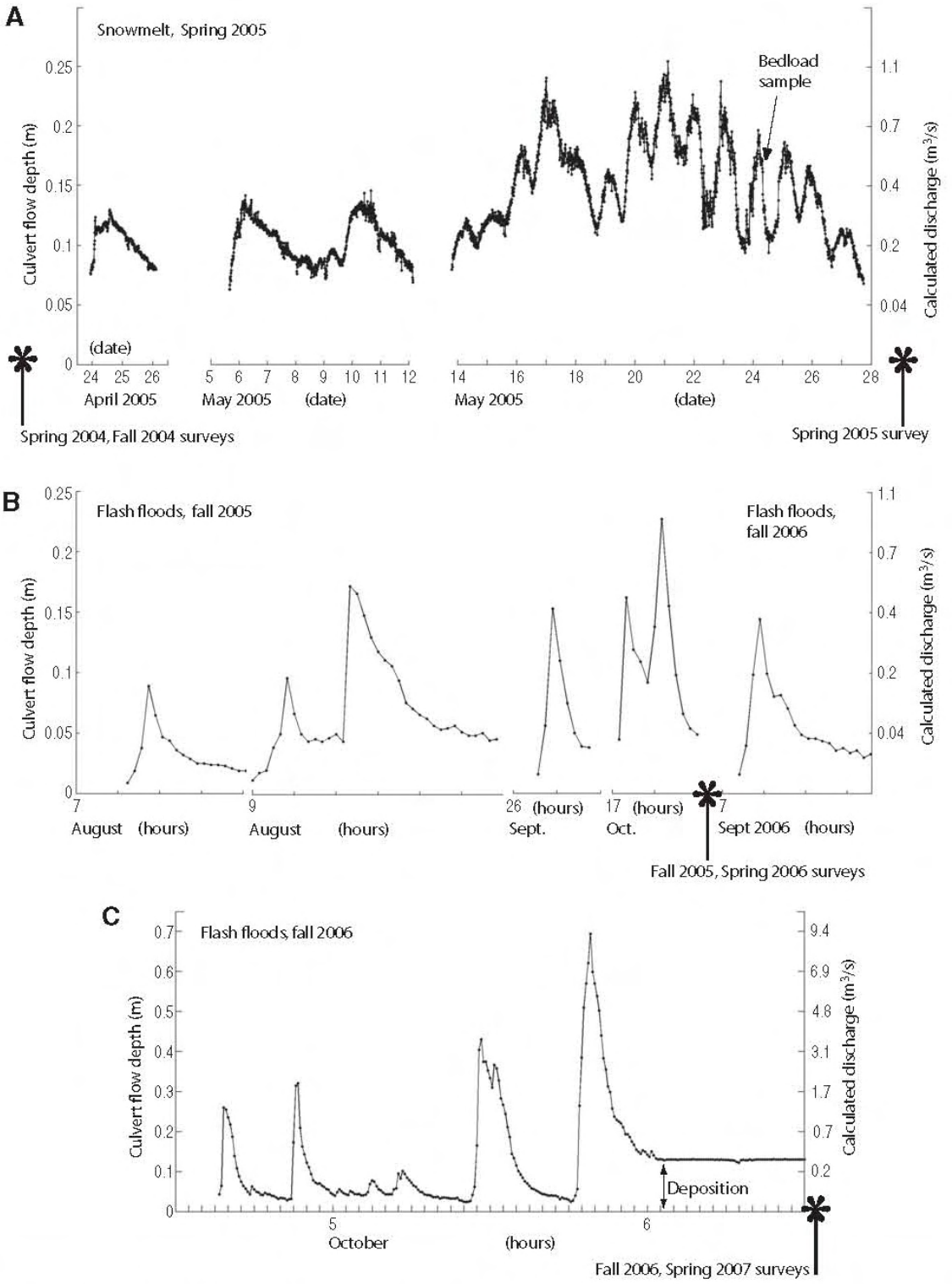


**Figure 3. Flow-depth and discharge hydrographs showing all of the flow events observed in this study. Data have not been smoothed, although some spikes were removed from the snowmelt record (A). Tick marks on the abscissa represent days (of the month) for the plots of spring 2005 snowmelt (A). Tick marks on the flash-flood plots represent hours (B and C). Note the different vertical scale of the fall 2006 flash floods (C). Each individual data point represents 10 min in all plots. The timing of our topographic surveys relative to the flow record is indicated.**

Alluvial cover along the inner channel decreased due to snowmelt runoff; increased due to flash floods. Why? Higher sediment concentrations in rising limbs of flash floods?

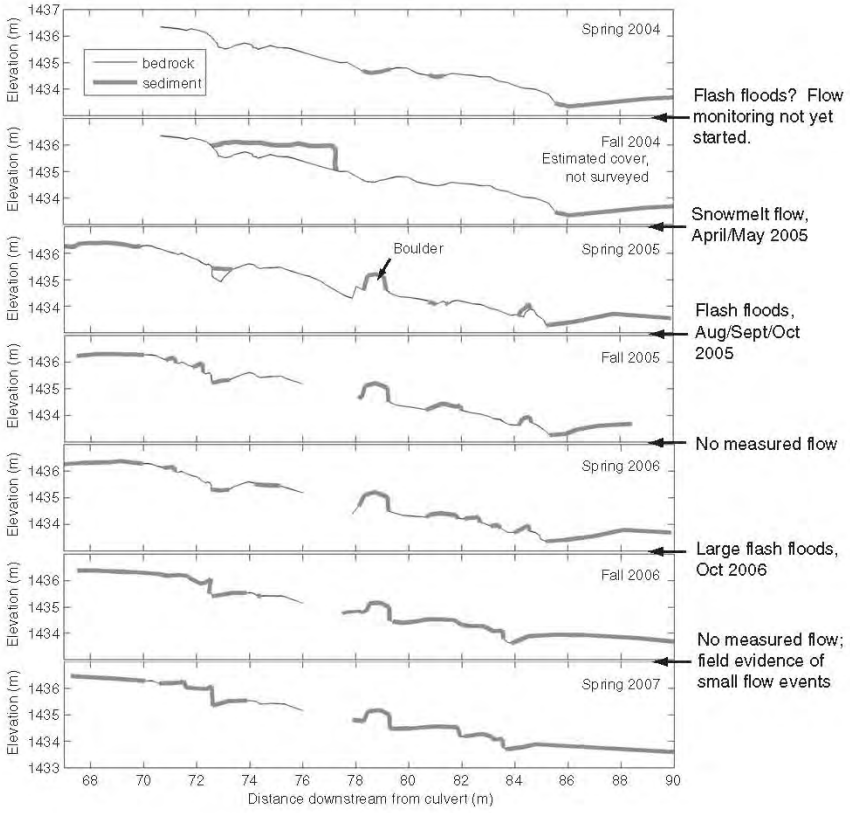


**Figure 5. Sediment deposition along the inner channel. The fall 2004 alluvial cover is estimated based on photographs and field notes, using the spring 2004 surveyed bedrock profile. Sediment deposition in the rest of the time steps was directly surveyed. Figure 3 shows when the surveys were done relative to the flow record. No flow was measured between fall 2005 and spring 2006; the differences in sediment cover between these time steps are relatively small, and either represent uncertainty in survey repeatability or that flow lower than what we can reliably measure occurred and modestly rearranged sediment in the channel. Between fall 2006 and spring 2007 low flow did occur (based on qualitative field observations of flow indicators) but was not recorded. The gap at 77 m is an undercut section of channel; bedrock bed elevations were measured in this reach in spring 2005 but not after. See text for transport history of boulder at ~78 m.**

Upstream of steep "flume mouth": Up to ~10 cm vertical bedrock incision from snowmelt flow.

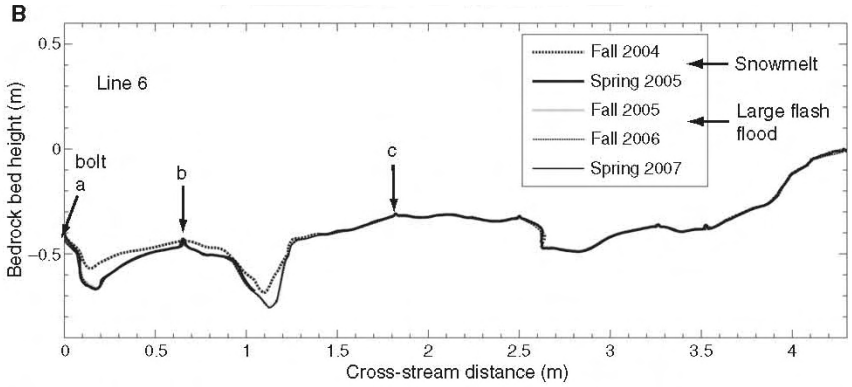


**Figure 7. (A) Photograph looking downstream at erosion line 6, located ~20 m upstream of the flume mouth (Fig. 2). Bolts a, b, and c are labeled. Photo taken in fall 2005; note the sediment filling both longitudinal grooves. (B) Line 6 repeat surveys, showing up to 100 mm of bedrock incision from spring 2005 snowmelt flow and negligible incision due to later flash floods. Surveyed lines are plotted in sequential order, and therefore later time steps cover the earlier ones. No bolts were lost due to bedrock erosion along this line; the initial bolt spacing was wider than the ~250 mm given in the methods section due to a limited supply of bolts at the time of installation.**

Erosion along inner channel from snowmelt flow, longitudinal profile

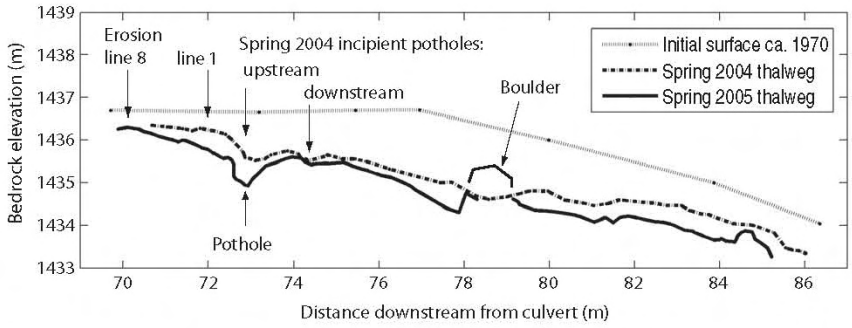


**Figure 8. Flume-mouth, inner-channel bedrock longitudinal profile, showing extensive bedrock erosion along its length due to spring 2005 snowmelt flow. An approximate initial bedrock surface prior to incision (ca. 1970) was reconstructed from surveys of the bedrock on either side of the inner channel. See text for transport history of boulder at ~78 m.**

Erosion along inner channel cross-section: nearly ½ m of bedrock incision from 3 weeks of snowmelt flow and sediment transport.

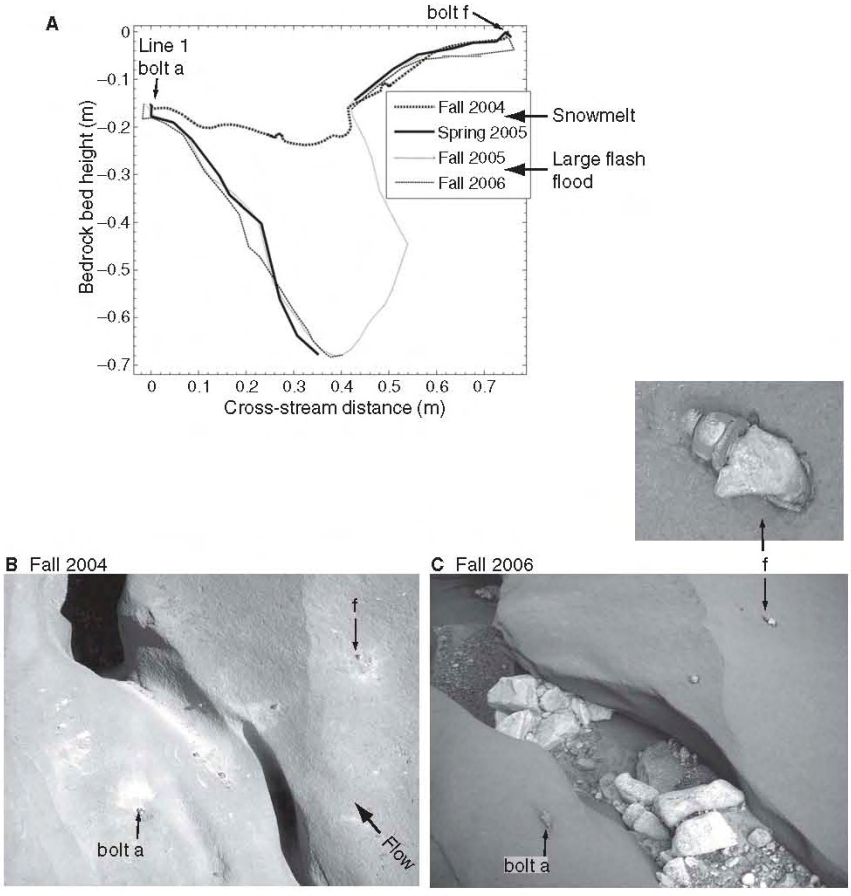


**Figure 9. Erosion line 1 (location in Fig. 8). (A) Repeat surveys of the topography between bolts. The fall 2005 survey was conducted with the total station in "reflectorless" mode from multiple viewpoints to accurately capture the undercut. No vertical exaggeration. (B and C) Photographs looking down from above on bolts in fall 2004 (immediately following installation) and in fall 2006. Distance between bolts a and f is ~750 mm. Bolt f was bent by sediment impacts during the fall 2006 flash floods. Flow toward upper left.**

# Pothole incision and morphology, along inner channel

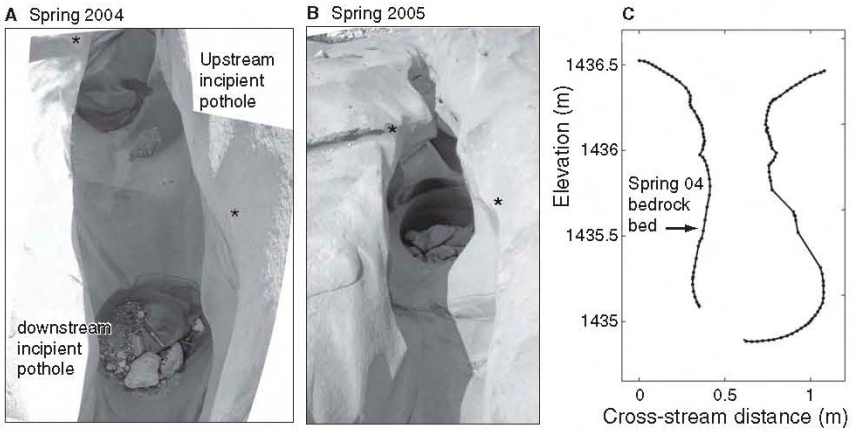


**Figure 11. Potholes. (A and B) Photographic comparison of the development of a pothole (spring 2004–2005). In spring 2004 two incipient potholes were present, but following spring 2005 snowmelt runoff, the downstream incipient pothole had eroded away while the upstream incipient form deepened ~500 mm to form a well-defined single pothole. Note somewhat different photograph scales and orientations. Asterisks mark matching locations in the two photographs. The spring 2004 image is a mosaic of two photographs. (C) Fall 2005 survey of the pothole cross section, measured with a total station in "reflectorless" mode, combining surveys from multiple locations to accurately capture undercuts. As discussed in the text, this detailed survey was completed in fall 2005, but the erosion that created the pothole resulted from spring 2005 snowmelt runoff.**

# Comparison to laboratory experiment morphology and erosion rate:

We have developed the same morphology (tortuous inner channel) in laboratory flume experiments. Our experimental erosion rates and patterns also explore how tools and cover effects are strongly modulated by evolving bed morphology.

Johnson and Whipple (2007), Feedbacks between erosion and sediment transport in experimental bedrock channels, *ESPL*, doi: 10.1002/esp1471

Johnson and Whipple (2010), Evaluating the controls of shear stress, sediment supply, alluvial cover, and channel morphology on experimental bedrock incision rate, J*GR-ES*

Starting from an approximately planer bed (in both sets of experiments), bedload transport becomes focused along interconnected topographic lows, focusing erosion (a positive feedback), and resulting in the incision of a narrow inner channel.

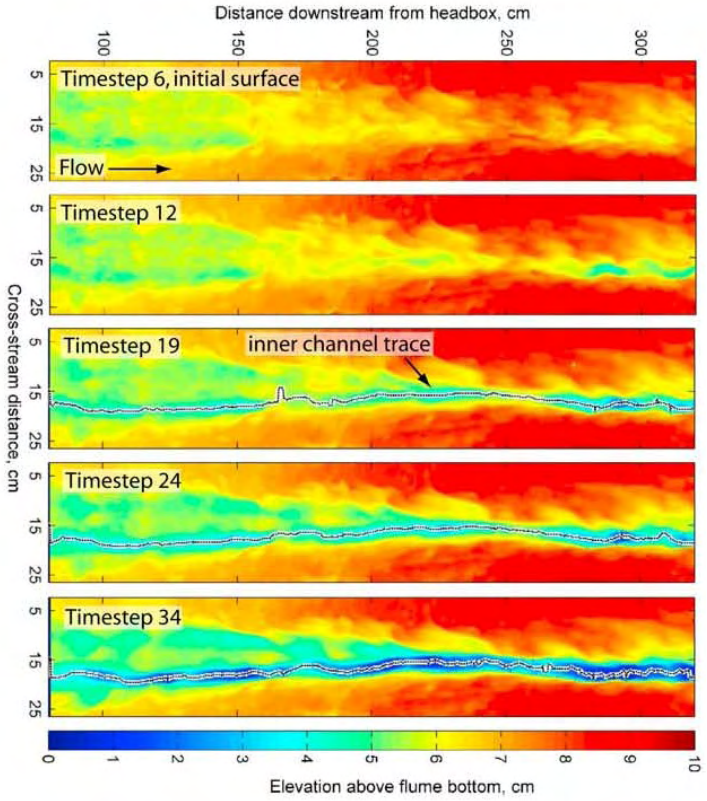


Figure 1. Bed topography in experiment A. The flume is 30 cm wide (starting at zero, x axis) and 4 m long (starting at 0, y axis). The area shown is the central subset of the flume we use for analysis (80–320 cm downstream from head box, 2.4–26.4 cm from the flume sidewall) to minimize possible inlet, outlet, and sidewall effects. Flow direction is indicated. Initially, the planar bed center was intentionally slightly lower than the sloping bed sides at the flume walls to inhibit sediment transport and incision at the sidewalls. Inner channel centerlines are indicated and described in the text.

Johnson and Whipple, JGR 2010

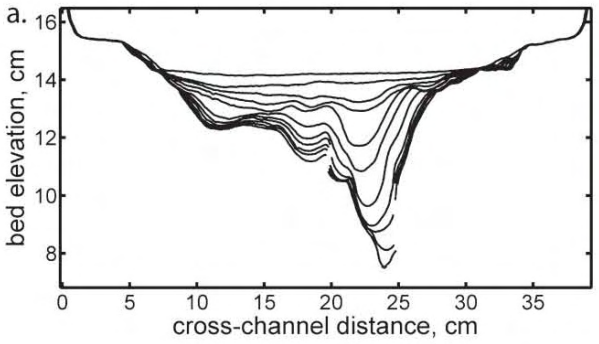


Measurements of sequential erosional topography at 10 per cent slope.

Johnson and Whipple, ESPL 2007

Sediment transport and erosion were focused along the developing inner channel. Initially, a positive feedback developed where more incision deepened the inner channel, catching more sediment and further increasing erosion.

Spatial pattern of sediment concentration : sediment transported through developing inner channel

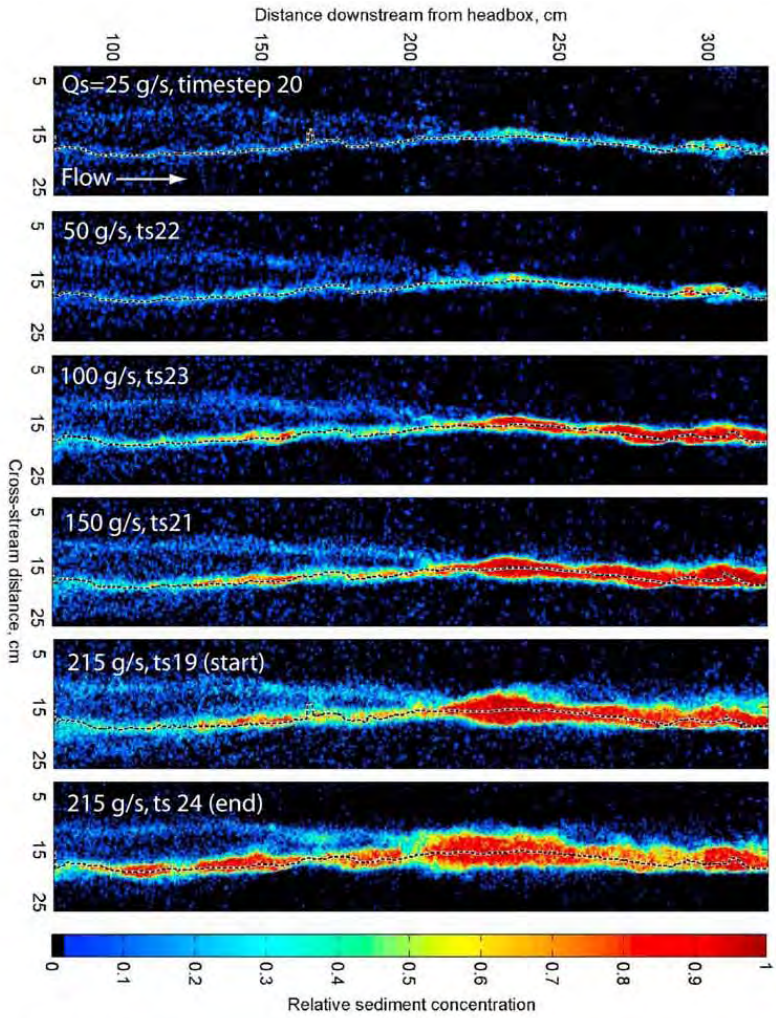


Figure 2. Relative sediment concentration on the flume bed during active transport for a series of time steps (19–24) with variable sediment flux, constant discharge, and 5 mm gravel. Inner channel centerlines are indicated. Time steps are shown in order of increasing sediment flux rather than chronologically. Bedload transport was strongly focused along the topographically low inner channel. These measurements were made using photographs of painted gravel in active transport and image analysis.

Johnson and Whipple, JGR 2010

Topography, erosion and local sediment concentration, shown here as f(Qs)

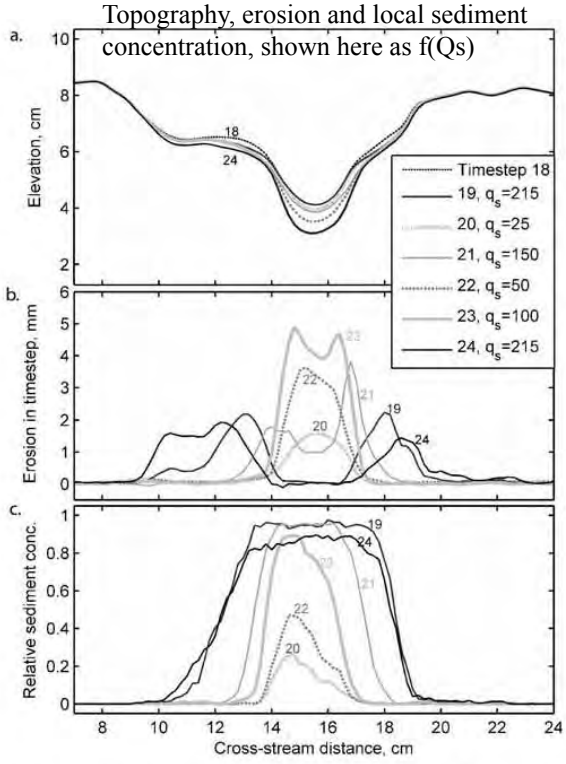


**Figure 4.** Variations in magnitude and location of erosion with changes in sediment flux averaged over a 10 cm long straight section of inner channel from 226 to 236 cm downstream. (a) Cross-section topography in sequential time steps. Lines from later time steps obscure earlier time steps. (b) Erosion in each cross section per time step. At low $Q_s$, erosion is focused in the inner channel. With increasing $Q_s$, inner channel erosion increases but then stops due to deposition, and erosion is focused higher up on the sides and above the inner channel. (c) Relative sediment concentration in each time step, showing how concentration saturates and spreads over a wider area.

Johnson and Whipple, JGR 2010

In both sets of experiments, tools effects (increasing erosion with increasing local sediment flux) and cover effects (decreasing erosion with increasing local sediment flux) were observed, but again, strongly influenced by local channel morphology.

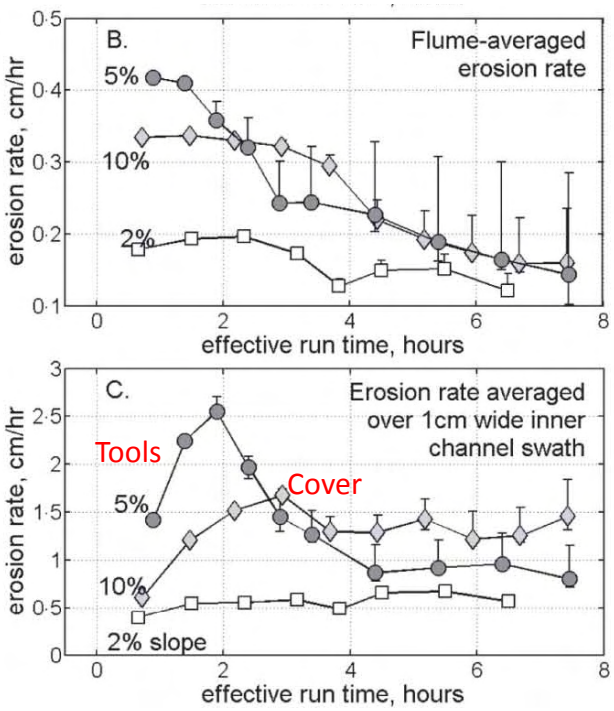


(b) Erosion rates for each timestep averaged over the measured flume area (30 cm wide by 300 cm long). The asymmetric uncertainty is primarily due to the data dropouts in the measured timestep topography, and the error bars represent minimum and maximum possible amounts of erosion given that few dropout locations eroded to the flume bottom by the end of the run. Most erosion by potholes unfortunately is not included because our method for measuring topography could not see the pothole bottoms. (c) Inner channel erosion rate calculated over a 1 cm wide by 300 cm long swath. The location of the 1 cm zone was chosen by eye to follow the path of highest erosion, and shifted between timesteps as the inner channel developed and migrated.

Johnson and Whipple, ESPL 2007

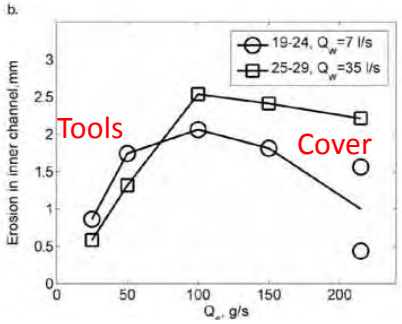


Erosion averaged along the axis of the inner channel per time step. Inner channel erosion rates are much higher than flume-averaged values.

Johnson and Whipple, JGR 2010

Morphologic similarities between field and flume (Johnson and Whipple, ESPL 2007)



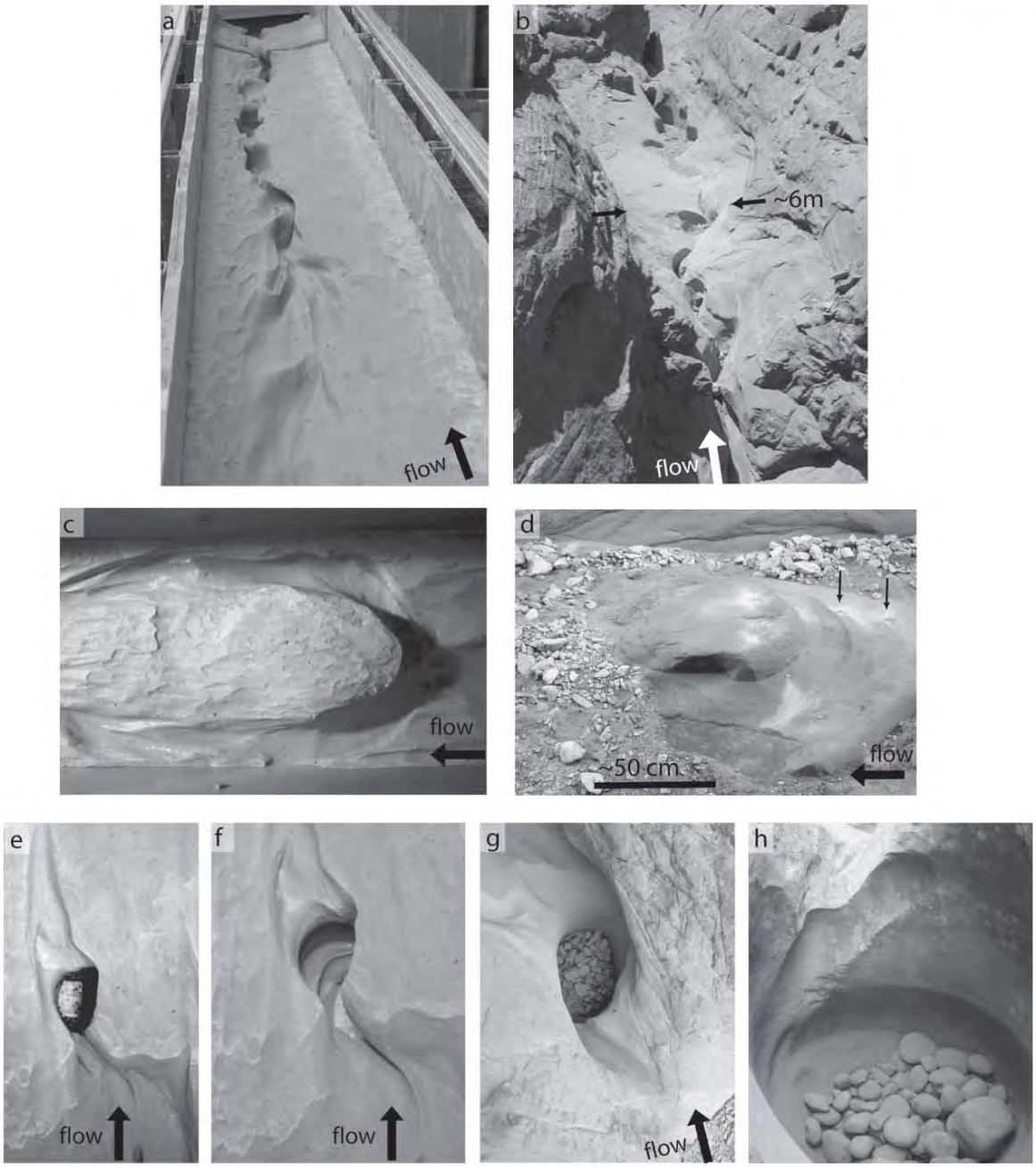


**Figure 3.** Comparisons of erosional features formed in flume and field. All the field photographs are channels and canyons draining the Henry Mountains of Utah that have incised into the relatively weak but unfractured Navajo Sandstone. (a) Oblique view looking downstream at the end of the 10 per cent slope flume experiment. Compare with 2(d). Flume width 40 cm. (b) A natural inner channel formed in the south fork of Maidenwater Creek. (c) View from above of experimental erosion around a broad protrusion molded into the bed of the first flume run. Flume width 40 cm. (d) Similar geometry of a trough in a Henry Mountains channel, initial condition unknown. White patches are pulverized rock from drilling bolt holes for erosion monitoring. (e), (f) Two views of a pothole formed in the fifth flume run in which the bed was molded to have vertical steps; the pothole occurred where the bed was initially horizontal and planar. Pothole diameter 5–6 cm; overall bed slope 10 per cent. (g) Field pothole (diameter ~ 60 cm) partially filled with sediment clasts. (h) Natural pothole, diameter ~2 m. This pothole is from the cascade of potholes shown in Figure 2 of Whipple (2004).




DOI: 10.1002/esp

Natural examples of same morphological feedbacks:
Peekaboo, Spooky and Coyote Narrows slot canyons, Escalante River drainage, UT

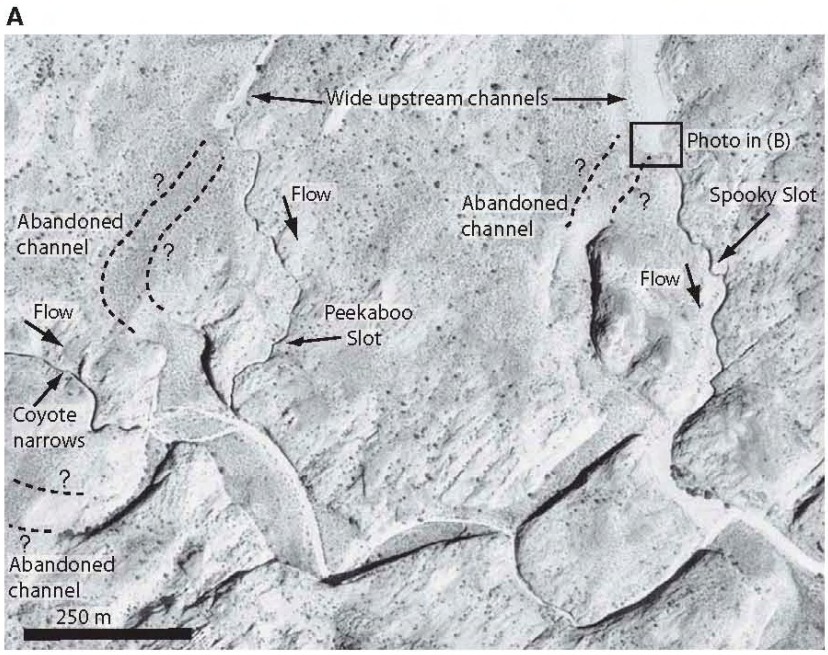


Figure 12. (A) Escalante canyons, aerial photograph (crop of Big Hollow Wash, Utah, digital orthophoto quadrangle) of Coyote Gulch and tributaries including the slot canyons Peek-aboo, Spooky, and Coyote Narrows (latitude 37.482N, longitude 111.216W). Rectangle shows approximate area of photo in 12B. Outlines of inferred abandoned channel segments are marked by dashed lines and question marks. (B) Photograph looking south of channel just upstream of Spooky slot canyon; note the start of the slot (shadowed bedrock). Sitting person is circled for scale. (C) A short distance downstream the active channel narrows greatly, forming Spooky slot canyon.

A less natural example: Fremont River Waterfall, in Capitol Reef National Park: a great place to stop on your way home (right on the highway). This is another example of a man-made step in the river, in this case by cutting off a meander bend during highway construction … in a National Park.

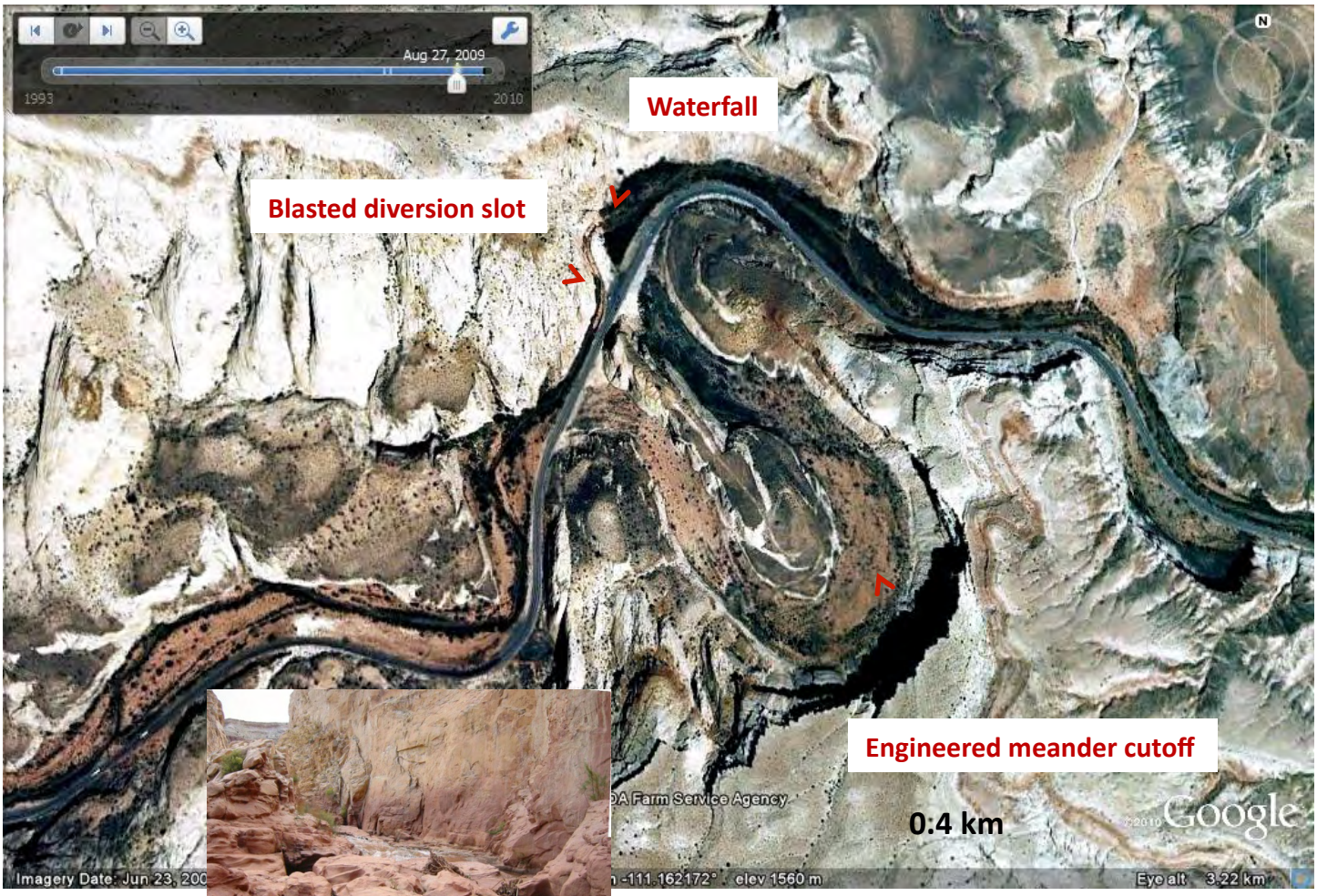


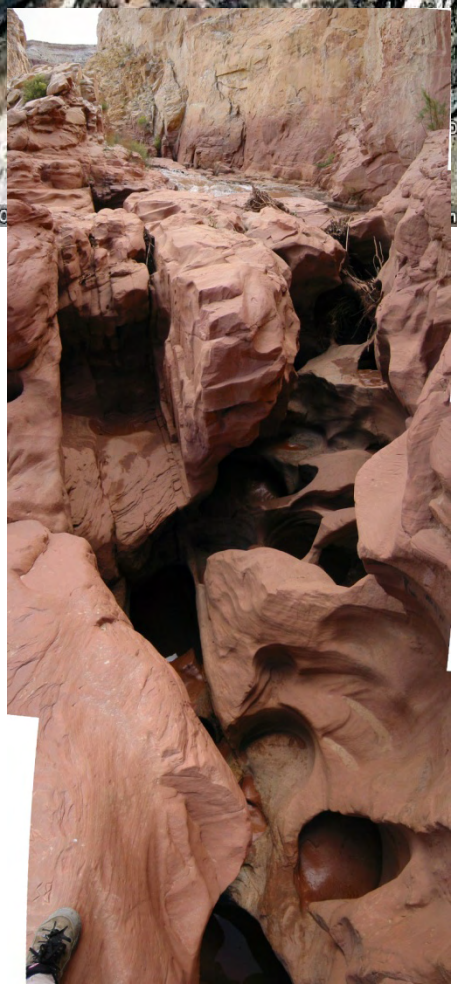

## Day 2 Stop 2: Comparing channel slopes, sediment supply, and incision in Trail Canyon and tributaries: Field evidence for cover effects at long timescales

Key topics at this site:

- Field evidence that alluvial cover can inhibit channel downcutting.
- The slope of incising bedrock channels can primarily be adjusted to the sediment load.
- Channels in this landscape have systematically different coarse sediment supply rates.

Most data and plots in this section are from the following paper:

JOURNAL OF GEOPHYSICAL RESEARCH, VOL. 114, F02014, doi:10.1029/2007JF000862, 2009



### Transport slopes, sediment cover, and bedrock channel incision in the Henry Mountains, Utah

Joel P. L. Johnson,[1] Kelin X. Whipple,[2] Leonard S. Sklar,[3] and Thomas C. Hanks[4]

Received 4 July 2007; revised 21 January 2009; accepted 26 February 2009; published 5 May 2009.

[1] Field data from channels in the Henry Mountains of Utah demonstrate that abundant coarse sediment can inhibit fluvial incision into bedrock by armoring channel beds (the cover effect). We compare several small channels that share tributary junctions and have incised into the same sedimentary bedrock unit (Navajo Sandstone) but contain differing amounts of coarse diorite clasts owing to the spatial distribution of localized sediment sources. Bedrock channels that contain abundant clasts (diorite-rich) have steeper longitudinal slopes than tributaries of these channels with smaller drainage areas and less sediment (diorite-poor). The diorite-poor tributaries have incised more deeply to lower average slopes and have more reach-scale slope variability, which may reflect bedrock properties, longitudinal sediment sorting, and incision at lower sediment supply. Diorite-rich channels have less bedrock exposed and smoother longitudinal profiles than diorite-poor channels. We find that (1) coarse sediment can mantle bedrock channel beds and reduce the efficiency of incision, validating the hypothesized cover effect in fluvial incision models; (2) the channel slope needed to transport the sediment load can be larger than that needed to erode bedrock, suggesting that the slope of incising bedrock channels can become adjusted to the sediment load; (3) when abundant sediment is available, transport capacity rather than thresholds of motion can be dominant in setting bedrock channel slope; and (4) cover effects can be important even when moderate amounts of bedrock are exposed in channel beds.

**Citation:** Johnson, J. P. L., K. X. Whipple, L. S. Sklar, and T. C. Hanks (2009), Transport slopes, sediment cover, and bedrock channel incision in the Henry Mountains, Utah, *J. Geophys. Res.*, *114*, F02014, doi:10.1029/2007JF000862.

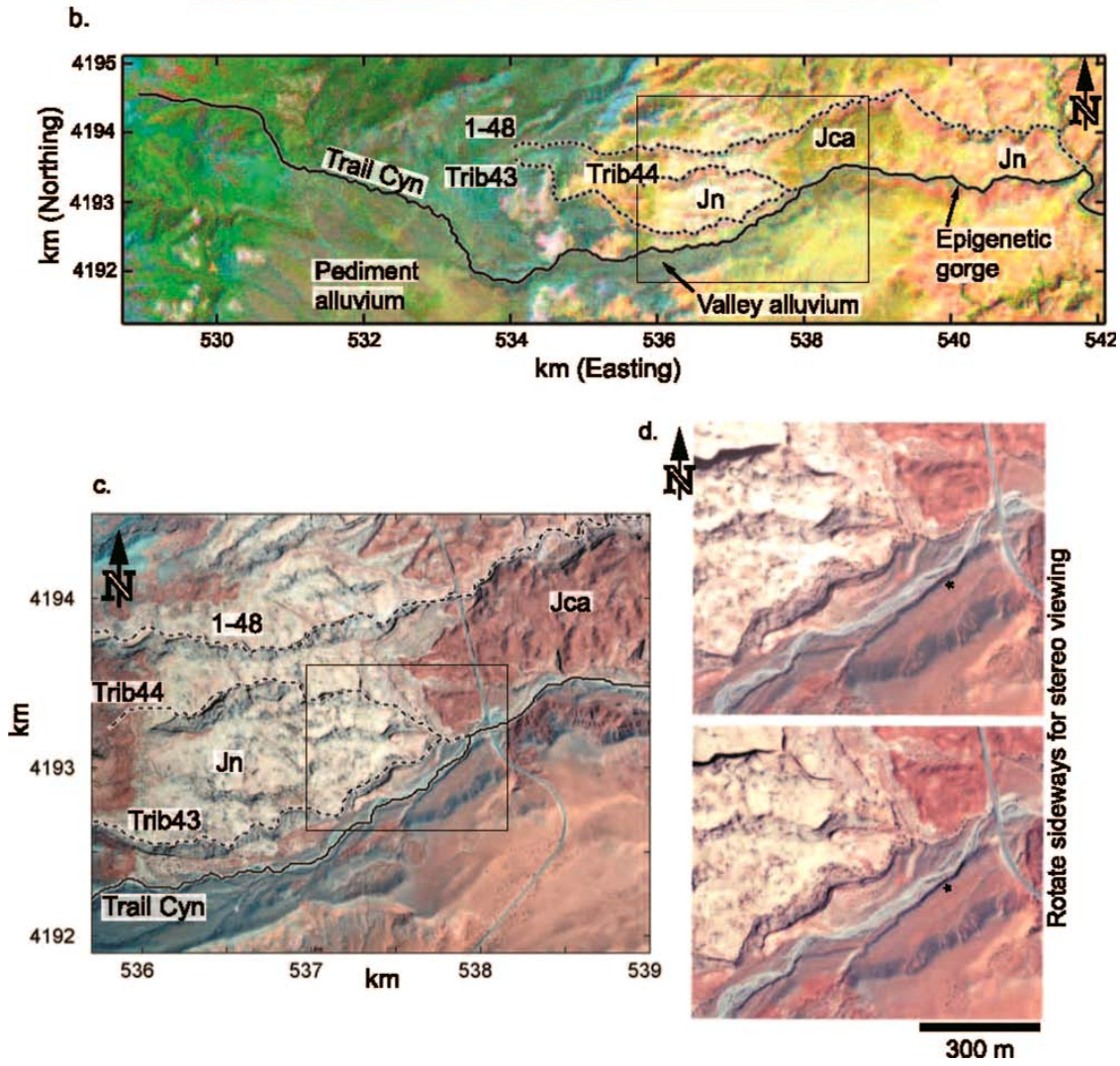


(b) Landsat image showing Trail Canyon and diorite-poor tributaries. Location indicated in Figure 1. Photograph of epigenetic gorge in Figure 6c. (c) Aerial photograph showing Trail and Maidenwater canyons. Note the difference between Jca (dark red), Jn (tan), and diorite-rich alluvium (gray) filling the Trail Canyon valley. Location shown in Figure 4b (rectangle). (d) Stereo air photographs showing the confluences of Trail Canyon, Trib43, and Trib44. Location indicated in Figure 3c. To view in stereo, rotate the page 90° clockwise, relax your eyes, focus on infinity, and let the images overlap. The asterisk is the ~13 m fill terrace similarly marked in Figure 6. Note that the Trib43 channel elevations are lower than the adjacent Trail Canyon.

**Citation:** Johnson, J. P. L., K. X. Whipple, L. S. Sklar, and T. C. Hanks (2009), Transport slopes, sediment cover, and bedrock channel incision in the Henry Mountains, Utah, *J. Geophys. Res.*, *114*, F02014, doi:10.1029/2007JF000862.

DEM longitudinal profiles of Trail Cyn and tribs

Slope-area data

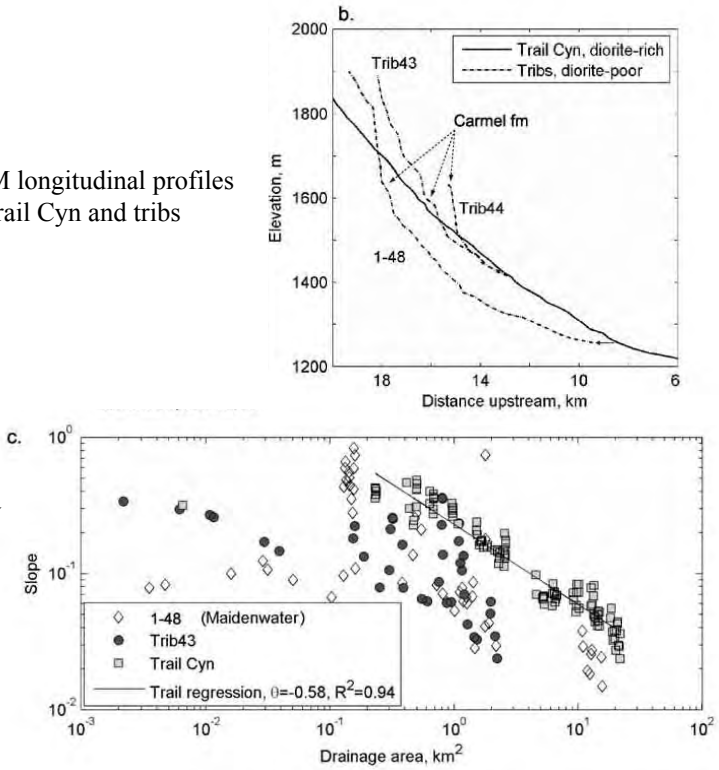


**Figure 4.** Channel profiles and slope area data. (a) Ticaboo Canyon profiles. Locations shown in Figure 3a. Channel 3 1 is offset by 1 km (*x* axis) for clarity. Near confluences, tributary slopes are lower than the main stem slope. (b) Trail Canyon, Trib43, Trib44, and 1 48 (Maidenwater); locations shown in Figure 3b. The tributary channels are incised more deeply to lower slopes than Trail Canyon in the vicinity of the confluences. Trail Canyon and 1 48 do not share a confluence directly but are both nearby tributaries of the larger Trachyte Creek. (c) DEM slope area data plotted for Trail Canyon, Trib43, and Maidenwater south. The diorite-poor channels have locally high slopes, but Trail Canyon has higher overall slopes at a given drainage area. Slopes were calculated over ~24.4 m of vertical elevation, which corresponded to two contour intervals in the original data (USGS 7.5′ quadrangles; contour interval 40 feet). No other smoothing was done.

Field surveys of longitudinal profiles

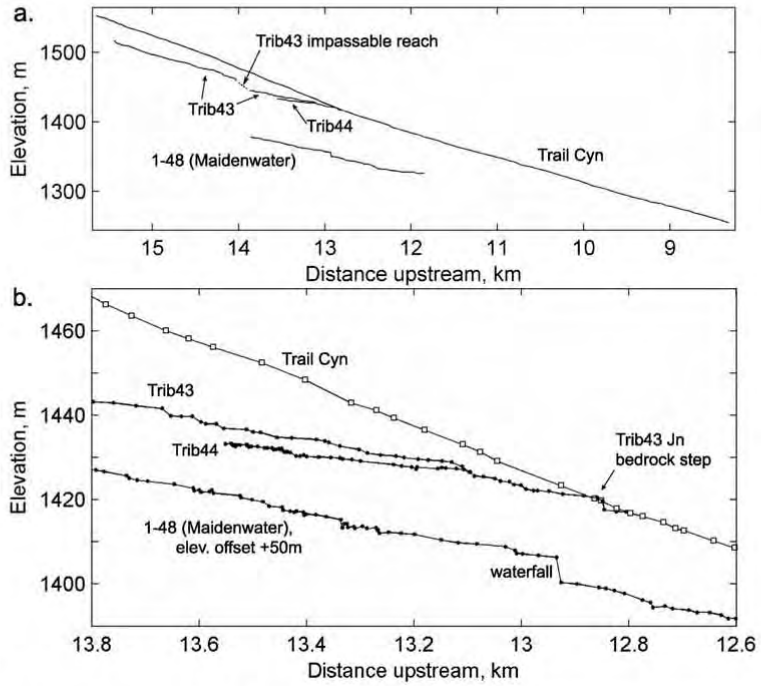


**Figure 5.** Field-surveyed channel profiles. (a) Complete distances surveyed along each channel. A steep impassable reach in Trib43 (dotted line, ~14 km upstream, 150 m long) was not surveyed. (b) A close-up view of surveyed reaches, showing differences in slope and profile smoothness. Survey points were chosen to capture changes in local slope (described in section 4), and so the smoother profile of Trail Canyon is not an artifact of the wider sample spacing. The Trib43 bedrock step is shown in Figure 6a. Maidenwater Canyon has a 5 m waterfall where the channel crosses a small carbonate-rich bed within the Navajo Sandstone.

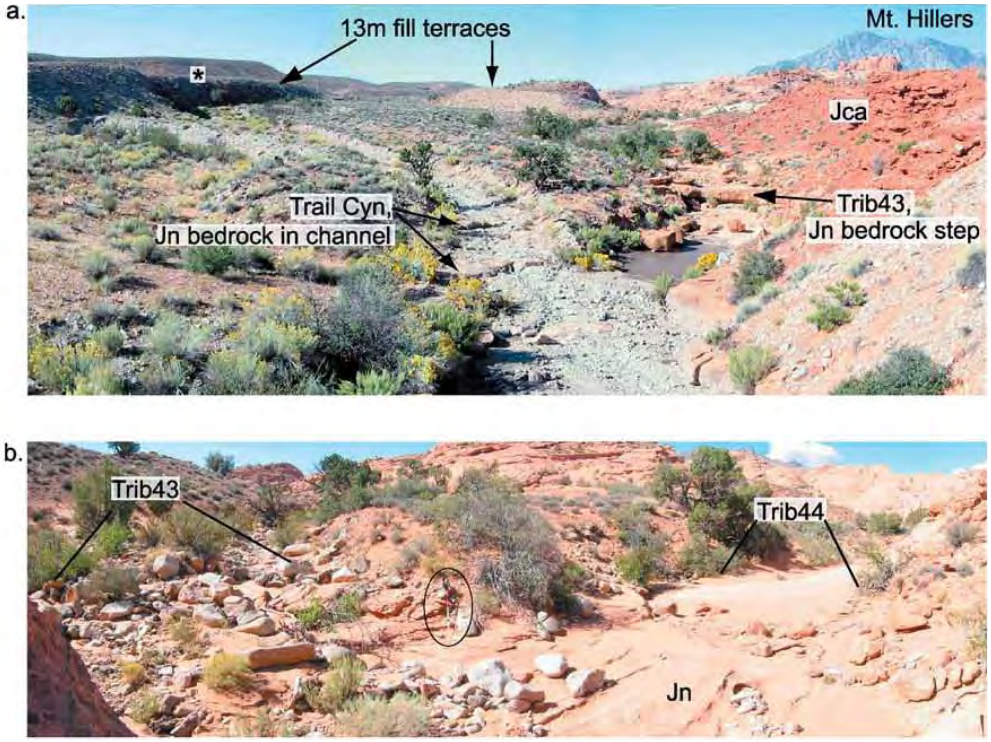


**Figure 6.** Photographs comparing tributaries. (a) The view looking upstream at the confluence of Trail Canyon (left) and Trib43 (right) shows differences in coarse sediment bed cover between the channels. The lithologically controlled step in Trib43 is apparent in the field-surveyed profile (Figure 5). Stratigraphically, the step occurs close to the top of the Navajo Sandstone (Jn). Darker weathered beds of the Carmel Formation (Jca) form the hillslope above. The asterisk corresponds to a ~13 m fill terrace marked in Figure 3d. (b) Confluence of Trib43 and Trib44, showing more coarse sediment bed cover in Trib43. The 1.75 m laser pole is circled for scale. (c) Epigenetic gorge downstream in Trail Canyon, location shown in Figure 3b. Note field assistant for scale.

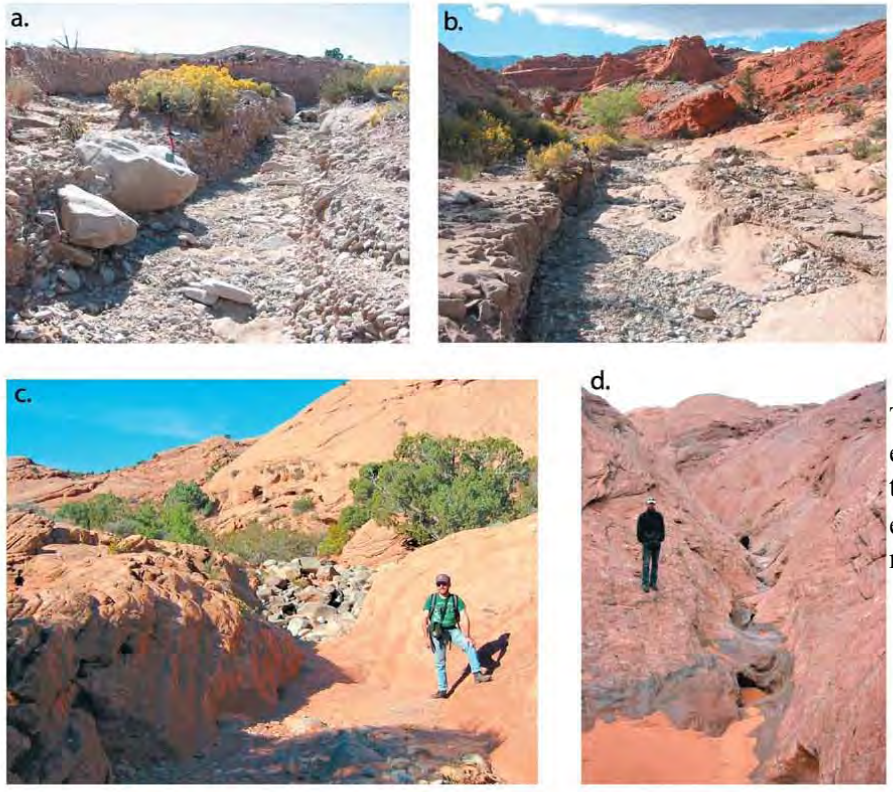


This is the downstream end of a slot canyon that can be easily explored, although it may be wet.

**Figure 7.** Field photographs showing channel morphology. (a) View upstream of the Trail Canyon channel. Note the imbricated cobbles in the foreground, the flat bed and rectangular channel cross section, and the active floodplain level with a higher fill terrace behind. The section of surveying rod visible is ~70 cm. (b) Bedrock exposed in the Trail Canyon bed and bank, looking upstream, 1.75 m surveying rod. (c) Trib43, looking upstream. In the background, just upstream of where Jn bedrock narrows, is a steep boulder jam of diorite and sandstone boulders and cobbles. The foreground sediment is sand, illustrating longitudinal sorting. (d) Trib44, looking upstream, showing potholes and fluvial sculpting at the start of a narrow slot. All of the visible sediment is sand.

More bedrock exposure = lower bedrock channel slope

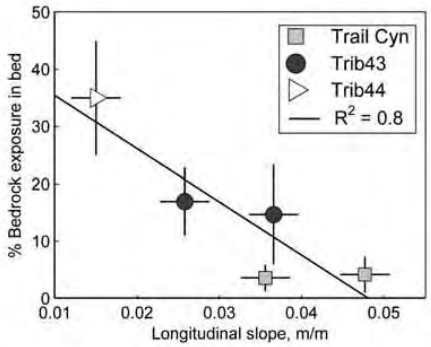


**Figure 9.** Reach-averaged slope plotted against percent bedrock exposure in the bed for Trib44 (distance upstream from Lake Powell 13.11 to 13.55 km), two reaches of Trib43 (12.81 13.87 km and 14.02 15.45 km upstream), and two reaches of Trail Canyon (upstream and downstream of the Trib43 confluence; 8.32 12.79 km and 12.82 15.65 km upstream). Together these reaches represent all of the surveyed distance along these channels (Figures 5 and 8).

Sediment size distributions in different channels

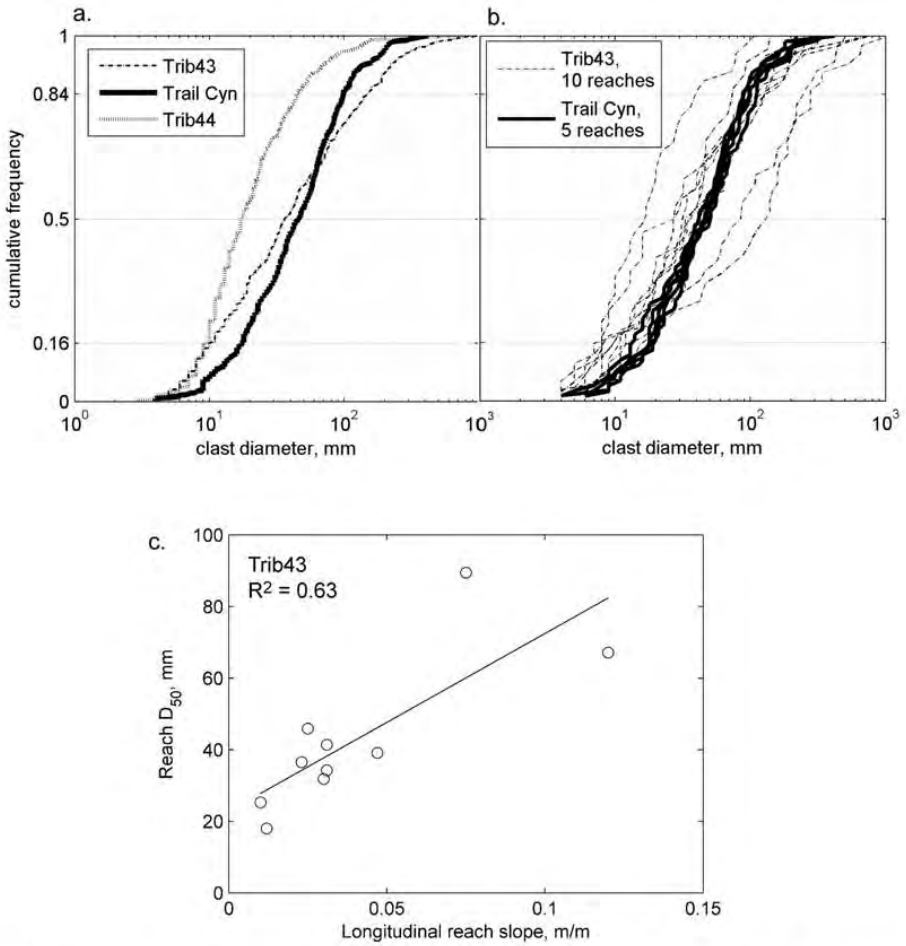


**Figure 10.** Pebble count sediment size distributions. (a) Total distributions (excluding sand) for each channel. Trail Canyon is better sorted than Trib43; both have larger coarse sediment (and much more of it) than Trib44. (b) Approximately 100 clast diameters were measured in each of 5 reaches of Trail Canyon, compared to ~50 clasts measured in each of 10 reaches of Trib43. Slope-dependent longitudinal sorting is strong in Trib43 and negligible in Trail Canyon. (c) Longitudinal slope plotted against $D_{50}$ for the 10 Trib43 reaches with separate pebble counts.

Simple steady-uniform flow calculations of shear stresses: flow well below bankfull will mobilize bed sediment



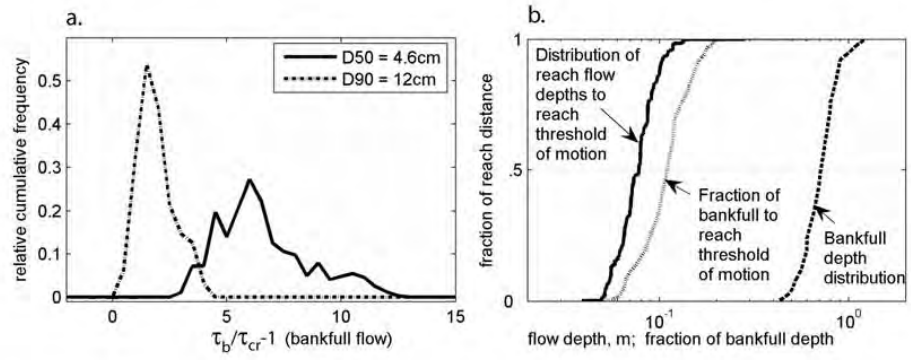


**Figure 11.** (a) Histograms represent the frequency of occurrence of excess Shield's stress ($\tau_b^*/\tau_{cr}^* - 1$) per unit distance downstream (i.e., accounting for differences in surveyed reach lengths) calculated for bankfull flow in Trail Canyon. Zero corresponds to the threshold of motion. (b) Cumulative distribution of flow depth in each reach necessary to reach the threshold of motion. Also plotted are the distribution of measured bankfull depths and the ratio of these two; that is, the fraction of bankfull flow depth necessary to reach the threshold of motion. The flow depths necessary to initiate sediment motion are nearly an order of magnitude smaller than bankfull flow.

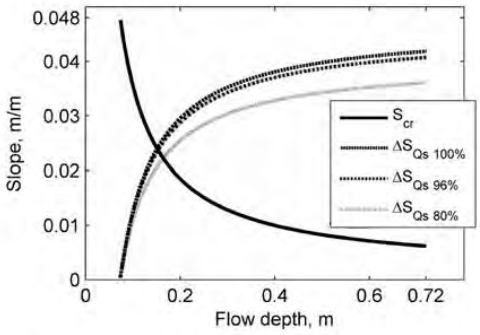


**Figure 12.** Components of total channel slope calculated using equations (5) and (6) as a function of flow depth based on reach-averaged Trail Canyon slope, width, and depth given in Table 1. At flow depths below ~0.08 m the threshold of sediment motion (for $D_{50}$ = 46 mm) is not exceeded. At flow depths greater than ~0.18 m, or ~25% of bankfull flow, the fraction of slope transporting the sediment load ($\Delta S_{qs}$) is larger than the fraction of slope that exceeds the threshold of sediment motion ($S_{cr}$).

**Citation:** Johnson, J. P. L., K. X. Whipple, L. S. Sklar, and T. C. Hanks (2009), Transport slopes, sediment cover, and bedrock channel incision in the Henry Mountains, Utah, *J. Geophys. Res.*, *114*, F02014, doi:10.1029/2007JF000862.

# Lidar coverage for Henry Mountains:

NCALM student grant to Skye Corbett (advisor Leonard Sklar)

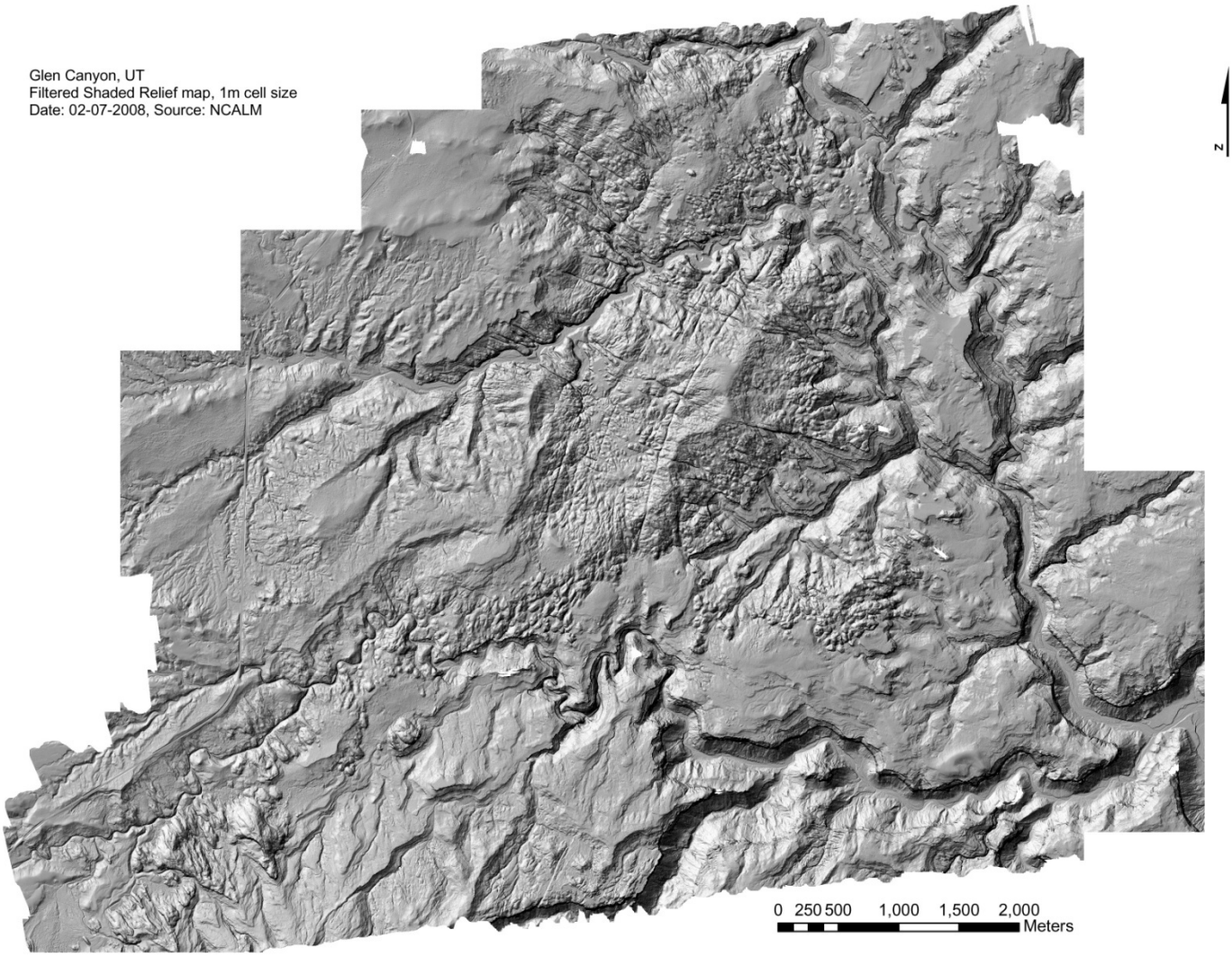

# Using Lidar and field surveys to quantify natural bedrock and alluvial reach roughness in relation to long-term sediment load.

Lindsay Olinde, PhD student, UT Austin

Plan for current and future work: to measure bed topography and various roughness metrics, and how they vary with sediment size distribution and long-term sediment supply. Using airborne lidar data, ground-based lidar, and field surveys.



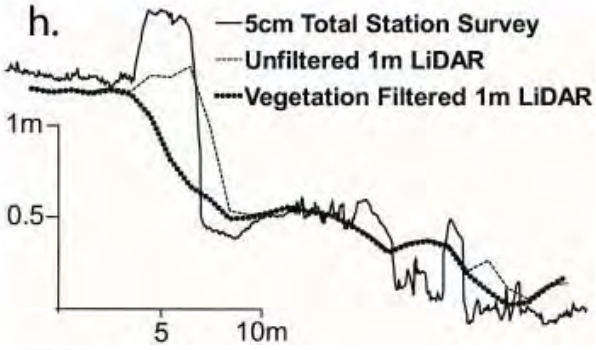


a. Location of Henry Mountains field site, and LiDAR shaded relief map showing surveyed reach in g and h. e. LiDAR-derived longitudinal profiles, linear trend (channel slope) removed. f. Power spectra for channels in e (over longer distances). Arrows highlight peaks with different amplitudes and wavelengths between the channels. g. Milk Creek, reach surveyed with total station. h. Comparison of total station survey and airborne LiDAR profiles.

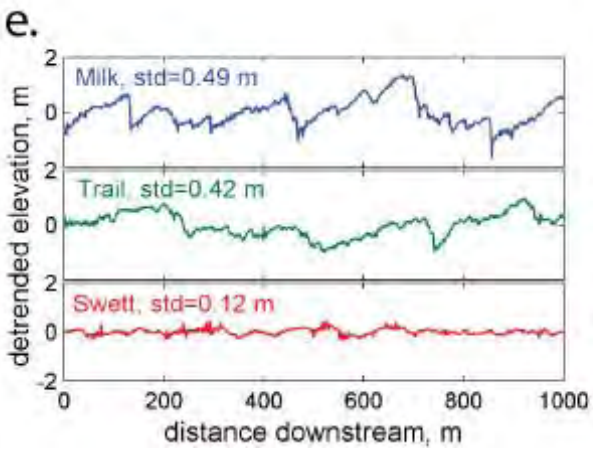


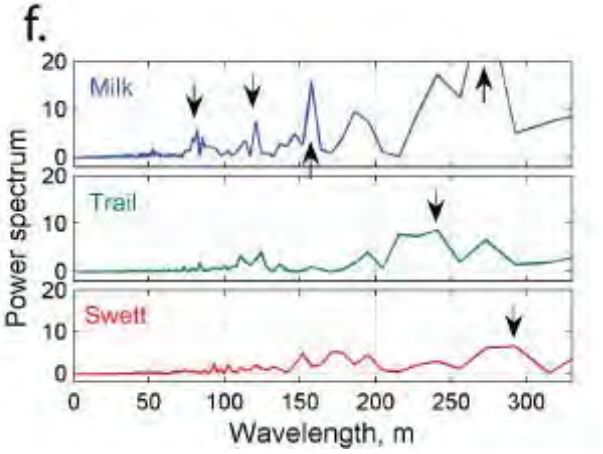

# Day 2 Stop 3: Epigenetic gorges in Trail Canyon

**Earth Surface Processes and Landforms**
*Earth Surf. Process. Landforms* **33**, 1993–2009 (2008)
Published online 12 March 2008 in Wiley InterScience
(www.interscience.wiley.com) **DOI:** 10.1002/esp.1650

## Epigenetic gorges in fluvial landscapes

W. B. Ouimet,[1]*† K. X. Whipple,[2] B. T. Crosby,[3] J. P. Johnson[1] and T. F. Schildgen[1]
[1] *Department of Earth, Atmospheric, and Planetary Sciences, Massachusetts Institute of Technology, Cambridge, MA, USA*
[2] *School of Earth and Space Exploration, Arizona State University, Tempe, AZ, USA*
[3] *Department of Geosciences, Idaho State University, Pocatello, ID, USA*

*Correspondence to: W. B. Ouimet, Department of Earth, Atmospheric, and Planetary Sciences, Massachusetts Institute of Technology, Cambridge, MA 02139, USA.
E-mail: wouimet@geosc.psu.edu
†Now at Department of Geosciences, Penn State University, University Park, PA 16802, USA.

Received 22 July 2007;
Revised 15 November 2007;
Accepted 26 November 2007

### Abstract

**Epigenetic gorges form when channels that have been laterally displaced during episodes of river blockage or aggradation incise down into bedrock spurs or side-walls of the former valley rather than excavating unconsolidated fills and reinhabiting the buried paleovalley. Valley-filling events that promote epigenetic gorges can be localized, such as a landslide dam or an alluvial/debris flow fan deposit at a tributary junction, or widespread, such as fluvial aggradation in response to climate change or fluctuating base-level. The formation of epigenetic gorges depends upon the competition between the resistance to transport, strength and roughness of valley-filling sediments and a river's ability to sculpt and incise bedrock. The former affects the location and lateral mobility of a channel incising into valley-filling deposits; the latter determines rates of bedrock incision should the path of the incising channel intersect with bedrock that is not the paleovalley bottom. Epigenetic gorge incision, by definition, post-dates the incision that originally cut the valley. Strath terraces and sculpted bedrock walls that form in relation to epigenetic gorges should not be used to directly infer river incision induced by tectonic activity or climate variability. Rather, they are indicative of the variability of short-term bedrock river incision and autogenic dynamics of actively incising fluvial landscapes. The rate of bedrock incision associated with an epigenetic gorge can be very high (>1 cm/yr), typically orders of magnitude higher than both short- and long-term landscape denudation rates. In the context of bedrock river incision and landscape evolution, epigenetic gorges force rivers to incise more bedrock, slowing long-term incision and delaying the adjustment of rivers to regional tectonic and climatic forcing.** 

**Keywords: epigenetic gorge; landslides; river incision; strath terraces; landscape evolution**

### Conclusions

Epigenetic gorges are a prevalent feature in rivers with valley-filling and re-incision sequences. Valley-filling events that promote epigenetic gorges can be related to landslides (landslide deposits and stable landslide dams), debris flows, alluvial fans or widespread fluvial aggradation. Re-incision results from shutting off the increased sediment flux or simply re-working a localized deposit. Epigenetic gorges form when landslides or alluvial fans push rivers against opposite valley walls and become entrenched into bedrock, or more generally after a period of fluvial aggradation when a river incises into the fill and is superimposed on a bedrock spur of the former bedrock valley.

Epigenetic gorges highlight the intermittent and episodic nature of bedrock incision in actively incising rivers both spatially and temporally. They are related to autogenic processes within actively incising rivers, indicating that isolated bedrock gorges and mixed bedrock–alluvial channels are part of the regular process of long-term incision. Incision can be rapid, then dormant, rapid then dormant. Epigenetic gorges also have important implications in the context of bedrock river incision and landscape evolution. They are a process by which valleys widen their bedrock valleys; they slow the overall long-term river incision and transient adjustment as rivers often have to re-incise a certain percentage of their bedrock gorges, enhancing the landslide influence in general. The rapid incision occurs in part because of the high number of tools for incision (fluvial sediments) that build up behind the dam and the high stream power associated with river channels these bedrock gorges.

# What is an epigenetic gorge?

An epigenetic gorge is a bedrock-walled river channel segment that forms as rivers incise into valley-filling deposits and become superimposed on bedrock spurs or entrenched into side-walls of the former valley (Hewitt, 1998) (Figure 1). The term 'epigenetic' refers to the secondary nature of these bedrock gorges, occurring after the formation of the original gorge, and is related to the terms 'epigenetic drainage' or 'epigenetic incision' (see, e.g., von Engeln, 1942). In recent literature, an epigenetic gorge has also been referred to as a 'valley spur cutoff', 'bypass gorge', 'superimposed gorge' or 'modern slot canyon' (James, 2004; Korup *et al.*, 2006; Hewitt, 2006; Pratt-Situala *et al.*, 2007, respectively). In fluvial settings, epigenetic gorges can form in association with landslide dams, alluvial fans or river incision and re-organization following widespread fluvial aggradation. Though not the focus of this paper, epigenetic gorges can also form in association with river blockages and aggradation related to eolian, glacial, volcanic or karst processes.

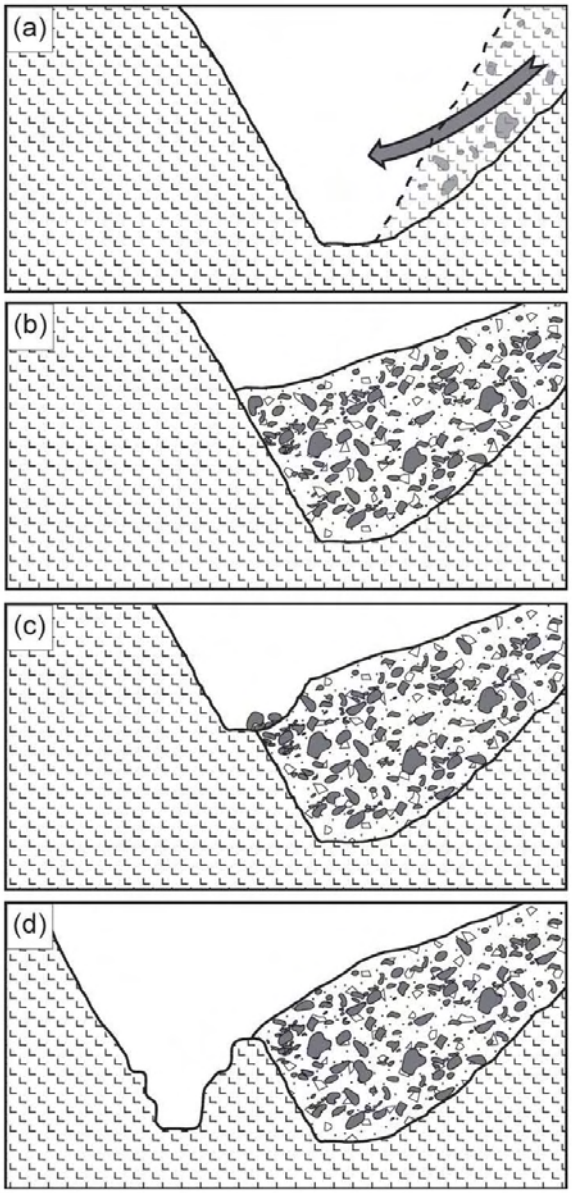


**Figure 1.** Conceptual model of how large landslide deposits and landslide dams can lead to the formation of epigenetic gorges. The particular example depicted shows an epigenetic gorge forming as a river incises into valley landslide deposits and becomes entrenched into side-walls of the former valley. Sequence: (a) initiation of a large landslide in an incised valley with bedrock valley walls; (b) landslide deposits fill the valley, forming a landslide dam; (c) river starts to cut down through the landslide debris while eroding the bedrock channel walls; (d) river establishes itself into bedrock, abandons the landslide debris and continues to cut an epigenetic gorge.

Trail Canyon: Epigenetic gorges here were formed by regional valley aggradation (presumably driven by changes in climate) followed by subsequent downcutting that happened to occur through bedrock. Alluvial fill terrace level ~10-15 m above current channels is widespread in this and other Henry Mountains watersheds with high sediment supply. May correspond to terrace level in another drainage dated by Cook et al. (2008) to ~13 ka

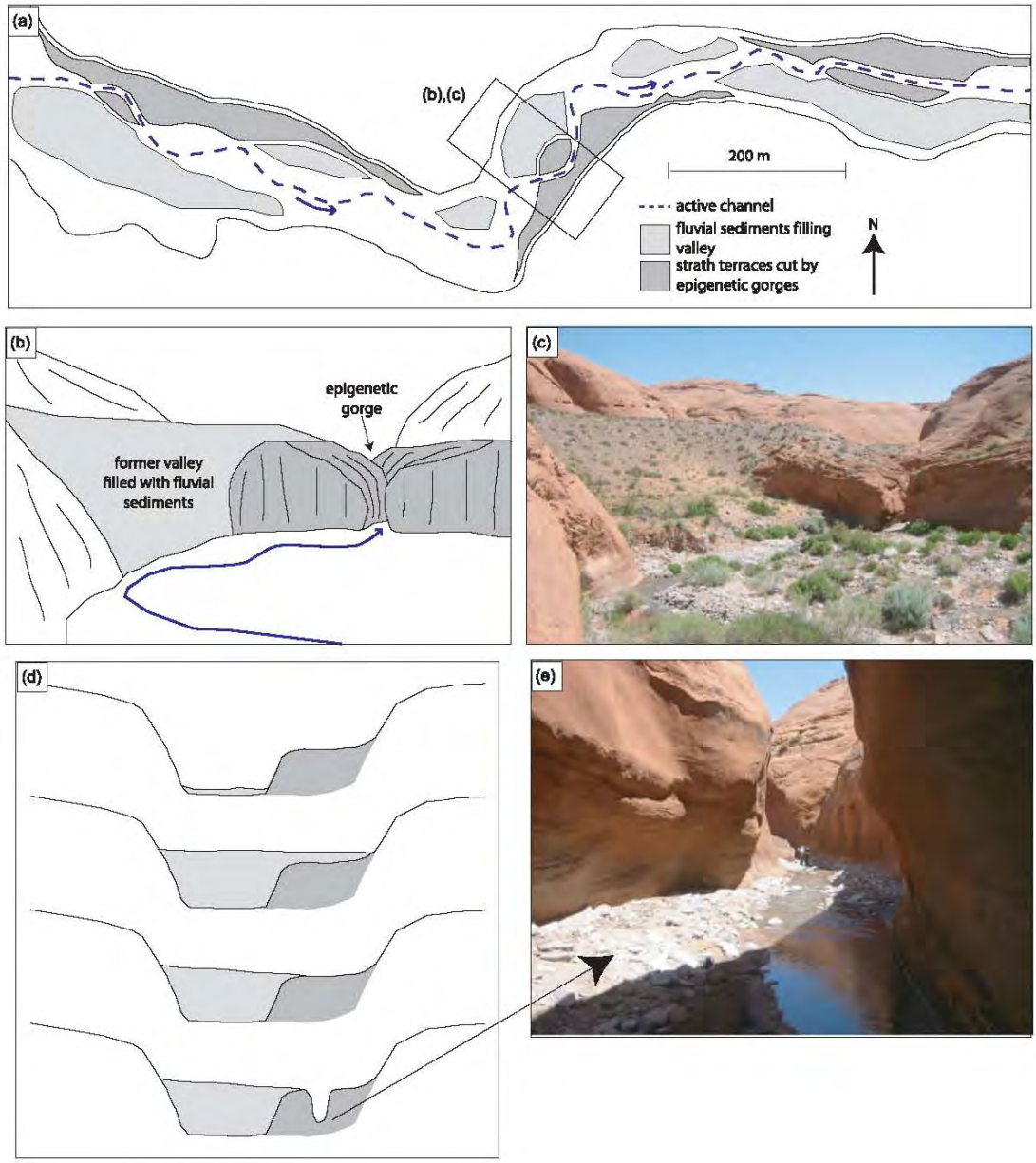


**Figure 6.** Epigenetic gorges in Trail Canyon, southeast Utah (GPS: 37·8876 North, 110·5398 West). Epigenetic gorges here are the result of river incision and re-organization following fluvial aggradation. (a) Map view of a 1·5 km stretch of Trail Canyon showing where three strath terraces have been cut by epigenetic gorges. Trail Canyon flows from left to right. (b), (c) Paired photograph and sketch of the middle epigenetic gorge viewed from upstream. (d) Schematic model of how fluvial aggradation in Trail Canyon led to the formation of these epigenetic gorges. (e) Photograph of new channel through the gorge. This figure is available in colour online at www.interscience.wiley.com/journal/espl

Other mechanisms for forming epigenetic gorges:
Landslide-induced egorge, Sichuan Province, China.

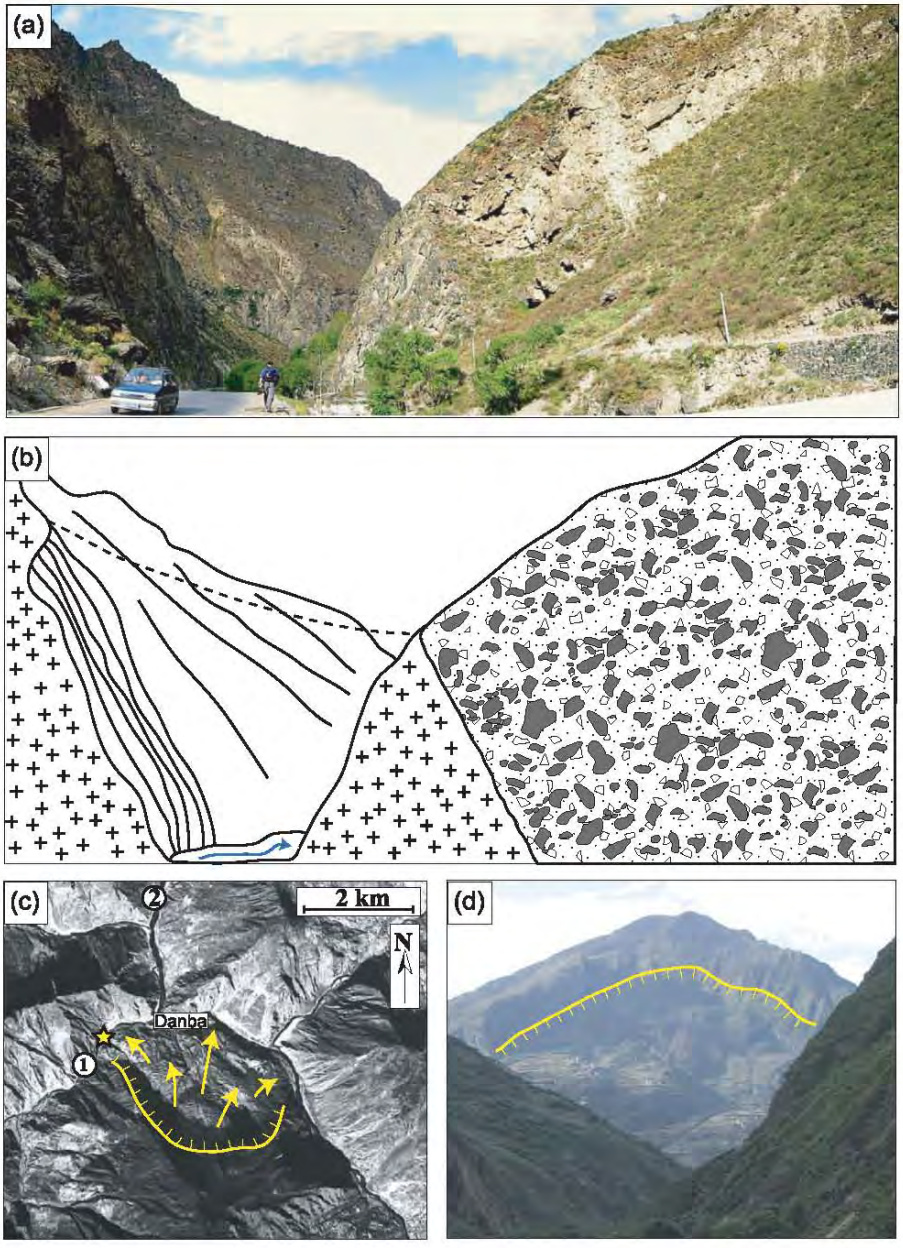


**Figure 2.** Landslide-induced epigenetic gorge located 1 km upstream of Danba along Dong Gu He River (GPS: 30·8787 North, 101·8735 West). (a), (b) Paired photograph and sketch of the epigenetic gorge viewed from upstream. (c) Corona image of Danba region highlighting the large landslide complex above the city. A star marks the epigenetic gorge location. Locations 1 and 2 indicate where photographs (a) and (d) were taken, respectively. (d) Photograph showing the landslide scarp above Danba. This figure is available in colour online at www.interscience.wiley.com/journal/espl

Landslide-induced epigenetic gorge, Sipia Falls, Peru.

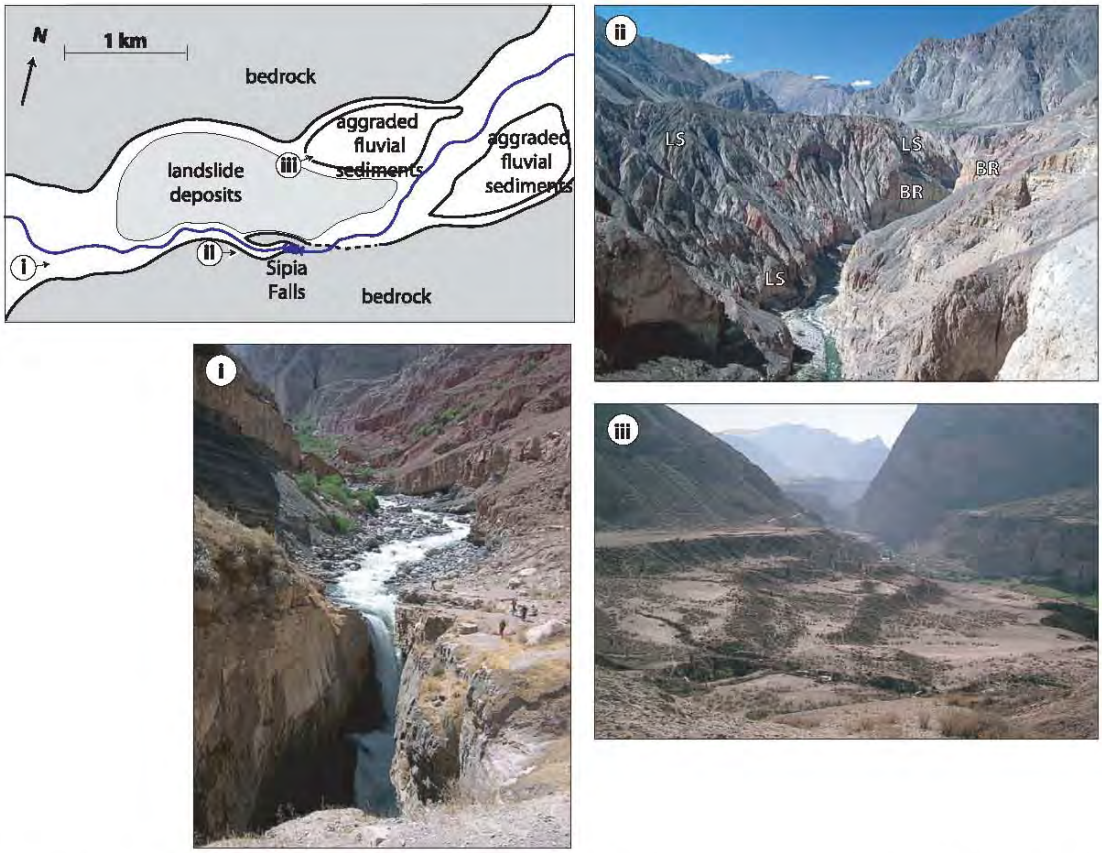


**Figure 5.** Landslide-induced epigenetic gorge at Sipia Falls within the Cotahuasi River canyon in southwest Peru (GPS: 15·2420 South, 72·9597 West). In the map sketch shown, the Cotahuasi River flows right to left. Locations i, ii and iii indicate where photographs (i), (ii) and (ii) were taken, respectively. In photograph (ii) LS denotes landslide deposits and BR denotes bedrock. This figure is available in colour online at www.interscience.wiley.com/journal/espl

New Zealand: Epigenetic gorges formed by alluvial fans pushing mainstem valley channels against bank. Subsequent mainstem downcutting formed epigenetic gorges.

Note also that the Escalante River slot canyons discussed previously are eolian-controlled epigenetic gorges.

*Aggradation Case Study: Waihuka River, North Island, New Zealand.* The Waihuka River is a trunk stream within the Waipaoa River catchment, located on the northeastern coast of the North Island of New Zealand. A pulse of incision initiated at ~18 ka propagated a wave of incision upstream through much of the Waipaoa River catchment, resulting in the incomplete dissection of an aggraded, low-gradient, relict landscape (Crosby and Whipple, 2006). Prior to incision, fluvial aggradation buried bedrock-floored river valleys between ~30 ka and 18 ka (Litchfield and Berryman, 2005). The bedrock lithology of the Waihuka catchment consists of Miocene clay-rich mudstones and siltstones interbedded with infrequent sandstone and carbonate beds (Mazengarb and Speden, 2000).

The cycle of river incision, aggradation and renewed incision in the Waipaoa basin resulted in the formation of epigenetic gorges, specifically documented along the Waihuka River (Crosby, 2006). The modern longitudinal profile of the Waihuka River (Figure 7) contains a distinct inflection at the exact location where the largest tributary enters the Waihuka. This tributary, the Parihohonu Stream, drains some of the most erosion resistant rocks in the Waihuka catchment, and 18 ka prior to incision produced a well defined alluvial fan that prograded out onto the floor of the Waihuka River valley. During aggradation, the expanding Parihohonu fan forced the Waihuka trunk stream laterally out of its paleochannel and against the opposite side valley wall. During post-aggradation incision, the channel incised into the bedrock along the valley wall rather than re-incising into the alluvium-filled paleochannel preserved under the fan. This same phenomenon was observed at three other location along the 14 km stretch surveyed along the Waihuka River. In the simplified field-surveyed longitudinal profile of the Waihuka River (Figure 7), the positive inflection in the elevation of the strath surface near the Parihohonu fan reflects a greater amount of local bedrock incision

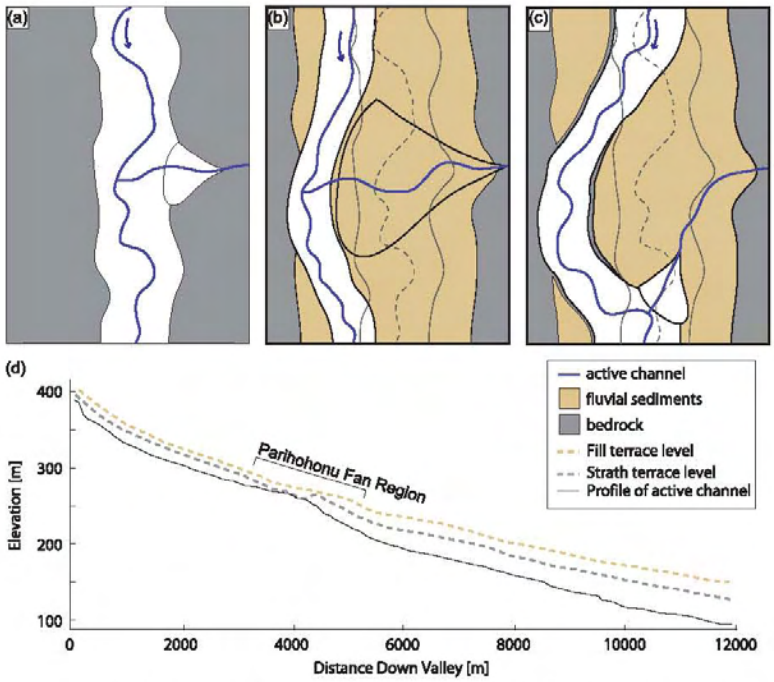


**Figure 7.** Waihuka River, North Island of New Zealand (GPS: 38·4449 South, 177·6240 East). (a)–(c) Schematic diagrams showing how fluvial aggradation and the influence of a side tributary fan may lead to the formation of an epigenetic gorge. The hypothetical river shown flows from top to bottom. (a) A pre-existing river valley bounded by bedrock with strath terrace levels. (b) Fluvial aggradation fills the valley to level higher than the strath terraces, with additional aggradation focused at a side tributary fan. This side tributary fan pushes the active course of the river to the west. Note the paleovalley and channel (dashed) shaded thinly in gray. (c) Incision into fill stays on the western side of the valley, eventually cutting incision bedrock that bounded the former channel. Note the paleovalley and channel (dashed) shaded thinly in gray. (d) River profile of the Waihuka River with mapped strath and fill levels projected above the profile. The convexity in the middle of the modern profile is the result of displacement between the pre- and post-aggradation Waihuka channels. The Waihuka experienced an epigenetic gorge incision scenario similar to that depicted in the schematic diagram. This figure is available in colour online at www.interscience.wiley.com/journal/espl


*Earth Surf. Process. Landforms* **33**, 1993–2009 (2008)
DOI: 10.1002/esp

One reason epigenetic gorges can matter:

Beware of interpreting incision rates from terrace ages as reflecting tectonic forcing. These averaged rates may primarily reflect autogenic channel dynamics and the history of sediment supply.

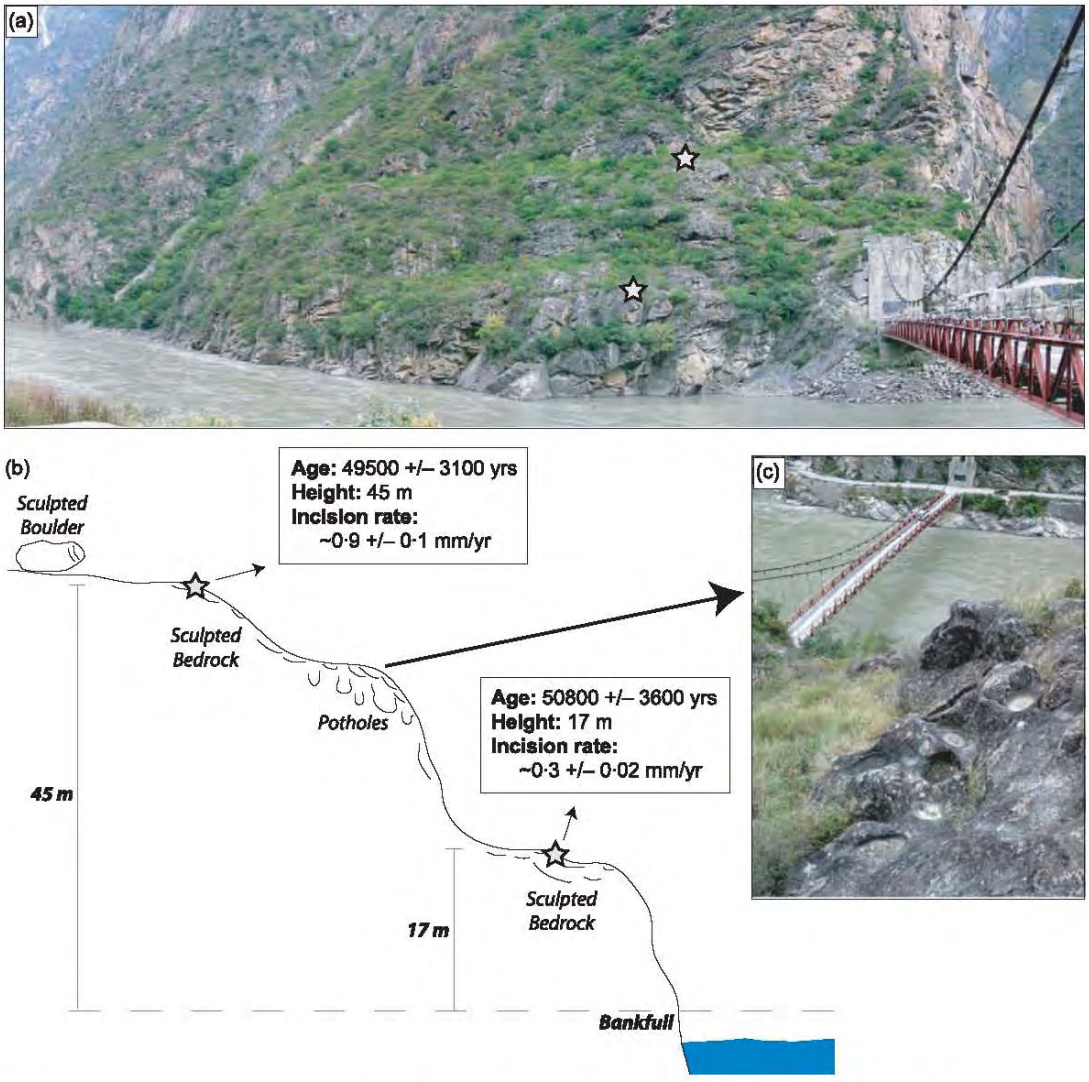


**Figure 8.** Bedrock straths along the Dadu River, ~45 km north of Luding (GPS: 30·2966 North, 102·1729 West). We dated two sculpted surfaces adjacent to the channel at this site, one 45 m above the present channel, the other 17 m. Both surfaces were dated at ~50 ka, within error of each other, yielding minimum incision rates of ~0·9 and ~0·3 mm/yr, respectively. These strath surfaces record rapid incision into fluvial sediment that had filled the Dadu River to a level at least 50 m above modern river elevation. This figure is available in colour online at www.interscience.wiley.com/journal/espl

# Day 2 Stop 4: Bedrock incision across a diorite laccolith

Topics: Rock strength, jointing, and erosional morphology
Rock properties control on hillslope-channel coupling

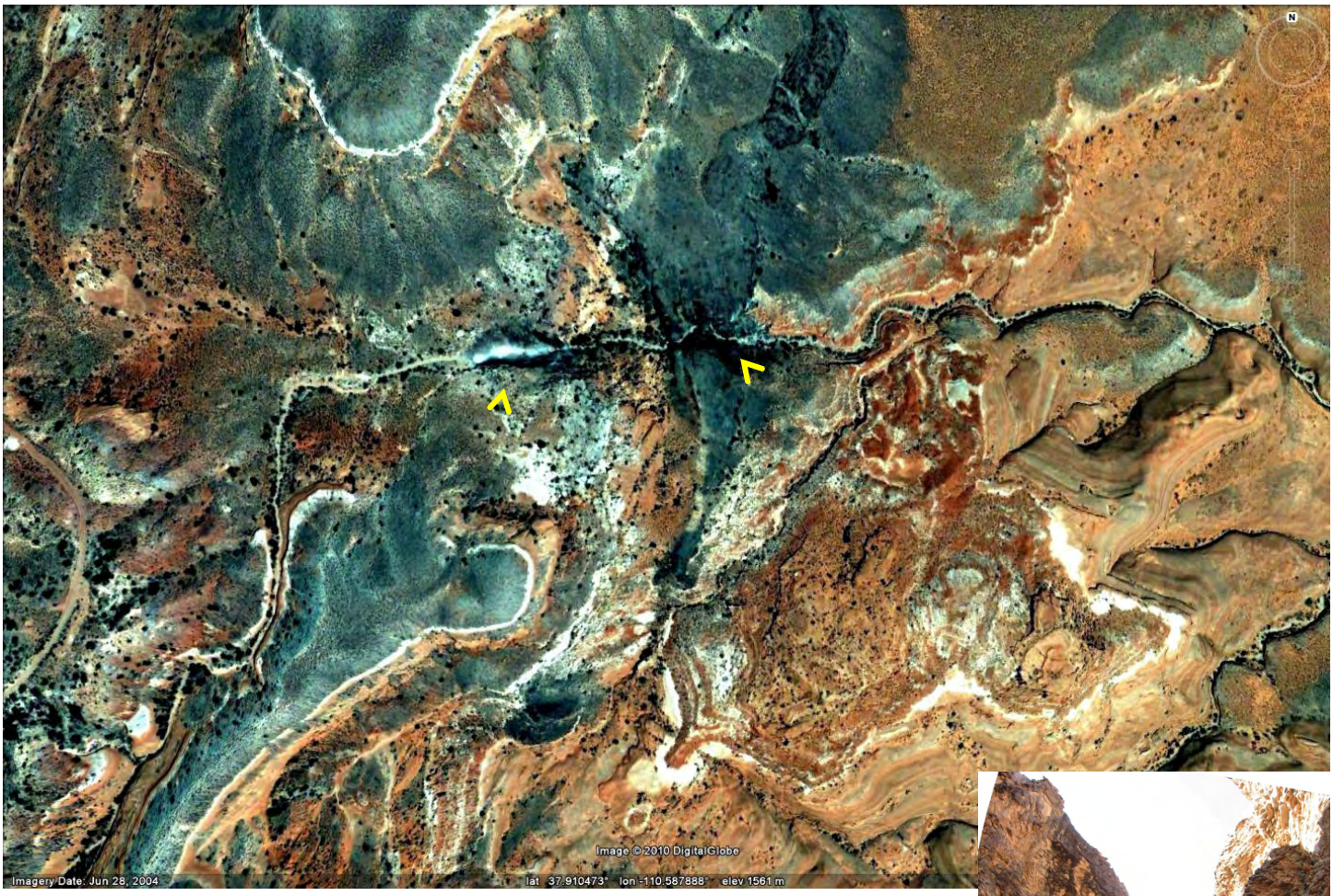


250 m

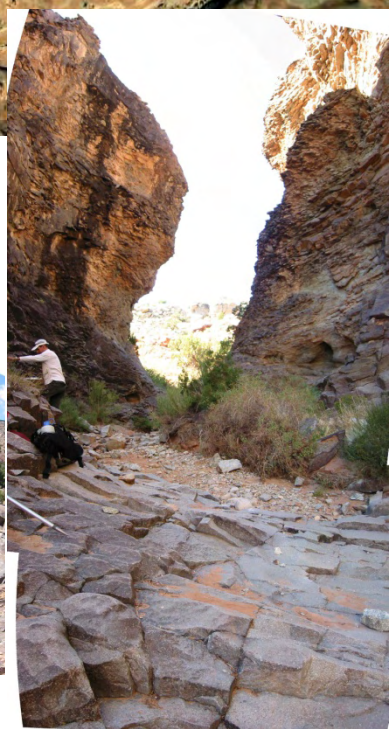

# Day 3: Dating surfaces, incision rates, and connections to the Colorado

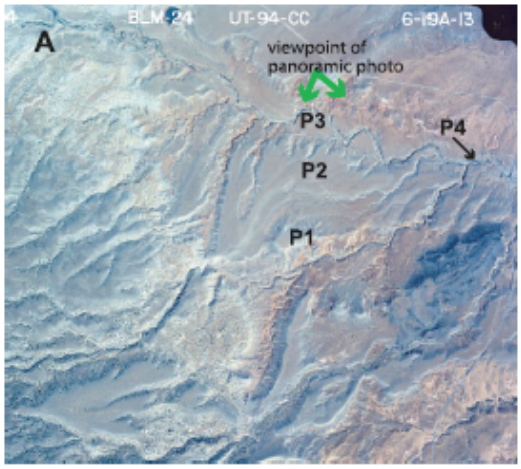


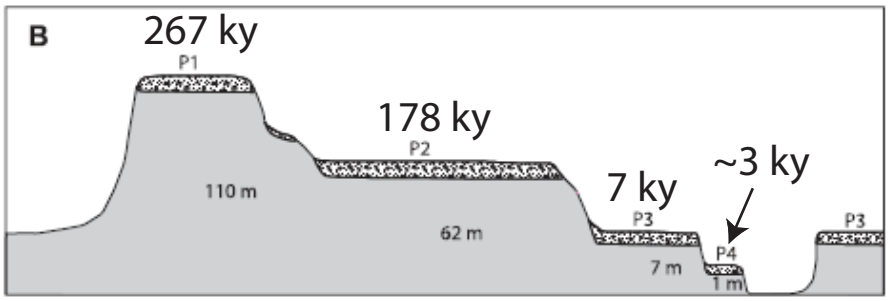


| Surface | Age (ky) | Height (m) | Incision rate (m/my) | ± |
|---|---|---|---|---|
| P1 | 267 | 110 | 412 | 21·4 |
| P2 | 178 | 62 | 348 | 28·3 |
| P3 | 13 | 7 | 527 | 8·4 |
| P4 | ~3? | 1 | ~330? | 19·2 |

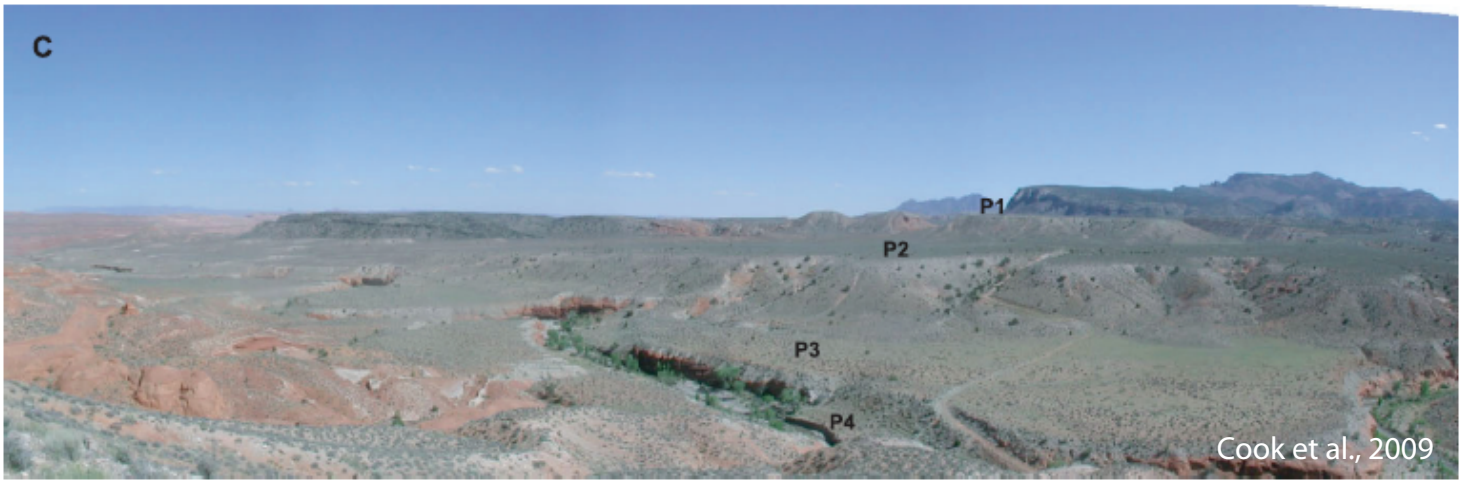


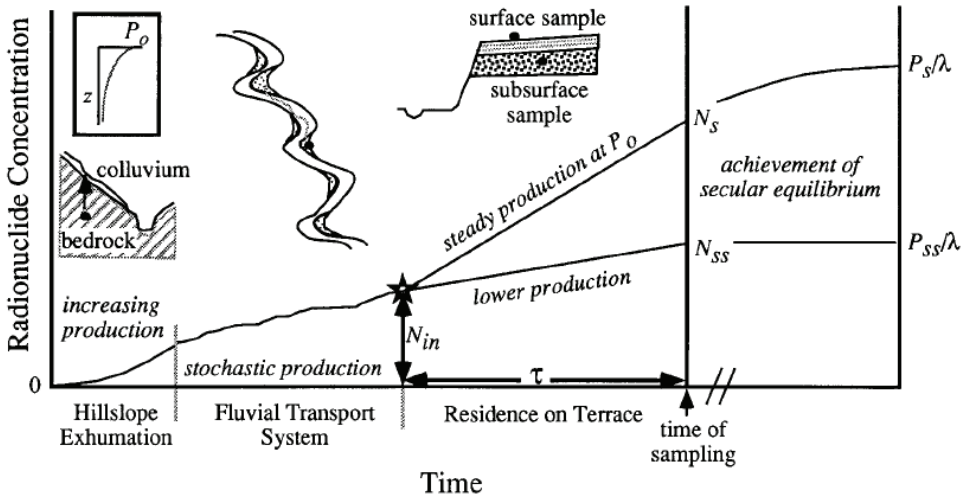


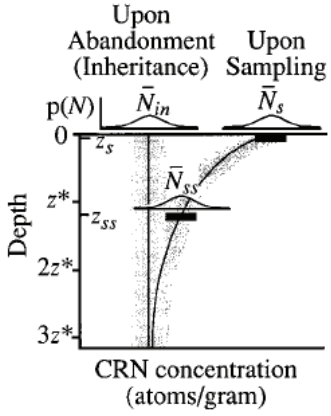


Anderson et al., 1996

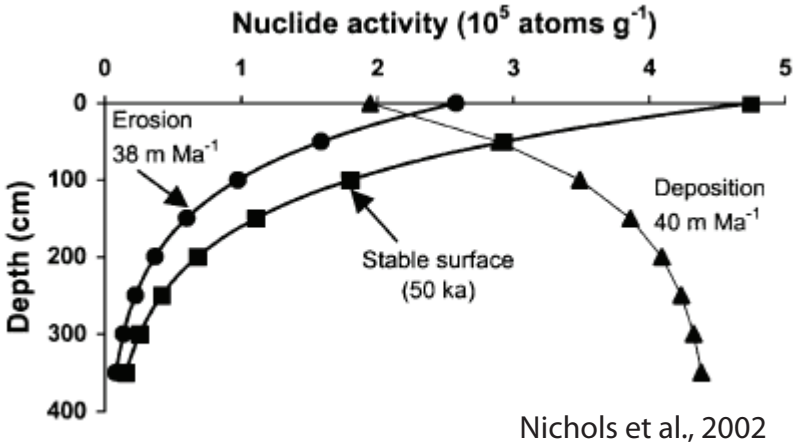


Nichols et al., 2002

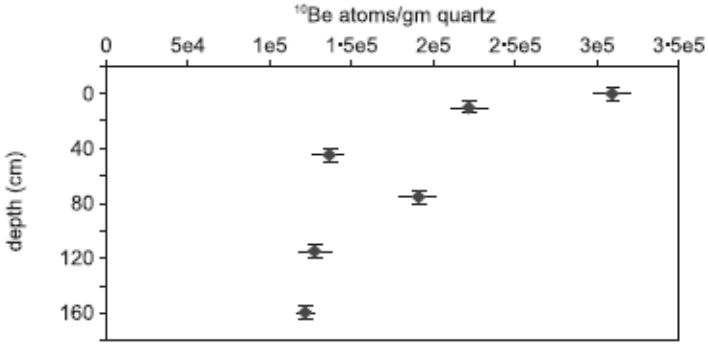


Cook et al., 2009

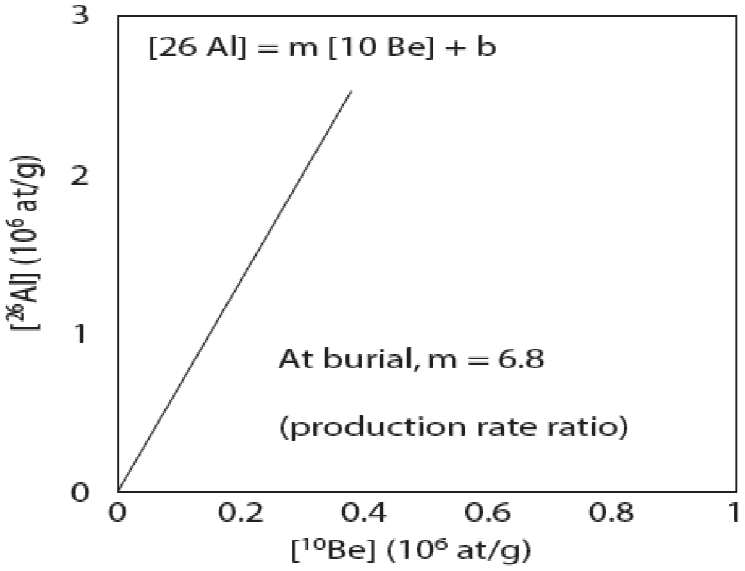


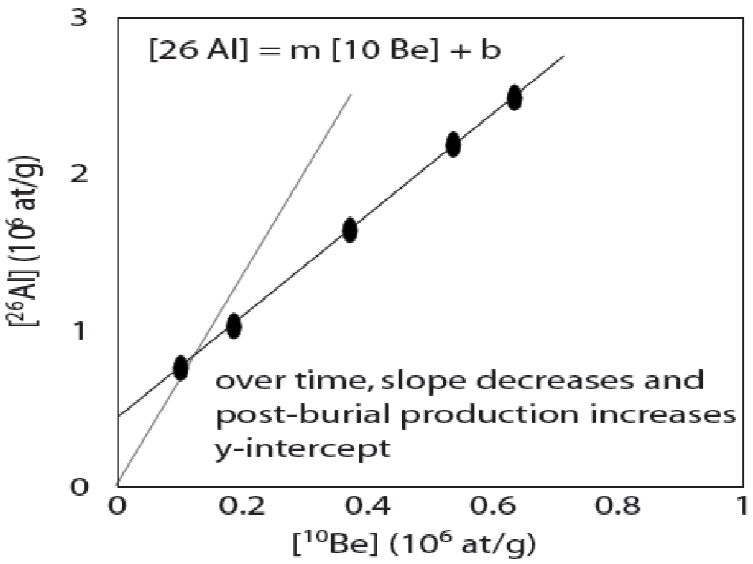


Simplified diagram of Al/Be ratios used for isochron cosmogenic burial dating. The slope of the line at the time of burial is the production ratio, generally 6.8, and decreases as decay occurs, i.e. as time goes by. Thus age is inversely proportional to slope. Inheritance provides the spread of points along the line. Post burial production of Aluminum increases the y-intercept (while Be is also produced) and erosion rates cause the line to not be exactly linear and must be corrected.

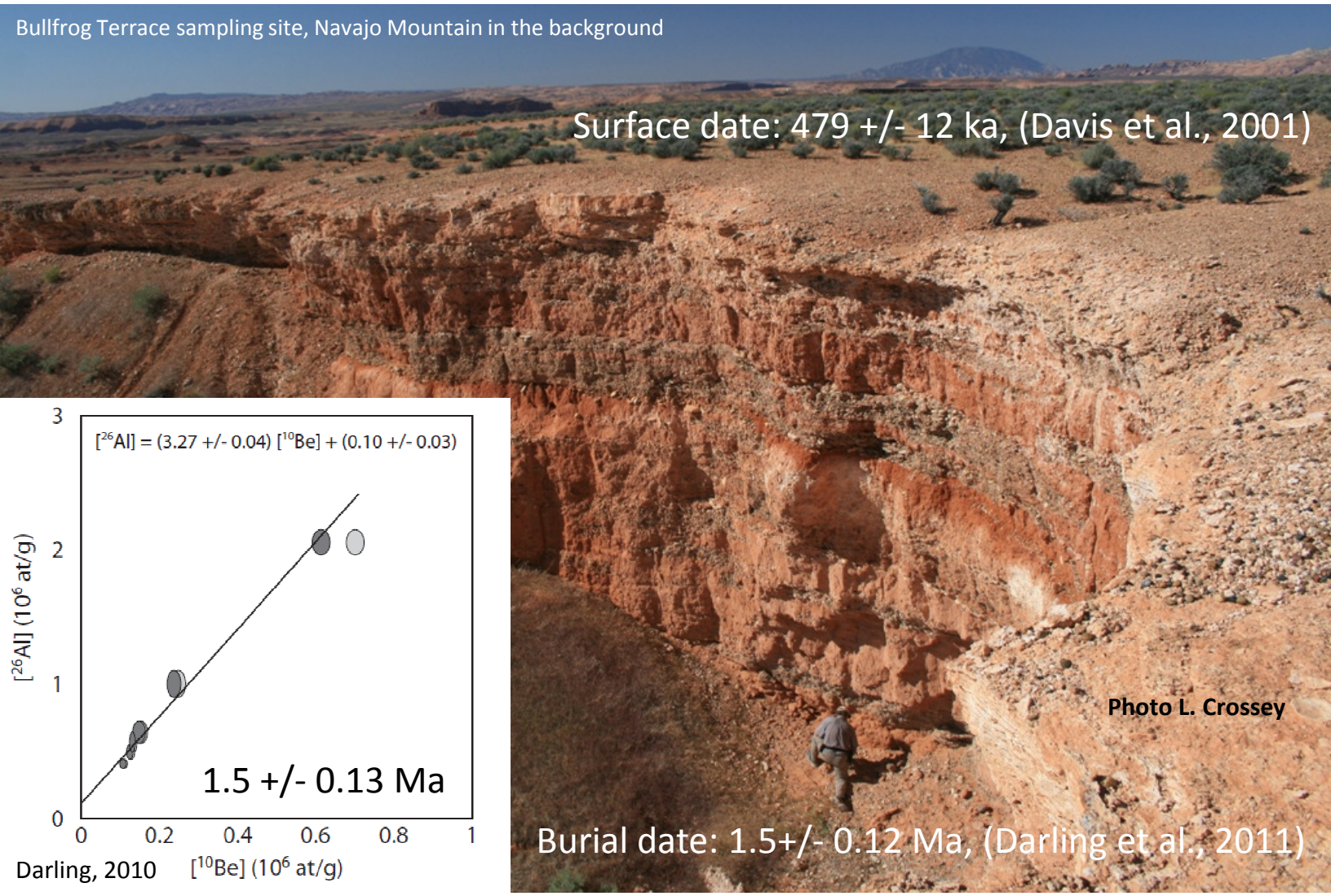





Darling, 2010

Isochron plots of $^{26}Al/^{10}Be$ data for determination of isochron dates. Measured data are shown in light gray with one-sigma error ellipses. Data linearized for regression are shown as darker ellipses, shifted to lower $^{10}Be$ concentrations (see Balco and Rovey, 2008). Regression equations are shown for each line, including errors in both slope and intercept. Errors in slope are calculated following York (1966) or from measurement uncertainty, whichever is greater.

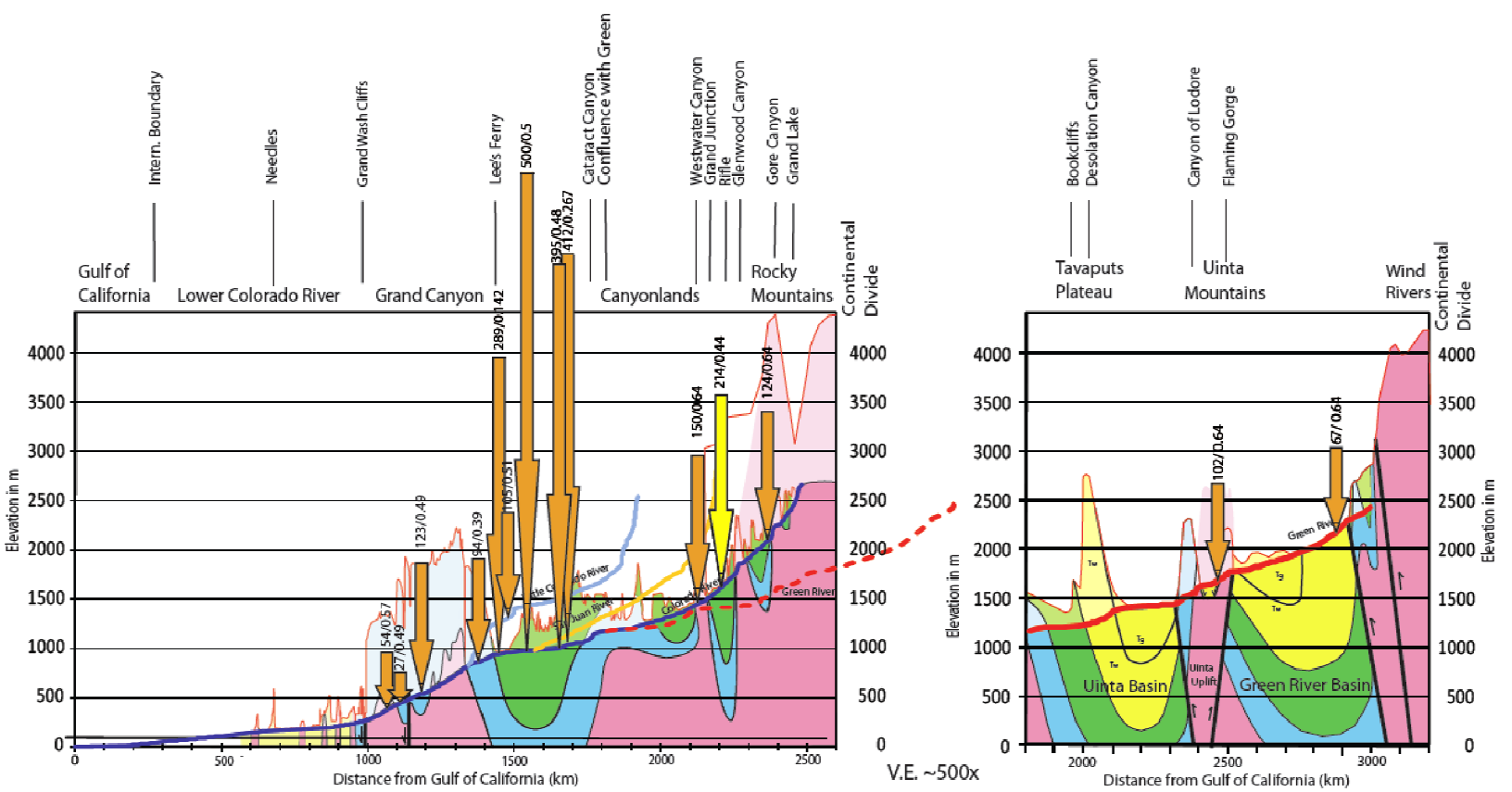


Short term rates on longitudinal profiles with schematic bedrock geology and canyon names. V.E. 500x. Yellow = Tertiary sedimentary rocks, Green = Mesozoic sedimentary rocks, Blue = Paleozoic sedimentary rocks, Pink = Precambrian igneous and metamorphic rocks. Compiled short term (less than 1 Ma) incision rates (including new data points); arrows are proportional to rate magnitude, horizontal bars within arrows represent strath elevation of dated terraces. These constraints show highly variable incision rates through time and space. 1 km elevation change = 100 m/Ma rate vector length.

Darling et al., 2011

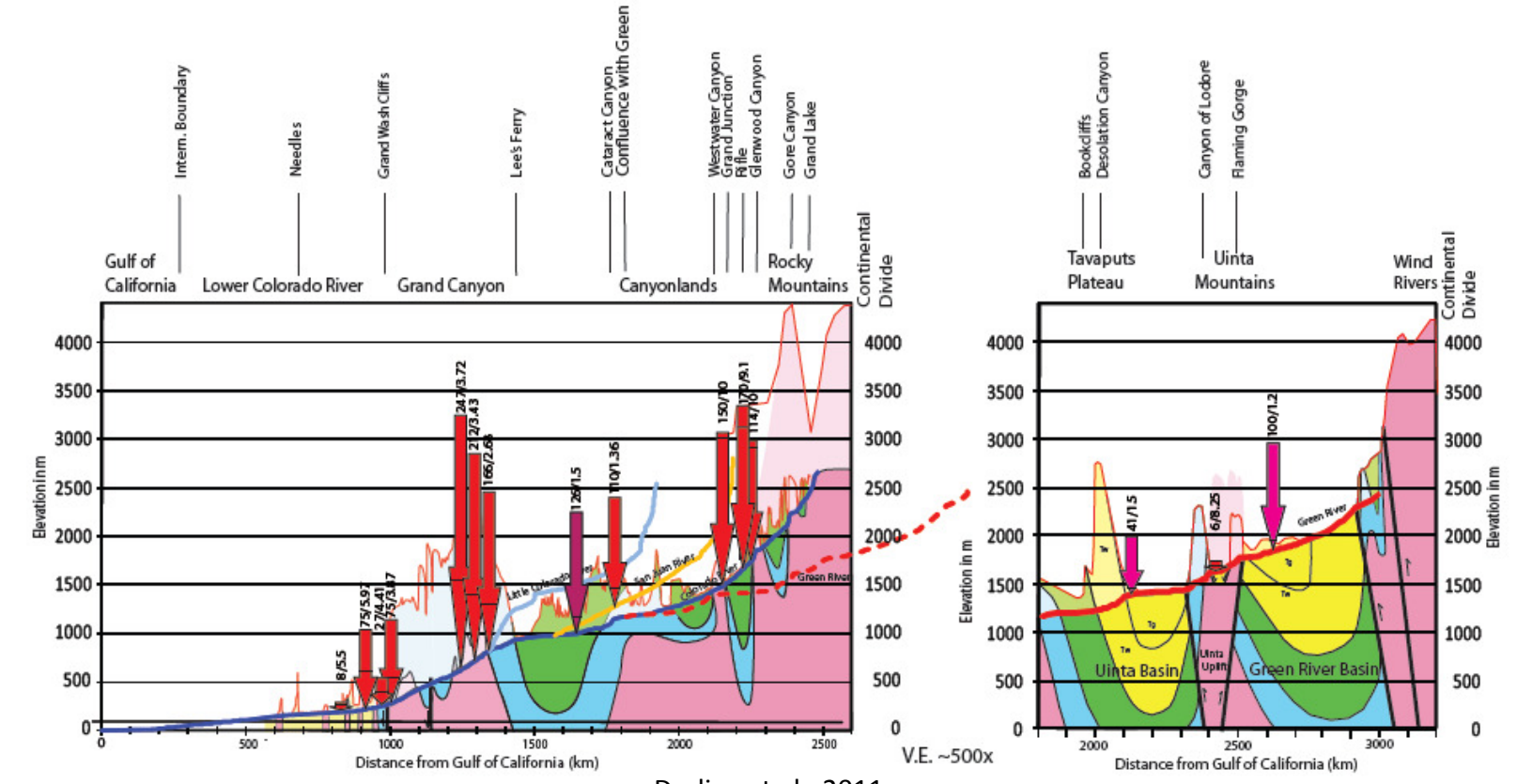


Darling et al., 2011

Long term rates on longitudinal profiles with schematic bedrock geology and canyon names. V.E. ~500x. Yellow = Tertiary sedimentary rocks, Green = Mesozoic sedimentary rocks, Blue = Paleozoic sedimentary rocks, Pink = Precambrian igneous and metamorphic rocks. Compiled long term (greater than 1 Ma) incision rates (including new data points); arrows are proportional to rate magnitude, horizontal bars within arrows represent strath elevation of dated terraces. 1 km elevation change = 100 m/Ma rate vector length.